5105-113
Solar Thermal Power Systems Project
Parabolic Dish Systems Development

DOE/JPL-1060-57
Distribution Category UC-62b

Cameron

Optimization of Dish Solar Collectors With and Without Secondary Concentrators

L.D. Jaffe

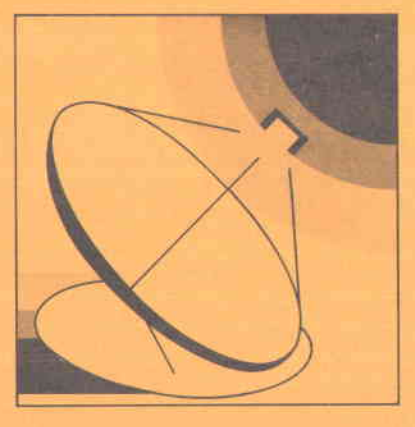

May 15, 1982

Prepared for
U.S. Department of Energy
Through an Agreement with
National Aeronautics and Space Administration
by
Jet Propulsion Laboratory
California Institute of Technology
Pasadena, California

JPL PUBLICATION 82-103

5105-113
Solar Thermal Power Systems Project
Parabolic Dish Systems Development

DOE/JPL-1060-57
Distribution Category UC-62b

Optimization of Dish Solar Collectors With and Without Secondary Concentrators

L.D. Jaffe

May 15, 1982

Prepared for
U.S. Department of Energy
Through an Agreement with
National Aeronautics and Space Administration
by
Jet Propulsion Laboratory
California Institute of Technology
Pasadena, California

JPL PUBLICATION 82-103

Prepared by the Jet Propulsion Laboratory, California Institute of Technology, for the U.S. Department of Energy through an agreement with the National Aeronautics and Space Administration.

The JPL Solar Thermal Power Systems Project is sponsored by the U.S. Department of Energy and forms a part of the Solar Thermal Program to develop low-cost solar thermal and electric power plants.

ABSTRACT

Methods for optimizing parabolic dish solar collectors and the consequent effects of various optical, thermal, mechanical, and cost variables are examined in this report. The most important performance optimization is adjusting the receiver aperture to maximize collector efficiency. Other parameters that can be adjusted to optimize efficiency include focal length, and, if a heat engine is used, the receiver temperature. The efficiency maxima associated with focal length and receiver temperature are relatively broad; it may, accordingly, be desirable to design somewhat away from the maxima.

Performance optimization is sensitive to the slope and specularity errors of the concentrator. Other optical and thermal variables affecting optimization are the reflectance and blocking factor of the concentrator, the absorptance and losses of the receiver, and, if a heat engine is used, the shape of the engine efficiency versus temperature curve. Performance may sometimes be improved by use of an additional optical element (a secondary concentrator) or a receiver window if the errors of the primary concentrator are large or the receiver temperature is high.

Such factors as receiver temperature affect not only efficiency, but also maintenance, reliability, and availability. All of these affect the cost of the energy produced, as does, of course, the initial installed cost of the collector itself. Both collector costs and efficiency have strong effects upon the cost of the energy produced; trade-offs of system performance versus system cost are needed.

PREFACE

William Revere and Peter Poon provided helpful information during the course of this work. Comments on the manuscript by James Bowyer, Philip Moynihan, William Owen, Louis Rubenstein, and Frank Surber led to significant improvements in the paper. The work was sponsored by the U.S. Department of Energy through an interagency agreement with NASA (NASA TASK RE-152; AMENDMENT 327; DOE/NASA IAA # DE-AM04-80AL13137).

CONTENTS

Tables

PART ONE

EXECUTIVE SUMMARY

EXECUTIVE SUMMARY

A dish solar collector consists of a dish concentrator with a receiver mounted at its focus. It provides a convenient means of converting solar energy into high-temperature heat, which may be either used directly or converted to mechanical or electrical energy.

This paper addresses problems of optimizing the optical characteristics of dish collectors for solar thermal power systems, presents methods for optimization, and examines the effects of various optical, thermal, and cost variables. Performance optimization may be done on the basis of the collector efficiency or, more narrowly, on the efficiency of the concentrator plus the receiver aperture; that is, the ratio: (net solar energy into the receiver aperture)/(direct sunlight incident on the concentrator). If the collector forms part of a system for production of mechanical work or electricity, performance optimization on the basis of system efficiency is preferable. For present purposes, this can be replaced by optimization on the basis of the combined efficiency of the concentrator, receiver, and engine; that is, the ratio: (engine output power)/(direct sunlight incident on the concentrator). The report primarily considers performance at rated load but devotes some attention to performance at part load. Part-load behavior can be important in determining performance on an annual basis because the system will probably run an appreciable fraction of the year under conditions of low insolation (incoming sunlight) or low demand.

The most important performance optimization for a dish collector is that of collector efficiency as a function of receiver aperture. If the receiver aperture is too large, thermal losses out the aperture will reduce efficiency unnecessarily. If the receiver aperture is too small, a significant fraction of the concentrated sunlight will not enter the aperture and will be lost, again reducing efficiency. The collector efficiency is rather sensitive to the choice of aperture. Other optimizations include collector efficiency versus focal length, and, if a heat engine is used, system efficiency versus receiver temperature. The efficiency peaks associated with focal length and receiver temperature are relatively broad, so the efficiency obtained is not

very sensitive to changes in these characteristics. In one example the temperature at which peak efficiency is achieved was 1000°C (1830°F), but at 675°C (1250°F) the efficiency was 95% of the peak efficiency. It may accordingly be desirable to design the system to operate at a temperature considerably below that corresponding to peak efficiency.

Performance optimization is quite sensitive to the slope and specularity errors of the concentrator. Slope errors in the concentrator optical surface result from the design, from inaccuracies in manufacturing and installation, and from deflections in service due to gravity, wind, and temperature changes. Minimizing slope errors is often key to the design of an efficient collector. Specularity spread (the angular spread of collimated light when reflected from a small or flat portion of a mirror) depends strongly on the mirror material: glass mirrors generally have better specularity than metal- or plastic-base mirrors. If the slope errors and specularity spread of a concentrator are high, the efficiency of the collector will tend to be low, especially at high receiver temperatures; slope errors and specularity are less important at low receiver temperatures.

Other optical and thermal variables affecting optimization are the reflectance and the blocking factor of the concentrator and the absorptance and thermal losses of the receiver. (The blocking and shadowing factor is the fraction of the sunlight that is not blocked or shadowed by elements of the concentrator, by equipment mounted on or near the concentrator or by nearby concentrators.) To reduce receiver losses, cavity receivers are almost always used in dish collectors. Cavity receivers have two advantages over open receivers: (1) For a given heat transfer area, cavity receivers provide a smaller exposed area for radiation and convection losses, and (2) the cavity design increases the effective absorptance for solar radiation.

If a heat engine is used, engine characteristics affect collector optimization, in particular the shape of the engine efficiency versus temperature curve. For this reason, in examples examined, the efficiency of systems with Brayton engines peaked at receiver temperatures 330-400°C (600-720°F) higher than did those with Rankine or Stirling engines.

Collector and engine performance at less than nominal insolation (part-load) should also be considered in striving for optimum annual performance.

Performance may sometimes be improved by the use of an additional optical element (a secondary concentrator) to provide additional concentration of the incoming sunlight or by the use of a window over the receiver aperture. These options are likely to be advantageous only if the errors of the primary concentrator are large or the receiver temperature is high. Use of a secondary concentrator significantly affects optimization of other components; thus, the optimum focal length of the primary concentrator and the optimum temperature of the receiver may be changed by the introduction of a secondary concentrator. Collector elements that in some circumstances may improve collector performance include wind screens and infra-red reflectors to return some of the emitted radiation to the receiver aperture.

Cost optimization of dish solar collectors and of dish solar thermal systems tends to be difficult because of the lack of reliable cost data. Hardly any dish collectors are beyond the prototype stage; costs and prices in volume production are therefore only estimates; costs of operation and maintenance are even more uncertain. To obtain meaningful data on the price differential between concentrators with different slope errors, for example, is almost impossible at present. Still more difficult is determining how this differential varies with the production rate. In this paper, therefore, discussion of cost trade-offs is limited to those in which the collector cost and efficiency are assumed to be known. Cost optimization is here made on the basis of the busbar energy cost of the electricity produced or the cost of the heat delivered, depending on the product. Other measures of cost, such as the cost per unit of installed capacity, could be utilized.

Projected collector costs are typically near 50% of total capital costs for a parabolic dish solar thermal power plant. In an example examined, a 1% increase in collector cost increased the cost of the electricity produced by 0.6%. A 1% decrease in collector efficiency increased the cost of electricity produced by 2%. As the efficiency continues to decrease, the cost of the electricity rises more rapidly; at low efficiencies, it is not possible to obtain low electricity cost even if the collector is free.

Slope error has a major effect on the efficiency that can be obtained and hence on the cost of electricity produced. It also can be expected to have a significant effect on the cost of manufacturing and installing a collector. Considering only the efficiency effect, in an example considered, the levelized busbar energy cost rose from about 70 mills/kW-h at a slope error of 0.5 milliradians to 130 mills/kW-h at 5 mrad and over 200 mills/kW-h at 10 mrad. The trade-off between manufacturing cost to attain a specific slope error and the resulting performance is thus quite important.

Changes in receiver temperature also affect efficiency, and therefore cost, if electricity or mechanical work is being produced. As mentioned above, system efficiency goes through a rather flat peak as the temperature is varied. High temperatures necessitate use of more expensive materials and tend to exacerbate problems of lifetime, reliability, and maintenance. (Maintenance and operations costs over a 30-year plant lifetime are projected as more than 50% of capital cost, in real dollars.) Thus, the optimum receiver temperature on the basis of cost will usually be well below that on the basis of efficiency.

In contrast, receiver aperture size, which has a strong effect on efficiency and hence on the cost of energy produced, has no significant direct effect on collector cost. Accordingly, the optimum receiver aperture on the basis of efficiency will also be optimum on the basis of cost.

The use of a secondary concentrator may sometimes permit attainment of adequate efficiency with a primary concentrator having larger slope errors than would otherwise be possible. The saving in cost of the primary may more than offset the cost of the small secondary. Because of efficiency considerations, this choice is likely to be advantageous only if the receiver temperature is high.

The cost/output ratio of a collector tends to be high at very small concentrator sizes because of the cost of concentrator drive and controls. It tends to be high at very large concentrator sizes because of the cost of concentrator structure: the output varies as the square of the linear dimension, but the structural weight and cost vary as the cube. Minimum cost per unit output is obtained at intermediate size (5- to 15-m-diameter).

The minimum is very flat. However, the whole system, not merely the collector, should be considered. If an engine is mounted on each collector, engine size and collector size must be matched. Very small engines (below 10 kW output) tend to be less efficient than larger ones and to cost more per unit output. This drives the cost optimum to somewhat larger sizes than if only the collector is examined.

Some typical characteristics pertinent to dish solar collectors for thermal power systems are:

Concentrator diameter	5-15 m
Concentrator slope error	1.5-10 mrad
Receiver type	Cavity
Receiver aperture diameter	0.1-0.5 m
Receiver temperature	
For production of heat	150°C (300°F) and up
For production of electricity or work	350-900°C (700-1650°F)
Anticipated for future production of electricity	to 1300°C (2400°F)
Collector efficiency	0.4-0.9

PART TWO

OPTIMIZATION OF DISH SOLAR COLLECTORS WITH AND WITHOUT SECONDARY CONCENTRATORS

SECTION I

INTRODUCTION

A dish solar collector (Figure 1) consists of a dish concentrator with a receiver mounted at its focus and provides a convenient method of converting solar energy into high-temperature heat. This heat may be either used directly or converted to mechanical or electrical energy. Dish concentrators may have a wide variety of optical, thermal, mechanical, and electrical configurations and may also differ in the materials and control systems used; many dish concentrators of current interest are reviewed in Reference 1. References 2 through 4 describe some receivers of interest for dish collectors. This report addresses problems of optimization of the optical characteristics of dish collectors for solar thermal power systems. Pertinent earlier work includes References 5 through 12.

SECTION II

METHODS FOR PERFORMANCE OPTIMIZATION

A. BASIS FOR PERFORMANCE OPTIMIZATION

The most fundamental decision in optimization is the choice of quantity to be optimized. For solar thermal power systems, one may optimize some measure of performance or some quantity that relates output and cost. Efficiency is a good measure of performance, but efficiency of what? Can the efficiency of the concentrator and the efficiency of the receiver be optimized separately? It turns out that the efficiency of the receiver is so strongly dependent upon the concentrator characteristics that a measure of concentrator performance which ignores the receiver is of little use, and vice versa. The size of the receiver aperture strongly affects both the solar power delivered to the receiver by the concentrator and the thermal power lost out the aperture by the receiver. A large receiver aperture permits more of the concentrated sunlight to enter the receiver but also increases radiative and convective losses out the aperture. Receiver aperture size thus must be optimized. This optimization interacts with the optimization of the concentrator itself: the concentrator performance needed depends upon the receiver aperture size. The temperature of the receiver is also important, as it strongly affects the loss out the receiver aperture and hence the optimization of the aperture size, which in turn is critical in evaluating collector performance. Such other receiver characteristics as losses out the walls do not react back so much on concentrator optimization and may or may not be considered. Therefore, the efficiency of the collector as a whole (concentrator and receiver together) must be optimized, with receiver temperature and receiver aperture size as key optimization parameters.

If the power system includes a heat engine for conversion of thermal to mechanical energy, there is an important interaction between the engine and the collector through the receiver temperature. The engine efficiency is strongly dependent on the engine inlet temperature, which usually approximates the receiver temperature. As the receiver temperature increases, the engine efficiency increases; however, the receiver thermal losses also increase, so

the receiver efficiency decreases. This interaction between the receiver and the engine efficiencies affects the choice of receiver temperature, which in turn affects the selection of receiver aperture. To optimize the efficiency of a solar thermal power system whose output is mechanical work or electricity, one must consider the dependence of engine efficiency upon temperature as a factor in optimizing the collector.

If the input to a receiver or engine varies, the receiver or engine losses do not vary in proportion because receiver and engine efficiencies depend on the input or, correspondingly, with the output. To optimize the performance of a plant that is to operate for years with varying insolation and varying demand, one should consider part-load as well as rated load efficiencies.

Solar power system components downstream of the engine, such as the alternator and power conditioning, usually do not interact strongly with collector performance and may ordinarily be disregarded in collector optimization.

This report, therefore, deals specifically with optimization of collector performance in terms of: (1) the efficiency of the concentrator plus receiver aperture; that is, the ratio (net solar energy into the receiver aperture)/(direct sunlight incident on the concentrator); and (2) the combined efficiency of the concentrator, receiver and engine; that is, the ratio (engine output power)/(direct sunlight incident on the concentrator). Relative values of engine efficiency are adequate for this purpose because multiplying all engine efficiencies by a constant will not affect the concentrator optimization. Performance at rated load will be considered for the most part, but some attention will given to performance at part load. (Direct sunlight, mentioned above, is sunlight that reaches the concentrator without having been scattered or reflected by the Earth's atmosphere or surface).

B. COLLECTOR PERFORMANCE CALCULATION WITH SIMPLE DISH CONCENTRATORS

The equation (modified from Reference 6) used for net rate of heat collection is

$$Q_c = IA\rho G\phi\alpha - A_r [\epsilon\sigma (T_r^4 - T_a^4) + h_c (T_r - T_a)] - A_w k (T_r - T_a) \quad (1)$$

where

Q_c = net rate of heat collection

I = direct solar flux incident upon a plane perpendicular to the sun line

A = optical area of the concentrator, projected on a plane perpendicular to the sun line

ρ = reflectance of the concentrator mirror (or transmittance of the concentrator lens)

G = the geometric blocking and shadowing factor (fraction of sunlight that is not blocked or shadowed by elements of the concentrator, by equipment mounted on or near the concentrator, or by nearby concentrators)

ϕ = the intercept factor = (concentrated solar power entering the receiver aperture)/(concentrated solar power reaching the focal plane)

α = the effective absorptance of the receiver for sunlight

A_r = area of the receiver aperture

ϵ = effective emittance of the receiver for thermal radiation

σ = Boltzmann's constant

T_r = temperature of the receiver, absolute

T_a = temperature (ambient) of the surroundings, absolute

h_c = effective convection coefficient

A_w = receiver cavity wall area

k = conduction coefficient

Equation (1) assumes that the concentrator is pointed close to the sun line. This will ordinarily be true for a dish concentrator during operation. Equation (1) also assumes that a cavity receiver is used, that the cavity can be treated as a black-body cavity (or hohlraum, with the receiver temperature taken as uniform and the receiver aperture area small compared to the cavity wall area); that one may neglect the fraction of energy radiated by the receiver which is returned to the receiver from the surroundings; that an effective convection coefficient, h_c, can be defined for the receiver aperture; and that the heat transfer coefficients, h_c and k, are independent

of temperature, of environmental effects such as wind, and of receiver aperture size. These are approximations that are likely to be adequate for optimization of the kind treated in this report. Equation (1) should generally give results with an accuracy of 5 to 10%.

The collector efficiency

η_{coll} = (rate of heat transfer to the working fluid)/(direct solar power incident upon the concentrator)

$= Q_c/IA$

$$= \rho G\phi\alpha - (1/IC)\left[\epsilon\sigma(T_r^4 - T_a^4) + h_c(T_r - T_a)\right] - (A_w/IA)k(T_r - T_a) \quad (2)$$

where

$$C = A/A_r, \text{ the concentration ratio} \quad (3)$$

The optical efficiency of the concentrator is defined as:

η_{opt} = (solar power delivered to the receiver)/(direct solar power incident upon the concentrator)

This is equal to

$$\eta_{opt} = \rho G\phi \quad (4)$$

Also

$$\eta_{coll} = \eta_{opt}\eta_{rec} \quad (5)$$

where the receiver efficiency

η_{rec} = (solar power delivered to the receiver)/(rate of heat transfer to the working fluid)

$$= \alpha - (1/\rho G\phi)\left\{(1/IC)\left[\epsilon\sigma(T_r^4 - T_a^4) + h_c(T_r - T_a)\right] - (A_w/IA)k(T_r - T_a)\right\} \quad (6)$$

C. PERFORMANCE OPTIMIZATION FOR SIMPLE DISH COLLECTORS

An optimization that is commonly done is that of selecting the receiver aperture area, A_r, to maximize the collector efficiency, η_{coll}, at a given receiver temperature, T_r, and with given values of ρ, G, α, ϵ, T_a, h_c, and k (see Equation 2). The geometric concentration ratio, C, is an explicit function of A_r (Equation 3). Increasing the receiver aperture, A_r, tends to decrease the collector efficiency, η_{coll}, by Equations (2) and (3) because

it increases the heat lost out the aperture by re-radiation and convection (the right-hand portion of Equation 2). The intercept factor, ϕ, is also a function of A_r because a larger receiver aperture will, in general, intercept more of the concentrated sunlight reaching the focal plane. This increases ϕ, and, by Equation (2), tends to increase the collector efficiency, η_{coll}. There is, therefore, a receiver aperture at which η_{coll} is maximum. To find this maximum, the intercept factor, ϕ, must be expressed as a function of the aperture size. To do this, it is necessary to know how the concentrated sunlight is spatially distributed in the focal plane.

For a given concentrator design, the flux distribution in the focal plane can be calculated by ray tracing, Monte Carlo, or cone optics methods. Ray tracing, even with a computer, tends to be tedious and somewhat expensive. Monte Carlo and cone optics calculations are less expensive. However, these methods still involve considerable cost and do not appear to be necessary for system studies and optimization although they are appropriate for detailed optical design of a selected concentrator. For optimization studies, less exact approximations are ordinarily adequate.

The approximation used here, devised by Duff and Lameiro (Reference 13), treats the flux distribution in the focal plane and the variables contributing to it as Gaussian distributions. For a point-focusing concentrator whose overall contour is that of a paraboloidal mirror, with a cavity or flat receiver, Duff and Lameiro find

$$\sigma_f^2 = \frac{\sigma_r^2}{R^2} = \delta^2 \frac{1}{\theta \tan^2 \frac{\theta}{2}} \left[\frac{-1}{3 \sin^3\theta \cos\theta} + \frac{2 - \cos\theta}{3 \sin^3\theta} + \frac{2 - 2\cos\theta}{\sin\theta} \right.$$

$$\left. + \frac{4 \sin\theta}{3 \cos\theta} - \ell n \tan\left(\frac{\pi}{4} + \frac{\theta}{2}\right) + \ell n \tan\left(\frac{\pi}{4} - \frac{\theta}{2}\right) \right] \qquad (7)$$

For a point-focusing concentrator (mirror or lens) whose overall contour is planar, with a cavity or flat receiver, Duff and Lameiro find

$$\sigma_f^2 = \frac{\sigma_r^2}{R^2} = \delta^2 \frac{1 + 2\cos^2\theta}{3\theta \cos\theta \sin\theta} \qquad (8)$$

Here (see Figure 1):

$\sigma_f = \sigma_r/R$ = standard deviation of the (Gaussian) flux distribution in the focal plane, in units of concentrator radius.

σ_r = standard deviation of the (Gaussian) flux distribution in the focal plane, in units of length.

R = radius of concentrator.

θ = rim angle of the concentrator, as seen from its focus (angle between the focus-to-vertex axial direction and the rim direction).

$$\delta^2 = (2\sigma_{slope})^2 + \sigma_\omega^2 + \sigma_p^2 + \sigma_{sun}^2 \qquad (9)$$

σ_{slope} = standard deviation of the (Gaussian) slope errors of the concentrator.

σ_ω = standard deviation of the (Gaussian) specularity spread of the optical surface(s).

σ_p = standard deviation of the (Gaussian) pointing error of the concentrator.

σ_{sun} = standard deviation of the (Gaussian) angular spread of the incoming direct sunlight.

Also, the rim angle, θ, is related to the focal length, F, of the concentrator by

$$f_r = F/D = (1 + \cos\theta)/(4 \sin\theta) \qquad (10)$$

for a paraboloidal concentrator (see Figure 1)

and

$$f_r = F/D = 1/(2 \tan\theta) \qquad (11)$$

for a planar concentrator, where

f_r = focal ratio

F = focal length

D = $2R$ = diameter of concentrator

The Duff-Lameiro approximation for paraboloidal mirrors resembles that of Aparisi (References 14 and 15) and is very close to the Aparisi approximation

for rim angles less than 45° (Figure 2). However, the Aparisi approximation

$$\sigma_f^2 = \sigma_r^2/R^2 = \delta^2/\sin^2\theta \qquad (12)$$

indicates that the size of the focal spot, σ_f, decreases continuously as the rim angle, θ, increases over the range from 0 to 90°. The Duff-Lameiro approximation for a paraboloidal mirror indicates that the focal size decreases to a minimum and then increases as the rim angle increases (see Figure 2). The latter characteristic accords with the results obtained with the more exact calculations of cone optics and ray-tracing, whereas the Aparisi result does not (Reference 16). When a wide range of rim angles are to be considered, the Duff-Lameiro approximation appears, therefore, preferable. Also, Aparisi did not provide an expression for planar concentrators; Duff and Lameiro did (Equation 8).

Duff and Lameiro did not include the σ_ω^2 term in Equation (9), but Wen et al (see Reference 10) have used it. The Duff-Lameiro derivation assumes that

$$\theta >> 2\sigma_{slope} + \sigma_\omega + \sigma_p + \sigma_{sun}$$

which should be true for all practical concentrators. More significantly, it assumes that the concentrator slope errors, the concentrator specularity, the pointing errors, and the angular distribution of direct sunlight are all normally distributed (Gaussian). This is probably a reasonable first approximation for slope errors though one may expect a different variance for circumferental slope errors than for radial. For lens concentrators, a term to account for spectral dispersion should be added to Equation (9). The angular distribution of a light beam after specular reflection from a flat glass mirror appears to be adequately described by a Gaussian distribution, but if reflection is from a metal or polymeric mirror, the sum of two normal distributions may be needed for a good description (Reference 17). The pointing errors are probably Gaussian to a first approximation; their distribution will depend upon the control scheme used. For solar radiation, a Gaussian angular distribution is a rather crude approximation, though its accuracy depends on atmospheric conditions (Reference 18). Unless the concentrator is unusually

accurate, however, σ_{sun}^2 is considerably smaller than $(2\sigma_{slope})^2 + \sigma_\omega^2 + \sigma_p^2$ (see Equation 9), so the inexactness of the solar representation has little effect upon the flux distribution in the focal plane (Reference 10). Equations (7) and (8) are probably accurate within 10% for most cases of practical interest.

Utilizing Equation (7) or (8), the flux distribution in the focal plane is

$$J(r) = IA\rho G \frac{1}{2\pi\sigma_f^2} e^{-r^2/2\sigma_r^2} \tag{13}$$

where

$J(r)$ = flux distribution in the focal plane as a function of r

r = radial distance from the focal point in the focal plane.

Then

$$\phi = 1 - e^{-r^2/2\sigma_r^2} \tag{14}$$

$$= 1 - e^{-A_r/2\pi\sigma_r^2} \tag{15}$$

$$= 1 - e^{-A_r/2\pi R^2\sigma_f^2} = 1 - e^{-A_r/2A\sigma_f^2} \tag{16}$$

$$= 1 - e^{-1/2C\sigma_f^2} \tag{17}$$

or

$$C = 1/(2\sigma_f^2 \ln \frac{1}{1-\phi}) \tag{18}$$

Figure 3 shows the geometric concentration ratio attainable with a paraboloidal mirror as a function of the slope error and the intercept factor, based on Equations (18), (12), and (9).

Substituting Equation (15) in Equation (1), differentiating with respect to A_r, and setting the result equal to zero, we find that the heat collected, Q_c, and the collector efficiency, η_{coll}, are maximized when

$$\phi = 1 - 2\sigma_f^2[\epsilon\sigma(T_r^4 - T_a^4) + h_c(T_r - T_a)]/I\rho G\alpha \qquad (19)$$

This value of ϕ may be inserted in Equation (18) to give C, and these values of ϕ and C may then be used in Equation (2) to determine the maximum collector efficiency.

D. SYSTEM PERFORMANCE CALCULATION

The overall efficiency of the solar thermal power system is taken as

$$\eta_{sys} = \eta_{coll}\eta_{pc}\eta_{pp} \qquad (20)$$

where

η_{pc} = efficiency of power conversion
η_{pp} = efficiency of power processing

Power conversion here designates the subsystem that converts the thermal energy from the receiver into mechanical or electrical energy. For a system producing electricity, the power conversion subsystem ordinarily consists of a heat engine, perhaps gearing, a generator, perhaps a rectifier, and auxiliaries. Then

$$\eta_{pc} = \eta_{eng}\eta_{gear}\eta_{gen}\eta_{rect}\eta_{aux} \qquad (21)$$

where

η_{eng} = engine efficiency
η_{gear} = gearing efficiency
η_{gen} = generator efficiency

η_{rect} = rectifier efficiency

η_{aux} = factor to account for parasitics

For a system producing mechanical output, the power conversion subsystem consists of the heat engine, perhaps gearing, and auxiliaries. For a system producing only thermal output, there is no power conversion and $\eta_{pc} = 1.0$.

Power processing here refers to elements of the power system, downstream of power conversion, which transmit and condition the energy. For an electrical system, it may include an inverter, cables, transformers, switchgear, and perhaps battery storage. For a mechanical system it may include mechanical or hydraulic power transmission and perhaps storage. For a thermal system it may include piping, pumps, valves, and perhaps thermal storage. One may also include in the power processing efficiency the power consumption for the controls, for starting, and for power plant buildings (such as lighting, heating, and air conditioning). The boundary between power conversion and power processing is somewhat arbitrary and may be chosen differently for different system designs.

It is sometimes convenient to express the efficiency of the engine in terms of the Carnot efficiency. Thus,

$$\eta_{eng} = v(T_i - T_o)/T_i \tag{22}$$

where v = engine effectiveness = (engine efficiency)/(Carnot efficiency)

T_i = engine inlet temperature, absolute,

T_o = outlet temperature of the engine thermodynamic cycle, absolute

Also,

$$T_i = T_r - \Delta T \tag{23}$$

where ΔT is the temperature drop between receiver and engine.

E. EFFECTS OF SECONDARY CONCENTRATORS

In optical terms, a simple solar concentrator is one in which the sunlight is reflected or refracted once by a single optical element (a mirror or lens). A compound concentrator is one in which the sunlight is reflected and/or refracted more than once through the use of two or more optical elements. If two are used, the first element that the sunlight strikes is called the primary concentrator and the second element is called the secondary concentrator.

A collector may include a secondary concentrator for any of several reasons. For example, the secondary may be used to fold the optical path, thus shortening the structure and permitting placement of the receiver (with the power conversion subsystem if one is used) in a more convenient location. It may be used to improve the optical performance by increasing the geometric concentration ratio or the intercept factor. Different types of secondaries may be used for different purposes; they are reviewed in References 19 and 20. Attention in this report is confined to secondaries intended to improve optical performance. Examples are sketched in Figure 4 (a, b, c, and d).

By adding a suitable secondary, the flux distribution at the focus can be confined to a smaller area than is possible by using only a primary concentrator (for any practical primary design). The geometric concentration ratio can thus be increased at a given intercept factor, or vice versa. This can reduce receiver aperture losses or increase receiver temperature, which in turn can increase power conversion efficiency. These advantages must be weighed against the light loss associated with the reflectance or transmittance of the secondary mirror or lens.

F. PERFORMANCE CALCULATION AND OPTIMIZATION FOR COMPOUND COLLECTORS

When a simple concentrator is replaced by a primary plus a secondary concentrator, the basic equations (Equations 1, 2 and 4) for collector performance need be modified only by setting

$$\rho = \rho_1 \rho_2 \tag{24}$$

where subscript 1 refers to the primary concentrator and subscript 2 refers to the secondary concentrator.

One may likewise write the blocking and shadowing factor, G, the intercept factor, ϕ, and the geometric concentration ratio, C, as the products of corresponding separate quantities for the primary and secondary or may consider them as factors for the compound concentrator (primary and secondary together).

The flux distribution in the focal plane of a secondary with good performance is, however, not well approximated as Gaussian; rather, it is close to rectangular: i.e., nearly uniform in the center, dropping sharply to near zero at a definite radius (Reference 21). This affects the receiver aperture optimization. With such a flux distribution, the receiver aperture, to a first approximation, should be set equal to the area over which the flux is uniform, and the fraction of the flux from the secondary that enters the receiver aperture is then 1.0. With some secondary concentrator designs, the receiver aperture can coincide with the exit aperture of the secondary concentrator (Figure 4b, c, and d).

The fraction of the flux from the primary that is intercepted by the secondary should also be optimized. A secondary used to improve performance will usually be located near the focal plane of the primary. As a first approximation, therefore, the flux distribution at the entrance aperture of the secondary may be approximated by Equation (8) or (9) but spread radially by a proportionality factor to account for the wider distribution in a plane not coincident with the focal plane.

On this basis, the intercept factor of the compound collector is determined by how much of the primary flux enters the secondary. That is,

$$\phi \simeq \phi_1 \tag{25}$$

where ϕ_1 is the fraction of the primary flux near the focal plane that enters the secondary.

The geometric concentration ratio at this intercept factor is affected by the design of the secondary, and may be written as

$$C = C_{1s}C_2 \tag{26}$$

where

C_{1s} = geometric concentration ratio with primary concentrator alone

C_2 = multiplicative increase in geometric concentration ratio due to the secondary concentrator

The C that can be attained by using a secondary is limited in two ways. First, C cannot exceed the theoretical limit

$$C_{max} = 1/\sin^2\psi \tag{27}$$

at an intercept factor of 1.0. Here ψ is the half-angle of the sun as seen from Earth, about 4.65 milliradians. C, therefore, cannot exceed $1/(4.65 \times 10^{-3})^2$ or about 46,000. This is rarely limiting; rather, C is constrained in practice by C_2, which cannot exceed a value that depends on the focal ratio of the primary (References 22 and 23), and is generally not more than 30 (Figure 5). This limiting C_2 is independent of δ and hence of σ_{slope}, σ_{spec}, and σ_p. Practical secondary designs can come close to the theoretical C_2; because C_2 is small, it is insensitive to slope errors and specularity of the secondary.

On the basis of the above, for a compound collector the optimum intercept factor and geometric concentration ratio, analogous to Equations (19) and (18), are:

$$\phi = 1 - 2\sigma_f^2[\epsilon\sigma(T_r^4 - T_a^4) + h_c(T_r - T_a)]/I\rho G\alpha C_2 \tag{28}$$

$$C = C_2/(2\sigma_f^2 \ln \frac{1}{1-\phi}) \tag{29}$$

If the secondary is large, it will block some sunlight that would otherwise enter the primary concentrator aperture, thus decreasing the geometric blocking factor G in Equation (28). This may require iteration to arrive at an optimum compound collector. Because the secondary size depends on its optical design and is not a function of C_2 alone, the added blockage will not be evaluated here.

G. SYSTEM PERFORMANCE OPTIMIZATION

If the system provides mechanical or electrical power, another performance optimization is that of optimizing the overall system efficiency with respect to receiver temperature. As the receiver temperature increases, the receiver losses increase and the collector efficiency falls (Equation 2). The engine inlet temperature is closely coupled to the receiver temperature; as the engine inlet temperature is increased the engine efficiency and, therefore, the power conversion efficiency rises. Because of these opposing effects, the overall system efficiency (Equation 20) will be maximum at some temperature.

To optimize the system efficiency, it is necessary to know the variation in power conversion (or engine) efficiency as a function of inlet temperature. Given this relationship, one may then find the system efficiency at various temperatures by numerical calculation, using Equation (2) and (20), and so locate the maximum. Even if the power conversion effectiveness, v, is independent of temperature, so that Equation (22) provides a simple expression for η_{pc} as a function of T_i, substitution of Equations (2), (21), (22) and (23) in Equation (20) gives a fifth-power relation that requires numerical solution:

$$T_o\left\{\rho G\phi\alpha I - \frac{1}{C}[\epsilon\sigma(T_r^4 - T_a^4) + h_c(T_r - T_a)] - \frac{A_w}{A}k(T_r - T_a)\right\}$$

$$- (T_r - \Delta T)(T_r - \Delta T - T_o)\frac{1}{C}(4\epsilon\sigma T_r^3 + h_c - \frac{A_w}{A}k) = 0 \qquad (30)$$

Computer techniques for obtaining numerical results from the equations mentioned are obviously useful and have been utilized in this work.

Both the collector efficiency optimization and the system efficiency optimization mentioned are for a fixed insolation, I. The insolation will, however, vary as a function of time. If detailed records of insolation versus time are available for a site, the output for a given design may be calculated for each short time interval and sum to give the total output over a year selected as typical. The insolation data are typically in form of insolation measurements at 15-minute intervals, recorded on magnetic tape, which are input to a computer program calculating annual output. By computing the annual output for various receiver apertures or temperatures, the optimum based on yearly output may be determined. The results will differ from site to site.

This report does not consider specific sites. Rather, it uses the simpler but less exact approach of optimizing on the assumption that an insolation is selected as a typical operating point and the collector is optimized at this insolation.

SECTION III

RESULTS OF PERFORMANCE OPTIMIZATION

Examples in this report are based primarily on two power systems. One is an idealized system whose characteristics are given in Table 3-1. The other is the baseline system whose characteristics are given Table 3-2; it was chosen primarily because useful cost calculations were already available since a similiar system was used as a baseline in the cost analyses of Revere (Reference 24) and Rosenberg and Revere (Reference 25).

A. EFFECTS OF OPTICAL EFFICIENCY AND GEOMETRIC CONCENTRATION RATIO

Figures 6a and 6b illustrate the effects of optical efficiency and geometric concentration ratio upon collector performance. For these plots the intercept factor, the receiver temperature, and other collector characteristics were held constant at the values listed for the idealized and baseline systems, respectively (see Tables 3-1 and 3-2). (To permit changes in the geometric concentration ratio and optical efficiency, the slope error and the reflectance were allowed to vary). Figures 6a and 6b show that collector efficiency is very strongly dependent on optical efficiency. At low geometric concentration ratios, the collector efficiency is also very strongly dependent on geometric concentration ratio, but at higher geometric concentration ratios collector efficiency becomes almost independent of geometric concentration ratio.

B. RECEIVER APERTURE OPTIMIZATION

Figures 7a and 7b are plots of collector efficiency versus geometric concentration ratio for the idealized and baseline systems. The slope error was held constant for these plots, and the intercept factor allowed to vary. Shown in these figures are the intercept factor, the solar heat absorbed by the receiver, and the receiver thermal loss. The curves display maxima in collector efficiency at the geometric concentration ratio and intercept

Table 3-1. Characteristics of Idealized System (unless otherwise stated)

Concentrator type: paraboloidal mirror

Overall concentrator shape: paraboloidal

I	=	800 W/m^2
ρ	=	1.0
G	=	1.0
ϕ	=	0.98[a]
C	=	2500[a]
f_r	=	0.6
σ_{slope}	=	2.0 mrad
σ_ω	=	0.5 mrad
σ_p	=	0.0
σ_{sun}	=	2.3 mrad
α	=	1.0
ϵ	=	1.0
T_r	=	1185 K = 912°C = 1674°F[b]
T_a	=	293 K = 20°C = 68°F
h_c	=	0.0
k	=	0.0
ΔT	=	0.0
T_o	=	293°K = 20°C = 68°F
v	=	0.5
η_{pp}	=	1.0

[a]If not optimized
[b]If not varied

Table 3-2. Characteristics of Baseline System (unless otherwise stated)

Concentrator type: paraboloidal mirror

Overall concentrator shape: paraboloidal

I	=	800 W/m^2
ρ	=	0.95
G	=	0.967
ϕ	=	0.978[a]
C	=	2500[a]
f_r	=	0.6
σ_{slope}	=	2.2 mrad
σ_ω	=	0.5 mrad
σ_p	=	0.0
σ_{sun}	=	2.3 mrad
α	=	0.982
ϵ	=	0.998
T_r	=	1198 K = 925°C = 1700°F[b]
T_a	=	293 K = 20°C = 68°F
h_c	=	16.0 W/m^2K
A_w/A	=	0.015
k	=	0.737 W/m^2K
ΔT	=	20.0 K = 20°C = 36°F
T_o	=	323 K = 50°C = 122°F
η_{pc}	=	0.346

Variation of η_{pc} with T_r: as shown for Brayton system in Figure 17b.

η_{pp}	=	0.95

[a] If not optimized
[b] If not varied

factor given by Equations (18) and (19): about C = 2500 and ϕ = 0.988 for the idealized system; C = 2400 and ϕ = 0.981 for the baseline system. The peak is fairly sharp, illustrating the importance of optimizing the receiver aperture. A drop in geometric concentration ratio from 2500 or 2400 to 2000 or 1800 has very little effect on efficiency, but a drop to 1000 will appreciably lower efficiency. Below some limiting value of geometric concentration ratio (140 to 190 for these examples), the collector heat loss becomes equal to the solar energy entering the collector, and the efficiency falls to zero. Above the peak geometric concentration ratio, the efficiency falls because of the decrease in intercept factor.

In a practical concentrator, it may be desirable to select a receiver aperture different from that giving maximum efficiency. For example, it may be desirable to increase the aperture size beyond this optimum to reduce heating of the aperture lip by the concentrated sunlight.

Typical receiver aperture diameters are 0.1 to 0.5 m for concentrator diameters of 6 to 13 m, providing geometric concentration ratios of 100 to 3000. Geometric concentration ratios below 500 may be considered low for dish collectors; ratios above 2000 may be considered high. The corresponding intercept factor is typically 0.9 or more. Typical optical efficiencies are 0.7 to 0.95 (see Reference 1).

C. EFFECTS OF REFLECTANCE AND BLOCKING FACTOR

The optimum values of geometric concentration ratio and intercept factor are dependent upon the product of the reflectance and the blocking-shadowing factor. Table 3-3 illustrates the effect of changing these quantities. A moderate decrease in reflectance or blocking factor produces a corresponding decrease in collector efficiency; the optimum geometric concentration ratio is increased slightly; the optimum intercept factor decreases very slightly.

Typical values of reflectance are 0.8 to 0.95; the blocking-shadowing factor is typically higher than 0.9.

Table 3-3. Effects of Reflectance and Blocking-Shadowing Factor upon Optimization of Receiver Aperture

Quantity	Idealized System Case 1[a]	Idealized System Case 2	Baseline System Case 1[a]	Baseline System Case 2
Reflectance, ρ	0.95	0.80	0.95	0.80
Blocking/shadowing factor, G	1.00	0.90	0.967	0.90
ρG	0.95	0.72	0.919	0.72
Optimal geometric concentration ratio, C_{opt}	2530	2735	2415	2570
Optimal intercept factor, ϕ_{opt}	0.987	0.983	0.981	0.976
Optimal collector efficiency, η_{coll}	0.932	0.656	0.805	0.614

[a](Case 1 is listed in Table 3-1 or 3-2. Characteristics not stated here are same for Case 1 and Case 2.)

D. EFFECTS OF SLOPE, SPECULARITY, AND POINTING ERRORS

An error in slope of a (primary) concentrating mirror deviates the reflected beam through an angle twice the slope error. A deviation due to lack of specularity or to a pointing error deviates the reflected beam, with respect to the receiver aperture, by once the specularity or pointing deviation. Thus the flux distribution at the focal point, the intercept factor, and the collector efficiency are strong functions of the slope error and less strong functions of the specularity and pointing errors (Equations 9, 7, 8, 13-19, and 2). Figure 8 shows the effect of slope error upon the collector efficiency and intercept factor. Figure 9 shows the effect of specularity spread; the effect of pointing error is similar.

As these figures indicate, the collector efficiency attainable with an optimized receiver aperture depends on the concentrator errors, as do the optimum geometric concentrator ratio and intercept function. If the

concentrator errors are high, the attainable collector efficiency, the optimum intercept factor, and the optimum geometric concentration ratio will be low. As the concentrator errors decrease, the optimized efficiency, geometric concentration ratio, and intercept factor increase toward limiting values.

Dish concentrators typically have slope errors of 1.5 to 10 mrad; a slope error less than 2.5 mrad is usually considered low; a slope error more than 5 mrad may be considered high. The specularity spread is typically about 0.5 mrad for glass mirrors and 2 to 10 mrad for plastic film and metal mirrors. The pointing error may range from 1 to 10 mrad. The size of these errors, together with the reflectivity and blocking factor, may be taken to indicate the quality of the concentrator. (Low errors, high reflectivity, and high blocking-shadowing factor correspond to high quality.) These factors may also correlate with the cost of the concentrator.

E. EFFECTS OF FOCAL RATIO AND OVERALL SHAPE OF CONCENTRATOR

The effect of focal ratio or, equivalently, concentrator rim angle (Equation 12) upon collector efficiency is shown in Figure 10. According to this figure (Duff-Lamerio approximation) the efficiency is maximum at a focal ratio of about 0.43 (rim angle about 60°) for a mirror concentrator having an overall paraboloidal shape and at a focal ratio of about 0.22 (rim angle 67°) for a mirror or lens with an overall planar shape. These focal ratios (rim angles) are only approximate and depend on the approximations chosen for calculating the flux distribution near the focal point (Equations 7 and 8). For a more exact solution, a more exact method such as cone optics should be used. Such calculations (References 26 and 27) indicate that the focal ratio that provides maximum efficiency for an overall paraboloidal shape depends on the intercept factor and varies from a focal ratio of 0.6 (rim angle 45°) at an intercept factor close to 1.0 to a focal ratio of 0.4 or less (rim angle 65° or more) at intercept factors below 0.8 (Figure 11).

To show the effect of slope error upon the focal ratio giving maximum efficiency, the curves of Figure 10 are plotted for both σ_{slope} = 2 mrad and σ_{slope} = 10 mrad. The focal ratio for maximum efficiency is seen to be independent of slope error.

Figure 10 suggests that performance will be slightly better if the overall concentrator contour is flat rather than paraboloidal. This comparison is incomplete, however. If the flat concentrator is a Fresnel mirror, the individual facets will block some of the light reflected from adjacent facets, unless gaps are left between facets, and such gaps will reduce the effective concentrator area or the angles of illumination of the receiver aperture. (Alternatively, facet edges can be beveled to prevent blocking, but then sunlight striking the bevels will be reflected away from the receiver and so lost.) If the flat concentrator is a Fresnel lens, similar blocking effects will occur; but in addition one must consider spectral dispersion of the transmitted light and the fact that the effect of lens surface slope errors upon the angular deflection of the sunlight will generally be much less than that of mirror surface slope errors. Accordingly, examination of the effect of concentrator shape needs to be more detailed than that represented by Figure 10.

Other considerations may also influence the choice of focal ratio. A short focal ratio reduces the length, weight, and cost of structure to support the receiver and power conversion equipment. If the concentrator is a paraboloidal mirror, a short focal ratio means that the surface must be curved more sharply, which may increase fabrication difficulty and cost. If the concentrator is planar in overall shape, it will probably be impractical to obtain the very short focal lengths that Figure 10 suggests as desirable: practical simple lenses usually have focal ratios of 0.7 or more, and flat Fresnel mirrors with very short focal ratios have very high blockage or shadowing of facets by adjacent facets. Dish concentrator mirrors usually have focal ratios between 0.4 and 1.0, with 0.4 to 0.6 being most common.

F. EFFECTS OF RECEIVER TEMPERATURE

If the receiver temperature is increased, the thermal losses from the receiver of course increase. The re-radiation loss through the receiver aperture increases as the fourth power of the absolute temperature. The free convective loss out an open aperture probably also increases as the temperature to a power somewhat greater than one, though a linear approximation is used in

the computer model employed in this work. The forced convection (due to wind) and conduction losses increase approximately linearly with receiver temperature.

The result is that the collector efficiency falls as the receiver temperature is increased. Figure 12a illustrates this at fixed geometric concentration ratios. The efficiency fall-off is greater at low geometric concentration ratios. To reduce the receiver aperture losses, it is desirable to reduce the aperture size (increase the geometric concentration ratio): the geometric concentration ratio should be optimized separately at each temperature of interest (Figure 13). Even with this optimization, the collector efficiency continues to fall as the temperature rises and will eventually become zero at a temperature where the losses equal the solar energy into the receiver. This may be termed the "equilibrium temperature."

If the system produces only heat, the receiver temperature is dictated by the use that will be made of the heat. Because of the increase in receiver losses and in heat transport losses as the temperature rises, there is no advantage in running the receiver hotter than is required to satisfy the use. If, however, the heat is used to drive a heat engine for production of mechanical work or electricity, the effect of temperature upon engine performance must also be considered. The engine efficiency will almost always increase as the engine input temperature increases. The combination of collector efficiency decrease and engine efficiency increase as the temperature rises means that, for a given system, there is a receiver temperature at which the system efficiency is maximum. Thus, the temperature for maximum system efficiency may be optimized.

In Figure 14, the collector, power conversion, and system efficiencies are shown as functions of receiver temperature. These efficiencies are for a system in which the power conversion effectiveness is constant (power conversion efficiency a fixed fraction of the Carnot efficiency) and the receiver aperture is optimized separately at each temperature. Corresponding efficiency curves with a fixed intercept factor are shown in Figure 11. The system efficiency peak is evident in these figures. As for most dish systems, the peak is rather flat. In Figure 14, the peak ($\eta_{sys-max}$) occurs at

1000°C; the system efficiency is ($0.99\ \eta_{sys-max}$) at 850°C, ($0.98\ \eta_{sys-max}$) at 785°C, ($0.95\ \eta_{sys-max}$) at 675°C. Thus, the loss of system efficiency incurred by operating significantly below the peak may be rather small. An increase in operating temperature is likely to shorten equipment lifetime, increase maintenance and maintenance cost, require use of more expensive materials, etc. Thus, the optimum temperature on the basis of cost will usually be lower than that on the basis of efficiency.

For convenience, the T_r at which system efficiency η_{sys} peaks may be written as T_{max}, and the $T_r < T_{max}$ at which η_{sys} is i times $\eta_{sys-max}$ as T_i, where i = 0.99, 0.98, 0.95, 0.90,....

Figure 15 shows the combined effects of receiver temperature and mirror slope error upon collector and system efficiency, with the receiver aperture optimized at each temperature. The receiver temperature for peak system efficiency decreases greatly as slope error increases. To obtain high system efficiency, both low slope errors and high receiver temperatures are needed.

In dish collectors providing heat to engines, typical receiver temperatures currently range from 350°C (700°F) to 900°C (1650°F); receiver temperatures up to perhaps 1300°C (2400°F) are being discussed for future use (Reference 28). For process heat, dish collectors are being used for temperatures as low as 150°C (300°F) (Reference 29).

G. EFFECT OF ENGINE TYPE

The variation of power conversion efficiency with temperature depends on the engine type. Accordingly, the engine type affects the shape of the curve of system performance versus receiver or engine inlet temperature and the temperature at which system performance is maximum. This in turn influences the selection of the receiver aperture and of the concentrator to be used.

To a first approximation, the effectiveness of a Rankine or Stirling engine is independent of engine inlet temperature. The effectiveness (fraction of Carnot efficiency) may be as low as 0.2 for an engine with very low efficiency and perhaps as high as 0.6 for an engine with very high

efficiency, but these differences in effectiveness merely multiply the system efficiency by different constant factors; they do not change its shape, so do not change the collector optimization. Brayton engines, however, typically have an effectiveness that increases with increasing inlet temperature. (Their efficiency is a larger fraction of the Carnot efficiency at high inlet temperature than at low.) The Brayton system efficiency is therefore maximum at a higher inlet temperature than is that for Rankine or Stirling engines (Figures 16 and 17). This drives the receiver design toward higher receiver temperatures and, therefore, small receiver apertures (high geometric concentration ratios, Figure 18); this in turn drives the concentrator design toward higher performance (high reflectance, blocking factor, and intercept factor, and correspondingly low mirror and pointing errors, Figure 19).

Note that for the examples shown in Figures 16 and 17 the effectiveness-temperature relationship of a Brayton engine leads to a receiver temperature for maximum system efficiency, T_{max}, which is 330 to 400°C higher than that for an engine with constant effectiveness. The shapes of the peaks are almost identical. In the Brayton system, for example, the temperature at which the system efficiency reaches 0.99 of the peak efficiency ($T_{0.99}$) is 115-125°C below the peak temperature T_{max}, $T_{0.98}$ is 160-170°C below T_{max}, $T_{0.95}$ is 270-275°C below T_{max} and $T_{0.90}$ is 375-405°C below (see Figure 17). The corresponding numbers for constant-effectiveness systems, such as Rankine or Stirling, are 125-130, 185-190, 275-305, and 385-415°C. For the idealized and baseline systems $T_{0.90}$ is 345 to 410°C higher when the Brayton engine is used than when the engine has an effectiveness versus temperature curve characteristic of a Rankine or Stirling cycle. With the concentrators listed, the geometric concentration ratio, optimized at these receiver temperatures, is 3620 (idealized system) or 3250 (baseline system) with the Brayton engine; it is 2660 (idealized system) or 2480 (baseline system) with the Rankine or Stirling engines (Figures 16 and 17). An examination of the effect of changing slope error would show that a low concentrator slope error would provide a greater performance improvement with the Brayton engine than with the Rankine or Stirling.

In dish collector systems, the engine inlet temperature of Rankine engines is typically 350 to 600°C (700 to 1100°F), of Stirling engines 700

to 800°C (1300 to 1500°F), of Brayton engines 800 to 900°C (1500 to 1650°F); considerably higher temperatures are anticipated for future Brayton engines (see Reference 28). Receiver temperatures are slightly higher than engine inlet temperatures; the difference is usually less than 50°C (100°F).

H. EFFECT OF RECEIVER ABSORPTANCE AND RECEIVER LOSSES

Receiver radiative, convective, and conductive losses all enter into the collector energy balance (Equations 1 and 2) and so affect the receiver aperture optimization (Equations 18 and 19), as well as the temperature at which the system efficiency peaks if the system output is mechanical or electrical energy. Thus, the receiver emittance and coefficients of convection and conduction enter into the optimization. The receiver absorptance also enters into the optimization (Equations 1, 18, and 19).

Note, however, that the absorptance, α, and emittance, ϵ, in Equation 1 are the effective quantities for the receiver aperture. A cavity receiver is designed to approximate a black-body cavity, and the effective absorptance and emittance of its aperture tend to be high (typically above 0.95), even if the absorptance and emittance of the internal wall are not (Figure 20). Also, the absorptance and emittance tend to be coupled: for receiver temperatures of interest for point-focusing systems, it is difficult to find materials with high absorptance and low emittance. (The absorptance and emittance are not identical because they pertain to different wavelengths: the absorptance to the solar spectrum at the Earth's surface, which peaks at about 0.5 μm, and the emittance to the spectrum emitted by the receiver, which peaks at wavelengths varying from about 4.7 μm for a receiver temperature of 350°C (700°F) to 1.8 μm for a receiver temperature of 1300°C (2400°F). The receiver and solar spectrum overlap, however; hence the difficulty of finding materials with high absorptance for solar radiation and low emittance for receiver radiation.)

Point-focusing systems are occasionally designed with open flat or spherical receivers rather than with cavity receivers. Cavity receivers, however, are almost always used because they have two advantages:

(1) In a cavity receiver, the exposed area at receiver temperature for outgoing radiation and convection is no greater than the exposed area for incoming solar radiation (both are the receiver aperture area). This is generally not true for open receivers.

(2) The cavity design increases the effective absorptance as compared to that of an open receiver (see Figure 20). This improves performance (Equation 1). The effective emittance is also increased by the cavity design, but this is usually less important because since the first term in Equation (1), involving α, is larger than the term involving ϵ in any practical collector. (Q_c must be positive).

Because the effective absorptance and emittance of cavity receivers tend to be close to 1.0, differences encountered in these quantities among different cavity receiver designs do not have much effect on collector performance optimization (Table 3-4).

Convective losses from a receiver aperture are difficult to measure and there are no well-established theoretical expressions for them. Moreover, these losses change as the angle of the aperture to the horizontal changes during the day and as the wind speed and direction change (see Reference 31 for recent work on this problem). Table 3-4 gives an example of the effect of a change in aperture convective loss upon collector optimization. The effect of closing the receiver aperture with a window will be discussed in a subsequent section.

Conductive losses from the receiver depend on the dimensions and material of the receiver and can be significantly modified by changing the thickness and conductivity of the insulation between the cavity and the exterior of the receiver. Exterior characteristics affecting the losses from the outside of the receiver to the surroundings are probably less significant. An example of the effect of a difference in conductive loss upon collector performance optimization appears in Table 3-4.

In the examples of Table 3-4, halving the absorptance of the receiver cavity wall causes a slight drop in efficiency but has almost no effect on the

Table 3-4. Effect of Heat Transfer Coefficients Upon Collector Performance Optimization

Baseline system except as noted. Receiver aperture optimized at each temperature.

Baseline values: $\alpha = 0.982$, $\epsilon = 0.998$, $h_c = 16.0$ W/m^{2}K, $k = 0.737$ W/m^{2}K, $A_w/A = 0.015$, $T_r = 925^oC$

Coefficients	$T_r = 925^oC$				$T_r = T_{max}$					$T_r = T_{0.95}$				
	C	ϕ	η_{coll}	η_{sys}	T_{max} ^oC	C	ϕ	η_{coll}	η_{sys}	$T_{0.95}$ ^oC	C	ϕ	η_{coll}	η_{sys}
Baseline														
$\alpha_{wall} = 0.59$ $\epsilon_{wall} = 0.93$	2410	0.981	0.805	0.265	1295	3250	0.948	0.698	0.320	1025	2560	0.975	0.781	0.304
$\alpha_{wall} = 0.30$ $\alpha = 0.941$	2440	0.980	0.768	0.252	1295	3290	0.945	0.662	0.304	1015	2620	0.974	0.746	0.289
$\epsilon_{wall} = 0.46$ $\epsilon = 0.970$	2400	0.982	0.807	0.265	1300	3260	0.947	0.696	0.322	1030	2600	0.975	0.782	0.303
$\alpha_{wall} = 0.30$ $\alpha = 0.941$ $\epsilon_{wall} = 0.46$ $\epsilon = 0.970$	2420	0.981	0.770	0.253	1295	3260	0.947	0.666	0.305	1015	2600	0.974	0.748	0.289
$h_c = 32$ W/m^2	2480	0.979	0.797	0.262	1295	3310	0.945	0.690	0.317	1020	2660	0.973	0.774	0.301
$h_c = 80$ W/m^2	2660	0.973	0.776	0.255	1295	3490	0.936	0.667	0.306	1010	2820	0.967	0.755	0.291
$k = 1.474$	2410	0.981	0.792	0.260	1295	3250	0.948	0.680	0.312	1010	2580	0.976	0.771	0.297

temperature of maximum system performance (T_{max}) or on the optimum concentration ratio and intercept factor. Halving the emittance of the wall has negligible effect on performance or optimization. Doubling the convection coefficient increases the optimum geometric concentration ratio slightly but has no other appreciable effect on performance or optimization. Increasing the convection coefficient by a factor of 5 produces a further slight increase in optimum geometric concentration ratio and a slight drop in efficiency. Doubling the conduction coefficient causes a slight drop in efficiency with no appreciable effect on optimum temperature, concentration ratio, or intercept factor.

Typical cavity receiver efficiencies in dish collectors range from a low of about 0.6 to a high of 0.95 or greater. Because the receiver losses increase with temperature, high receiver efficiency is more likely to be attained at low rather than at high receiver temperature. Relatively high receiver efficiency for a given receiver temperature may be considered to indicate high receiver quality.

Typical dish collector efficiencies range from about 0.4, which would be considered low, to 0.9, which would be considered very high.

I. EFFECTS OF INSOLATION LEVEL AND PART-LOAD PERFORMANCE

The direct insolation, I, varies with site, time of day, time of year, and weather from a low of zero to a high of about 1,100 W/m^2 at the surface of the Earth. (It may occasionally be somewhat higher at high-altitude sites.) Typical insolation design points for dish collectors are 700 to 1,000 W/m^2.

Suppose a dish thermal system is operating at its design point and the insolation then falls, because of a change in weather. After a transient, the power output of the collector must fall to match the insolation. (The transient may be long if thermal storage is included in the collector. Storage is not considered here). If the collector is supplying process heat, this heat will usually be needed at a fixed temperature, so the operating strategy will probably be to keep the receiver temperature constant and vary the flow rate of the working fluid to match the insolation.

Suppose the collector is providing heat to a power converter. The thermal loss terms in Equation (3) vary inversely with the insolation, I, whereas the first term is independent of insolation. The curve of η_{coll} versus T_r will therefore fall and become steeper as the insolation I decreases (Figure 21). The curve of η_{pc} versus T_r remains unchanged, as, to a first approximation does the value of η_{pp}. The curve of η_{sys} versus T_r is the product of the curves for η_{coll}, η_{pc}, and η_{pp}. When the insolation falls, this curve will peak at a lower temperature than it does for high insolation (see Figure 21). If the system was initially operating at or near T_{max}, it will be desirable to drop T_r to match the new, lower, T_{max}. If, however, the system was initially running well below T_{max} (perhaps for reasons of cost), it may be desirable to continue running at this temperature rather than reduce T_r: presumably the T_r selected is satisfactory, and lowering it will only mean operation further from T_{max} and hence at still lower η_{sys}. This means that the mass flow rate of the working fluid should be reduced to match the insolation. Implications in turn depend on the design of the power conversion and power processing subsystems. For example, is the engine speed constrained to a constant multiple of 60 Hz to maintain synchronism with the electric grid? If both speed and inlet temperature must be kept constant, what can be varied to change the mass flow rate? In Stirling engines it is usually possible to change the operating pressure and hence the density of the working fluid. Some Brayton engines have guide vanes to change the flow impedance. In other engines no suitable operating parameter may be available, and it may be necessary to maintain speed and allow inlet temperature to fall, thus decreasing efficiency. The part-load performance of different engines varies and depends on the parameter used to accommodate load changes (temperature, speed, pressure, flow impedance). System optimization for part-load operation therefore depends heavily upon the power conditioning and power processing characteristics. Dish collector power systems may be shut down at direct insolation lower than 300 to 500 W/m^2 because the power produced is insufficient to supply system losses (unless the plant is provided with energy storage or can operate off fuel as well as sunlight.)

A dish module is often connected to a power sink that will accept all its output. If this is not so, and there is no provision for energy storage, it may be necessary, when demand is low or insolation high, to match the input

and output by lowering the system efficiency. This may be done by dumping energy from the power conversion or power processing subsystem, by reducing the receiver temperature (if this can be done), by permitting the receiver temperature to rise above T_{max} (if this is permissible), by pointing slightly off-sun (if this does not damage the receiver aperture plate) or, if necessary, by shutting down. If multiple modules are used to supply a common demand, it should be possible to shut down some and keep others running.

J. EFFECTS OF SECONDARY CONCENTRATOR

Figure 22 gives examples of collector and system efficiencies as functions of receiver temperature, with and without a secondary concentrator. The secondary concentrator provides an increase in geometric concentration ratio and, when the receiver aperture is optimized, an increase in intercept factor. This does not always increase collector efficiency, however. At low receiver temperatures and moderate secondary reflectance, the reflectance loss is greater than the improvement at the receiver aperture, and performance is better without the secondary than with it. At higher temperatures the receiver aperture losses are more important; if the receiver temperature and secondary reflectance are high enough, the secondary concentrator can improve performance.

Performance with a secondary concentrator is sensitive to the reflectance or transmittance of the secondary: note the difference between the performances of secondaries with reflectances 0.90 and 0.95 in Figures 22a and b. If a secondary is to be of help, it should have very high reflectance or transmittance.

The characteristics of the engine also enter into the tradeoff: Figure 21 is for a system that uses an engine whose effectiveness rises with receiver temperature. The performance of such a system tends to optimize at a fairly high receiver temperature, at which a secondary concentrator is likely to be advantageous. If the engine effectiveness did not rise with temperature, system performance would be maximum at a lower temperature, at which the secondary concentrator is less likely to be of use.

Figure 22 suggests that a secondary concentrator is more likely to be useful at long focal ratios than at short. Figure 23 compares the effects of focal ratio upon the performance of a simple and a compound concentrator. The collector efficiency with the simple paraboloidal mirror peaks at a focal ratio of 0.4-0.6, and falls markedly at longer focal ratios. With a secondary concentrator that provides maximum efficiency, the collector efficiency (Duff-Lameiro approximation) is almost constant over the whole range of f_r = 0.4-3.0. More exact calculations (References 22 and 23) indicate that the performance rises as the focal ratio increases (Figure 5). It may not, however, be desirable to go to a long focal length because of concentrator weight and cost considerations. These can sometimes be alleviated by using an optical configuration that folds the optical path after it leaves the primary mirror (Reference 12).

The overall geometric concentration ratio, optimized, is higher with the secondary concentrator than without, but the primary geometric concentration ratio of the compound concentrator is lower than that of the concentrator without secondary. The difference is, of course, due to the geometric concentration ratio of the secondary. The secondary concentration ratio optimizes only slightly above 1.0 at very short focal lengths (at which use of a concentrating secondary is unlikely to prove efficient). It optimizes at 10 or more at long focal lengths (see Figures 5 and 23).

It is of some interest to consider the effect of a secondary concentrator with primaries having various slope errors, specularity spread, or pointing error. As Figure 24 shows, a secondary concentrator is of more help when the accuracy of the primary is poor. In some cases, adding a secondary to a primary with moderate errors can provide performance equivalent to that of a more accurate primary alone.

Another consideration is that the reflectance loss at the secondary concentrator may not actually be a loss to the system. A small secondary, struck by all of the collected sunlight, will tend to heat well above ambient temperature. Depending on the system design, it may be advantageous to use the secondary concentrator to preheat the working fluid before it enters the receiver (or the recuperator of the power conversion subsystem). This permits

recovery of the solar energy lost in the secondary and at the same time provides active cooling of the secondary.

Figures 22 through 24 indicate that the use of a secondary concentrator is likely to improve performance only if the system can utilize to advantage a high receiver temperature or if the primary concentrator is somewhat inaccurate. The high receiver temperature may be used either to supply a demand for high-temperature process heat or to drive a heat engine whose performance increases markedly with inlet temperature.

K. EFFECTS OF WIND SCREENS AND INFRA-RED REFLECTORS

To reduce convective losses out the receiver aperture, a wind screen is sometimes used. The most common form is a portion of a cone (Figure 25a), with a cone angle at least as great as the rim angle of the concentrator. If such a screen does not extend beyond the shadow cast by the receiver and the power conversion equipment mounted with the receiver, it does not increase the blocking and shadowing factor. Quantitative data on the amount by which such a screen reduces convective loss are scarce.

An alternative is a portion of a sphere centered at the receiver aperture (Figure 25b) and confined to angles greater than the rim angle of the concentrator. This may be less effective aerodynamically than the cone in reducing convective losses, though data on losses from such shapes are almost non-existent. On the other hand, the spherical screen can serve another purpose: reducing radiative losses from the receiver aperture by reflecting some of the emitted radiation back into the aperture. To do this, the interior of the screen should have high reflectance in the near infrared (wavelengths of a few microns). Because of its spherical shape, if the screen is a perfect reflector, almost all the radiation from the aperture that strikes the screen will be reflected back into the aperture. If the concentrator rim angle is 60°, a screen outside of it will subtend 0.5 of a hemispherical solid angle and so could reflect back almost 0.5 of the emitted radiation. If the rim angle is 45°, the screen solid angle can be 0.7 of a hemisphere and so could reflect back almost 0.7 of the emitted radiation. Because cavity receivers are not black bodies, these limits are only

approximate; a more exact calculation would take into account the distribution of radiation within the receiver cavity.

The conical wind screen of Figure 25a is not very useful as an infrared reflector because the view angle of the receiver aperture, as seen from screen, is poor, and specular reflection at the screen will not return emitted radiation to the receiver. This conical design can, however, double as a secondary concentrator (see Figure 4b).

L. EFFECTS OF WINDOWS

In the discussion so far, it has been tacitly assumed that the receiver aperture is open to the air. The aperture may, however, be closed by a window. Sometimes the receiver cavity is designed to contain the working fluid, and it is undesirable to let this fluid escape out the aperture or to let cold air enter and mix with the working fluid. Another reason for a window is to eliminate convective heat loss out the receiver aperture. This advantage must then be traded against the loss of entering sunlight due to reflection and absorption by the window.

This is a difficult trade-off because data and theory for convective loss have not been adequate. The window loss is ordinarily 8% of the incoming sunlight or more, depending on the thickness and composition of the window. (Anti-reflection treatment may be useful.) A window to prevent convective heat loss may be justified if the convective loss without the window is higher than the window loss. The window also reduces the loss of outgoing radiation from the receiver, but this is usually a smaller effect. As the receiver temperature is increased, the loss per unit area of receiver aperature also increases. On the other hand, the receiver aperture size is usually decreased as the temperature rises; this tends to reduce loss out the aperture. It seems clear, however, that the usefulness of a window is greater at high receiver temperature than at low.

In the example shown in Figure 26, the collector and system efficiency above 900°C (1650°F) are higher with a window than without. Below 900°C efficiency is higher without a window.

The receiver temperature at which the system efficiency is greatest tends to be higher with a window than without one (see Figure 26). The window reduces the effect of temperature on receiver efficiency; the curve of system efficiency versus temperature is then more influenced by the engine efficiency, which tends to rise with engine inlet and receiver temperature.

A window is more likely to be advantageous when the concentrator errors are high because high concentrator errors lead to use of a large receiver aperture, and so to high convective loss if the aperture is open. In the example of Figure 27, collector efficiency with a slope error of 0.5 mrad is higher without a window than with one, over the entire range of temperatures examined (700° to 1450°C, 1300 to 2650°F); with a slope error of 5 mrad, the opposite is true.

It would be helpful to tailor the window's spectral characteristics to permit high inward transmission of solar radiation but low outward transmission of infra-red radiation from the receiver (Reference 33). Ideally, the window should reflect wavelengths longer than 2 or 3 μm. So far, no materials have shown to have both these desired spectral characteristics and adequate high temperature properties. Fused silica, though not a good infrared reflector, does absorb a significant fraction of the infrared radiation emitted at receiver temperatures, while transmitting almost all the solar radiation; the infrared absorption improves the performance of fused silica as a receiver window.

M. SYSTEM CONSIDERATIONS

As should be clear from the above, the performance optimization that can be done considering the collector alone is rather limited. We can optimize the focal length for a simple concentrator. We can optimize the receiver aperture if the required temperature for the working fluid is specified for a process heat demand, if the concentrator errors are fixed by manufacturing tolerances, and if the expected insolation is defined. Performance optimization beyond this generally requires that the rest of the solar thermal system be considered. If the system is to produce mechanical or electrical power, the efficiency of the engine as a function of inlet temperature and

part load will have to be considered in optimizing the receiver temperature and hence the receiver aperture. The pointing error of the concentrator affects collector optimization but is in turn affected by the design and optimization of the control subsystem. Clearly, it is desirable to optimize the performance of the entire solar thermal system and not of the collector alone.

Considerations other than efficiency and initial cost (discussed below) affect dish collector design. High receiver temperatures exacerbate problems of lifetime, reliability, maintenance, and the availability of suitable materials; the receiver is, therefore, usually designed to operate at a temperature lower than that at which efficiency is maximum. To reduce the heat flux on the lip of the receiver aperture, the aperture size may be increased beyond that at which efficiency is optimum. The choice of focal length may be influenced not only by efficiency but also by a trade-off between the additional length and structural weight required for a long focal length and the additional mirror area required for a fixed projected area when the focal length is very short. The latter is illustrated in Figure 28 for a paraboloidal mirror. Note that at focal ratio 0.6 the ratio of mirror area to projected area is 1.04, but for incremental area at the rim, the ratio is about 1.08. At a focal ratio of 0.4, the ratio of areas is 1.09, the ratio of incremental areas about 1.18. The corresponding equations are:

$$\frac{A_s}{A} = \frac{2}{3}\frac{1}{\sin^2\theta}\left[2\sqrt{2\,(1+\cos\theta)} - (1+\cos\theta)^2\right] \qquad (31)$$

$$\frac{dA_s}{dA} = \sqrt{\frac{2}{1+\cos\theta}} \qquad (32)$$

where A_s = surface area of the mirror.

SECTION IV

METHODS FOR COST OPTIMIZATION

Cost optimization is often more important, in principle, than performance optimization. Cost optimization of dish solar collectors and of dish solar thermal systems tends to be difficult in practice because of the lack of reliable cost data. Hardly any dish collectors are beyond the prototype stage. Costs or prices in volume production are therefore only estimates; costs of operation and maintenance are even more uncertain. To obtain meaningful information on the cost differential between, for example, a concentrator with a slope error of 2 mrad and a concentrator with a slope error of 4 mrad is almost impossible at present. Still more difficult is knowing how this differential varies with the production rate.

In the absence of useful data on the effect of design variables upon collector costs, this discussion is limited to cost trade-offs in which the collector cost and collector efficiency are assumed to be known. The results can be examined in terms of how much the purchaser of a solar thermal system would find it worthwhile to pay for certain desired characteristics.

A. BASIS FOR COST OPTIMIZATION

There is no point in optimizing on a collector or system cost alone because an inexpensive system that has zero performance is of no use. One may utilize a measure of cost/output ratio, such as mills/kW-h (electrical or thermal), or the invested $/kW of installed capacity. Costs to be considered include not only the price of a purchased concentrator but also such factors as transportation costs, cost of site and installation, costs of operation, maintenance, and replacement over the life of the plant. Energy cost and capacity cost are not the only important cost parameters: for instance, it may be worthwhile to increase the availablity of solar power over the year even if the cost per kilowatt-hour and the cost per kilowatt of installed capacity are thereby increased. In this paper, however, I use as a cost parameter for optimization the busbar energy cost (BBEC) in either of two variations. One

is the levelized busbar energy cost (abbreviated as $\overline{BBEC}$, where the overlining signifies "levelized"). This is the measure most commonly used by utility companies to evaluate alternative plant designs, and represents the fixed revenue per kilowatt-hour that a utility must receive for the energy produced by the plant during its lifetime in order to just cover the utility's lifetime costs for the plant. $\overline{BBEC}$ assumes revenue is a fixed number of dollars (or cents, or mills) despite the inflation that is assumed to take place in costs. The other variation is <u>real</u> levelized busbar energy cost ($BBEC_o$), which is the corresponding fixed revenue in <u>real</u> (non-inflated) dollars, and assumes that the actual number of current-year dollars received will inflate at the general inflation rate. $BBEC_o$ has some advantages over $\overline{BBEC}$ (Reference 34), including much less sensitivity to the inflation rate assumed to apply over the lifetime of the plant. The choice of $\overline{BBEC}$ or $BBEC_o$ has no significant effect on the optimizations discussed in this report, and energy costs in this report are given in terms of both. See Reference 35 for further discussion of busbar energy cost and how to calculate it. Though BBEC is most widely used for the cost of electrical energy, it can be used equally well for the cost of thermal energy.

B. COST CALCULATION AND OPTIMIZATION

Costs were calculated using the model for utility-owned solar power systems described by Doane, et al, in Reference 35. The quantities calculated were the levelized busbar energy costs, $\overline{BBEC}$ and $BBEC_o$. The economic assumptions are listed in Appendix A.

To reduce computing time and expense, cost sensitivities derived by Revere (see Reference 24) were used. These sensitivities, together with the baseline system to which they refer, are also described in Appendix A.

SECTION V

RESULTS OF COST OPTIMIZATION

A. EFFECT OF COLLECTOR COST

As Figure 29 indicates, the concentrator cost is expected to be the largest single item of capital cost in a dish solar thermal power system when produced in quantity. The collector (concentrator plus receiver) cost is typically projected as near 50% of the total capital cost.

Figure 30 shows estimated operations and maintenance (O&M) costs for the same system as Figure 29. Concentrator maintenance is the largest single item of O&M, typically projected near 40% of the total O&M. Note too that O&M costs are quite significant: in this example, such costs are more than 50% of the capital costs, over the 30-year design lifetime of the plant. (This is in constant (real) dollars. In current dollars, with the assumed cost escalation (inflation; see Appendix), O&M would be almost 150% of the capital cost.)

Since collector costs represent such a large portion of total plant costs, they have a strong effect upon the cost of the electricity produced. In the example given, a 1% increase in collector costs raises the cost of the electricity produced by 0.64% (Figure 31).

B. EFFECTS OF COLLECTOR PERFORMANCE

If the output is constant but the collector efficiency is decreased, the concentrator aperture area must be increased to gather more sunlight. This tends to increase the concentrator cost (initial and O&M) per unit of output. The same is true if the concentrator area is held constant and the output is allowed to fall. Figure 31 gives an example. For the system considered, a 1% decrease in collector efficiency increases the busbar energy cost by 2.0%.

The trade-off between collector efficiency and collector unit price can be examined by considering the collector efficiency and unit price for each

(fixed) BBEC. This is clarified in Figure 32. For the baseline system illustrated, with a collector efficiency of 0.80, the trade-off is: a 1% decrease in collector efficiency requires a 0.32% decrease in collector cost to maintain the same BBEC. At lower collector efficiencies, larger decreases in collector costs are needed for each percent decrease in collector efficiency; below some finite collector efficiency, the BBEC cannot be maintained even if the collector is free.

Figures 33 and 34 show the corresponding effect of optical efficiency alone (rather than collector efficiency), together with the effect of collector price and the corresponding trade-off. Figures 35 and 36 show the relations in terms of slope error, geometric concentration factor, and collector price for the same (baseline) system. If the slope error is too large, the BBEC cannot be attained no matter how low the concentrator cost. Figure 37 illustrates the effects of optical efficiency and of geometric concentration ratio upon BBEC; Figure 36 shows the trade-off between them.

C. EFFECT OF TEMPERATURE

If the system produces electrical or mechanical power, and the receiver and engine inlet temperatures are changed, both the collector efficiency and the power conversion efficiency are affected, as discussed earlier. The change in collector efficiency changes the required concentrator area and, therefore, the concentrator price; the change in power conversion efficiency changes the required size of concentrator, receiver, and engine. This affects prices for all of these elements. Furthermore, an increase in operating temperature will often require changes in the design and materials of the receiver and engine that in turn affect their prices. Also, with an engine and receiver of a given type, an increase in operating temperature is likely to lead to increased maintenance costs and perhaps lowered reliability and availability. These last factors are highly dependent upon the design. Because it is difficult to assign them general quantitative values, these factors will not be treated in this report. Some design variables, such as receiver aperture (geometric concentration ratio), will probably not have a significant effect on equipment price or maintenance cost.

Figure 39 illustrates the effect of geometric concentration ratio and slope error upon the busbar energy cost at various receiver temperatures for the baseline system. The effects of the independent variables upon subsystem efficiencies and of these efficiencies upon system costs are modeled, but effects upon cost of design, material and maintenance changes appropriate to the different temperatures are not. Figure 39 should therefore be used with caution. For the assumption made in constructing this figure, namely, that equipment and maintenance costs are not raised by low slope error or high receiver temperature, $\overline{BBEC}$ at the optimum temperature falls from 204 mills/kW-h at 10-mrad slope error to 122 mills/kW-h at 5 mrad and about 70 mills at 0.5 mrad; a $\overline{BBEC}$ of 200 mills/kW-h cannot be obtained if the slope error is 10 mrad. The optimum receiver temperature rises from about 700°C (1300°F) at 10 mrad to 925°C (1700°F) at 5 mrad and 1500°C (2730°F) or more at 0.5 mrad.

D. EFFECT OF MODULE SIZE

The effect of collector size upon the unit cost of the heat output should be considered. The price of the concentrator drive is not proportional to its size but tends to vary less strongly than the size. The price of controls for the collector itself is almost independent of collector size. For very small collectors, the price of drive and controls is high relative to the energy output and increases the cost of this energy. For very large dish collectors, the cost of structure becomes limiting: the area and the energy output increase as the square of the linear dimension; the weight and the cost of structure increase as the cube. There is accordingly a collector size that minimizes the cost of the thermal energy produced. For designs evaluated so far, this minimum occurs at diameters of 5 to 15 m. It is, however, very flat, so the cost of the thermal output is rather insensitive to collector size within this range.

To examine the collector alone may, however, lead to sub-optimization; the whole system should be considered. Parabolic dish solar power plants are comprised of modules, each of which consists of a collector, an associated engine-generator if one is used, and associated power processing equipment, cabling, and controls. Because these plants are so modular, the plant size

has little effect upon the selection of collector size (unless the plant is so small that only a single small collector is needed.) There are some economies of scale in the central station that are common to all the modules and includes elements of the power processing subsystem (such as switchgear and central inverters) and of the control subsystem; again this does not affect collector optimization. At the module level, however, if the plant produces electricity or mechanical work, the power conversion subsystem interacts with collector optimization. If there is a separate heat engine for each module, the size of the collector must match the size of the heat engine. Small heat engines tend to be less efficient than larger engines and almost always cost more per unit of output. To a lesser extent, this is also true for generators. If one were optimizing the power conversion subsystem alone, the optimum would probably be a large unit, perhaps a single large unit for the whole plant. If the size of the power conversion subsystem is to match that of the collector, it will tend to drive the collector to a size somewhat larger than the optimum for the collector considered alone. The size optimum is dependent on the efficiencies that can be obtained in engines of 5 to 15 kW; until now there has been little incentive to attain high efficiency in such small engines. The engine price is less important because it is typically small compared to the collector cost (Figure 21); engine O&M costs may or may not be important. For the baseline system used as an example, a 1% increase in power conversion efficiency decreases the busbar energy cost by 1%; a 1% increase in price of the power conversion subsystem increases BBEC by 0.11%.

REFERENCES

1. Jaffe, L. D., Dish Concentrators for Solar Thermal Power Systems: Status and Technological Development, Technical Report 81-43, Jet Propulsion Laboratory, Pasadena, California, January 1, 1981. Also, Preprint AIAA-81-2530, 2nd Terrestrial Energy Systems Conference, December 1981, Colorado Springs, Colorado. Accepted for publication, Journal of Energy.

2. Owen, W., Bank, H., Otth, D., Wright, C., and Hagen, T., "First Results of Steam Receiver Testing at JPL's Parabolic Dish Test Site," Proceedings 1981 Annual Meeting, American Section, International Solar Energy Society, pp. 415-418.

3. Hanseth, E. J., "Development, Solar Test, and Evaluation of a High-Temperature Air Receiver for Point-Focusing Parabolic Dish Applications," 2nd Terrestrial Energy Systems Conference, AIAA, December 1981, Colorado Springs, Colorado.

4. Osborn, D. B., Haskins, H. J., Conway W. A., and Wen, C. C., "Design and Test of a Solar Receiver for an Organic Rankine Cycle Engine," Proceedings ASME Solar Energy Div., 4th Annual Conference, Albuquerque, New Mexico, April 1981, pp. 449-457.

5. Lof, G. O. G., and Duffie, J. A., "Optimization of Focusing Solar Collector Design," Journal of Engineering for Power, Volume 85, pp. 221-228, 1963.

6. Selcuk, M. K., and Ward, G. T., "Optimization of Solar Terrestrial Power Production Using Heat Engines," Journal of Engineering for Power, Volume 92, pp. 173-181, 1970.

7. Duff, W. S., Lameiro, G. F., and Lof, G. O. G., "Parametric Performance and Cost Models for Solar Concentrators," Solar Energy, Volume 17, pp. 47-58, 1975.

8. Howell J. R., and Bannerot, R. B., "Optimum Solar Collector Operation for Maximizing Cycle Work Output," Solar Energy, Volume 19, pp. 149-153, 1977.

9. Wen, L., "Thermal Performance Trade-offs for Point-Focusing Solar Collectors," Proceedings Intersociety Energy Conversion Engineering Conference, San Diego, California, August 1978.

10. Wen, L., "Effect of Optical Surface Properties on High-Temperature Solar Thermal Energy Conversion," Journal of Energy, Volume 3, pp. 82-89, 1979.

11. Wu, Y. C., and Wen, L. C., "Solar Receiver Performance of Point-Focusing Collector System," ASME Preprint 78-WA/Sol-5, American Society of Mechanical Engineers, New York, 1978.

12. Pons, R. L., "Optimization of a Point-Focusing Distributed Receiver Solar Thermal Electric System," ASME Preprint 79-WA/Sol-11, American Society of Mechanical Engineers, New York, 1979.

13. Duff, W. S., and Lameiro, G. F., "A Performance Comparison Method for Solar Concentrators," Paper 74-WA/Sol-4, ASME Winter Annual Meeting, New York, November 1974.

14. Zakhodov, R. A., "Calculation of the Energy Distribution in the Radiation Field of Reflector-Type Solar Energy Devices," Geliotekhnika, Volume 1, No. 5, pp. 11-18, 1965.

15. Grilikhes, V. A., and Zakhodov, R. A., "Derivation of the Equation of Irradiance Distribution in the Focal Plane of Parabolodial Solar Concentrators," Geliotekhnika, Volume 7, No. 4, pp. 9-13, 1971.

16. Clark, T. B., "Comparisons and Results of Optical Analysis Techniques," Technical Report SCSE-013, Ford Aerospace & Communications Corporation, Newport Beach, California, 1978.

17. Pettit, R. B., "Characterization of the Reflected Beam Profile of Solar Mirror Materials," Solar Energy, Volume 19, pp. 733-741, (1977).

18. Wen, L., Huang, L., Poon, P., and Carley, W., "Comparative Study of Solar Optics for Parabolic Concentrators," Journal of Solar Energy Engineering, Volume 102, pp. 305-315, 1980.

19. Jaffe, L. D., and Poon, P., Secondary and Compound Concentrators for Parabolic Dish Solar Thermal Power Systems, DOE/JPL - 1060-43, 1981.

20. Jaffe, L. D., and Poon, P., "Secondary and Compound Concentrators for Parabolic Dish Solar Thermal Power Systems," Proceedings, 16th Intersociety Energy Conversion Engineering Conference, Volume 2, pp. 1752-1758, ASME, New York.

21. Welford W. T., and Winston, R., The Optics of Nonimaging Concentrators, Academic Press, New York, 1978.

22. Baranov, V. K., "Paraboloitoric Focone as Secondary Solar Energy Concentrator," Geliotekhnika, Volume 13, No. 5, pp. 18-25 (1977).

23. Welford, W. T., and Winston, R., "Design of Second Stage Nonimaging Concentrators," University of Chicago, Report to JPL (1979).

24. Revere, W., "System Influence Coefficients of Solar Thermal Power Systems," JPL private communication, February 29, 1980.

25. Rosenberg, L., and Revere, W., A Comparative Assessment of Solar Thermal Electric Power Plants in the 1-10 MWe Range, Technical Report 81-53, Jet Propulsion Laboratory, Pasadena, California, June 1981.

26. O'Neill, M. J., and Hudson, S. L., "Optical Analysis of Paraboloidal Solar Concentrators," Proceedings 1978 Annual Meeting, American Section, International Solar Energy Society, Volume 2.1, pp. 855-862.

27. Schrenk, G. L., in Clark, T. B., "Flux Distributions and Intercept Factors at the Focal Plane of Parabolic Reflectors," Technical Report SP3-010, Ford Aerospace and Communications Corporation, Newport Beach, California, 1978.

28. Pham, H. Q., and Jaffe, L. D., "Heat Engine Development for Solar Thermal Power Systems," Proceedings, 3rd Annual Conference on Systems Simulation, Economics Analysis/Solar Heating and Cooling Operational Results, Reno, Nevada, April 27-May 1 1981, ASME, New York, pp. 654-659.

29. Hauger, J. S., "A Fresnel Collector Process Heat Experiment at Capitol Concrete Products," Parabolic Dish Solar Thermal Power Annual Program Review Proceedings, DOE/JPL 1060-46, May 1981, pp. 217-221.

30. Heller, J., and Hyland, R. E., NASA Lewis Research Center, personal communication, 1980.

31. LeQuere, P., Penot, F., and Mirenayat, M., "Experimental Study of Heat Loss Through Natural Convection from an Isothermal Cubic Open Cavity," Proceedings DOE/SERI/SNLL Workshop on Convective Losses from Solar Receivers, Sandia Laboratory Report SAND81-8014, Livermore, California, October 1981, pp. 165-174. Also, Clausing, A. M., "An Analysis of Convective Losses from Cavity Solar Central Receivers," Solar Energy, Vol. 17, pp. 295-300, 1981.

32. Sanders Associates, Parabolic Dish Module Program Review #2, Doc. 82-LMK-011, Merrimack, New Hampshire, March 1982.

33. Jarvinen, P. K., "Heat Mirrored Solar Energy Receivers," AIAA Preprint 77-728, American Institute of Aeronautics and Astronautics, New York, 1977.

34. Chamberlain, R. G., internal communication, JPL, September, 1980.

35. Doane, J. W., O'Toole, R. P., Chamberlain, R. G., Bos P. B., and Maycock, P. D., The Cost of Energy from Utility-Owned Solar Electric Systems, A Required Revenue Methodology for ERDA/EPRI Evaluations, ERDA/JPL 1012-76/3, JPL Technical Report 5040-29, Jet Propulsion Laboratory, California Institute of Technology, Pasadena, California, June 1976.

36. Revere, W., JPL, private communication, 1981.

APPENDIX A

ASSUMPTIONS FOR COST CALCULATIONS

Cost calculations were based on those of Rosenberg and Revere (see Reference 25) and of Revere (Ref. 24). The economic assumptions were (see Reference 25):

Ownership	:	Investor-owned utility
Plant lifetime	:	30 yr
Cost of capital (discount rate)	:	0.086/yr
General escalation (inflation) rate	:	0.060/yr
Capital cost escalation rate	:	0.060/yr
Operating and maintenance cost escalation rate	:	0.070/yr
Effective income tax rate	:	0.40/yr
(Miscellaneous tax rate)/ (capital investment)	:	0.020/yr
(Insurance premiums)/ (capital investment)	:	0.0025/yr
Base year	:	1978
Year of commercial operation	:	1989-1990
Plant construction period	:	2 years (2/3 1988; 1/3 1989)

Revere (see Reference 24) derived cost sensitivities for the following baseline system:

Type of system:	Parabolic dish concentrator
	Brayton power conversion
	Output: electricity
Plant size:	5 MW electric
Storage:	None
η_{coll} =	0.74 (annual average)
η_{pc} =	0.28 (annual average)
η_{pp} =	0.95

The costs assumed for this baseline system, in 1978 $/m^2 of concentrator aperture area, were (see Reference 25):

Capital costs, installed:

Concentrator, including foundation ($18)	$86.00
Receiver and receiver support	17.00
Power conversion	34.30
Electrical transport	13.24
Controls and cables	15.00
Land & site preparation	15.28
Buildings	23.00
Architect-Engineer & construction management	0.10 x installed capital cost
Construction management	0.10 x installed capital cost
Shipping	0.015 x equipment price
Initial spares	0.05 x equipment price
TOTAL (rounded)	260.

Operating and maintenance

Operation	$0.35/yr
Concentrator maintenance	1.81
Power conversion maintenance	1.09
Controls maintenance	0.28
Buildings & ground maintenance	0.90
TOTAL	4.43

The $\overline{BBEC}$ calculated (see Reference 25) for this baseline system was 89 mills/kW-h (in 1978 $). This is at a capacity factor of 0.31, which was found to be optimum for the plant. [Capacity factor = (electrical energy produced per year)/(electrical energy produced if operating continuously at rated power for one year).] The corresponding $BBEC_o$ is 45 mills/kW-h (1978 $).

Revere (see References 24 and 36) derived the following influence coefficients for deviations from the baseline system:

> Concentrator or receiver cost delta of $\$1.804/m^2$ increases $\overline{BBEC}$ by 1 mill/kW-h.
>
> Delta in average collector efficiency of 0.566% decreases $\overline{BBEC}$ by 1 mill/kW-h (1978 $).
>
> Power conversion cost delta of $\$3.53/m^2$ increases $\overline{BBEC}$ by 1 mill/kW-h.
>
> Delta in average power conversion efficiency of 0.360% decreases $\overline{BBEC}$ by 1 mill/kW-h (1978 $).

For this work, all costs were converted to 1980 $, using a factor of 1.185 for escalation from 1978 to 1980.

Also, the effect of a change in efficiency upon BBEC is more appropriately expressed as a multiplicative rather than an additive change:

$$\frac{BBEC_2/BBEC_1}{\eta_{coll,1}/\eta_{coll,2}} = \frac{88/89}{0.74/0.74566} = 0.996 \simeq 1.00$$

$$\frac{BBEC_2/BBEC_1}{\eta_{pc,1}/\eta_{pc,2}} = \frac{88/89}{0.28/0.2836} = 1.001 \simeq 1.00$$

The ratio $BBEC_o/\overline{BBEC}$ for the stated economic assumptions is 0.506.

APPENDIX B
FIGURES

FIGURE CAPTIONS

Fig. 1 Dish solar collector: geometry.

Fig. 2 Size of focal spot vs. rim angle and focal ratio.

Compare Duff-Lameiro (Ref. 13) and Aparisi (Refs. 14, 15) approximations for paraboloidal mirrors. Also shown is Duff-Lameiro approximation for planar concentrators. All are for cavity or flat receivers.

Fig. 3 Geometric concentration ratio attainable for paraboloidal mirrors as function of slope error or size of focal spot and intercept factor.

Focal ratio $f_r = 0.5$. Angular spread of incoming direct sunlight, σ_{sun}, taken as 2.3 mrad. Specularity spread, σ_ω, and pointing error, σ_p, taken as 0.0. Thus

$$\delta^2 = (2\ \sigma_{slope})^2 + 2.3^2\ \text{mrad}^2$$

Focal spot relative size, σ_f, given by Duff-Lamiero approximation (Eq. 7).

Fig. 4 Examples of secondary concentrators to improve optical performance.

a) Fresnel lens
b) Conical (truncated, Axicon)
c) Compound elliptic concentrator
d) Hyperbolic trumpet

Fig. 5 Effect of focal ratio upon attainable geometric concentration ratio of single and compound concentrators.

Rectangular distribution of slope errors. Intercept factor = 1.0.

Adapted from Baranov (Ref. 22).

Fig. 6 Effect of optical performance upon collector efficiency.

Intercept factor constant for each system.

a) Idealized system, except as noted
b) Baseline system, except as noted

Fig. 7 Receiver aperture optimization.

a) Idealized system
b) Baseline system

Fig. 8 Effect of concentrator slope errors upon collector efficiency and intercept factor. Dotted line: receiver aperture optimized.

a) Idealized system
b) Baseline system

Fig. 9 Effect of specularity spread upon collector efficiency and intercept factor. Dotted line: receiver aperture optimized.

a) Idealized system
b) Baseline system

Fig. 10 Effect of focal ratio or rim angle upon collector efficiency.

Receiver aperture optimized for each focal ratio (or rim angle). Duff-Lameiro approximation. Idealized system.

Fig. 11 Effect of rim angle and geometric concentration ratio upon intercept factor.

Flat solar disk profile, diameter 32 arc minutes. Paraboloidal mirror, reflectance 1.0, slope error 3 arc minutes, no other errors.

After O'Neill and Hudson (Ref. 26).

Fig. 12 Effect of receiver temperature and geometric concentration ratio upon collector, power conversion and system efficiency.

Idealized system, except as noted; constant intercept factor (ϕ = 0.98), constant power conversion effectiveness.

a) Collector efficiency
b) Power conversion and system efficiency

Fig. 13 Effect of receiver temperature on collector efficiency, with and without optimization of receiver aperture at each temperature.

Idealized system except as noted.

Fig. 14 Effect of receiver temperature on collector, power conversion, and system efficiency.

Receiver aperture optimized at each temperature. Idealized system except as noted. Constant power conversion effectiveness.

Fig. 15 Effect of receiver temperature and concentrator slope error upon efficiency.

Idealized system except as noted. Receiver aperture optimized at each temperature. Constant power conversion effectiveness.

a) Collector efficiency
b) Power conversion and system efficiency

Fig. 16 Effect of receiver temperature on power conversion and system efficiency with engines of differing characteristics.

Idealized system, except as noted. Receiver aperture optimized at each temperature.

Constant power conversion effectiveness is characteristic of Rankine and Stirling systems. The numerical value of the effectiveness (here taken as v = 0.5) depends on the particular engine.

Brayton systems characteristically have an engine effectiveness that increases with engine inlet temperature. Brayton power conversion efficiencies shown here are based on engine efficiencies from Ref. 30 and alternator plus rectifier efficiency of 0.92.

a) Collector, power conversion, and system efficiencies.
b) System efficiency as fraction of maximum system efficiency; geometric concentration ratio; and intercept factor.

Fig. 17 Effect of receiver temperature on collector, power conversion, and system efficiencies with engines of differing characteristics.

Baseline system, except as noted. Other characteristics as in Fig. 16.

a) Collector, power conversion, and system efficiencies.
b) System efficiency as a fraction of maximum system efficiency; geometric concentration ratio; and intercept factor.

Fig. 18 Effect of receiver temperature and geometric concentration ratio upon collector and system efficiency.

Fixed intercept factor. Baseline system except as noted. Brayton power conversion effectiveness as in Fig. 16.

a) Collector efficiency
b) Power conversion and system efficiency

Fig. 19 Effect of receiver temperature and concentrator slope error upon efficiency.

Receiver aperture optimized at each temperature. Baseline system except as noted. Brayton power conversion efficiencies as in Fig. 16.

a) Collector efficiency
b) Power conversion and system efficiency

Fig. 20 Effective absorptance or emittance of receiver aperture vs. absorptance or emittance of interior wall for a cavity receiver. (Holraum approximation: aperture area small compared to total surface of cavity.)

Fig. 21 Effect of insolation level upon optimization of receiver temperature.

Receiver aperture optimized at each temperature. Idealized system.

Fig. 22 Effect of secondary concentrator on collector and system performance.

Baseline system except as noted. Focal ratios 0.6 and 1.0.

Secondary concentrator reflectances 0.90 and 0.95. Exit aperture of secondary concentrator coincident with receiver aperture. Secondary geometric concentration ratio maximized at each focal ratio of the primary concentrator (1.96 at $f_r = 0.6$; 4.43 at $f_r = 1.0$).

Receiver aperture (= secondary concentrator exit aperture) optimized at each temperature for each design.

a) Collector efficiency
b) System efficiency
c) Overall geometric concentration ratio
d) Intercept factor.

Fig. 23 Effect of focal ratio upon performance of simple and compound concentrators.

Based on Duff-Lameiro approximation for primary (Ref. 13). Idealized system except as noted.

Secondary concentrator reflectance 0.95. Exit aperture of secondary concentrator coincident with receiver aperture. Secondary geometric concentration ratio maximized at each focal ratio of the primary concentration.

Receiver aperture optimized for each design. Receiver temperature 1350°C (2460°F).

a) Collector efficiency.
b) Geometric concentration ratio and intercept factor.

Fig. 24 Effect of secondary concentrator on performance with primary concentrators of various accuracy.

Collector characteristics as for Fig. 23. Focal ratio 0.6.

a) Collector efficiency.
b) Geometric concentration ratio and intercept factor.

Fig. 25 Wind screens and infrared reflector.

a) Conical wind screen. Can also serve as secondary concentrator: compare Fig. 4b.
b) Spherical section wind screen. Can also serve as infrared reflector to return emitted radiation to receiver.

Fig. 26 Effect of window on collector performance at various concentrator slope errors and receiver temperatures.

Receiver aperture optimized. Baseline system, except as noted. With window, effective receiver absorptance 0.92 (due to reflection), convection coefficient 0.0, effective emittance 0.236, 0.245, 0.261, 0.288, 0.305, 0.322, 0.339, 0.356 at 704, 760, 871, 982, 1093, 1204, 1316, 1427°C respectively (based on data of Ref. 32.)

Fig. 27 Effect of receiver temperature on collector and system performance with and without a window.

Receiver aperture optimized. Baseline system except as noted. Receiver loss coefficients with window: same as for Fig. 26. Brayton power conversion effectiveness as in Fig. 16.

Fig. 28 Effect of focal ratio upon ratio of concentrator area to projected concentrator area.

Projection parallel to sun line. Paraboloidal reflector.

Fig. 29 Distribution of capital costs for solar thermal power plant. (Projected.)

System type: dish-Brayton electric. Production rate: 25,000 modules per year. Plant size: 5 MWe.

Based on data of Ref. 25.

Fig. 30 Distribution of operations and maintenance costs for solar thermal power plant as percent of total cost in constant dollars. (Projected.)

Same plant as Fig. 29. Plant lifetime 30 years.

Based on data of Ref. 25.

Fig. 31 Effect of collector price and efficiency upon cost of electricity produced. (Projected.)

Baseline system except as noted.

Fig. 32 Trade-off of collector price vs. collector efficiency at constant cost of electricity produced. (Projected.)

$\overline{\text{BBEC}}$ = 97 mills/kW-h. Baseline system, except as noted.

Fig. 33 Effect of optical efficiency and collector price upon cost of electricity produced. (Projected.)

Baseline system except as noted.

Fig. 34 Trade-off of collector price vs. optical efficiency, at constant cost of electricity produced. (Projected.)

Baseline system except as noted.

Fig. 35 Effect of slope error, geometric concentration ratio, and collector price upon cost of electricity produced (Projected.)

Baseline system except as noted. Receiver aperture optimized for each slope error. (For collector efficiencies, see Fig. 8b.)

Fig. 36 Trade-off of collector price vs. slope error and geometric concentration ratio, at constant cost of electricity produced. (Projected)

$\overline{\text{BBEC}}$ = 97 mills/kW-h. Baseline system except as noted. Receiver aperture optimized for each slope error.

Fig. 37 Effect of optical performance upon cost of electricity produced. (Projected.)

Baseline system except as noted. (For collector efficiencies, see Fig. 5.)

Fig. 38 Trade-off of optical efficiency vs. geometric concentration ratio at constant cost of electricity produced. (Projected.)

Baseline system except as noted.

Fig. 39 Effect of slope error upon cost of electricity produced at various receiver temperatures. (Projected.)

Baseline system except as noted. Receiver aperture optimized. Plant costs assumed to depend on efficiencies but to be otherwise independent of temperature. (For collector efficiencies, see Fig. 19; for power conversion efficiencies, see Fig. 17a.)

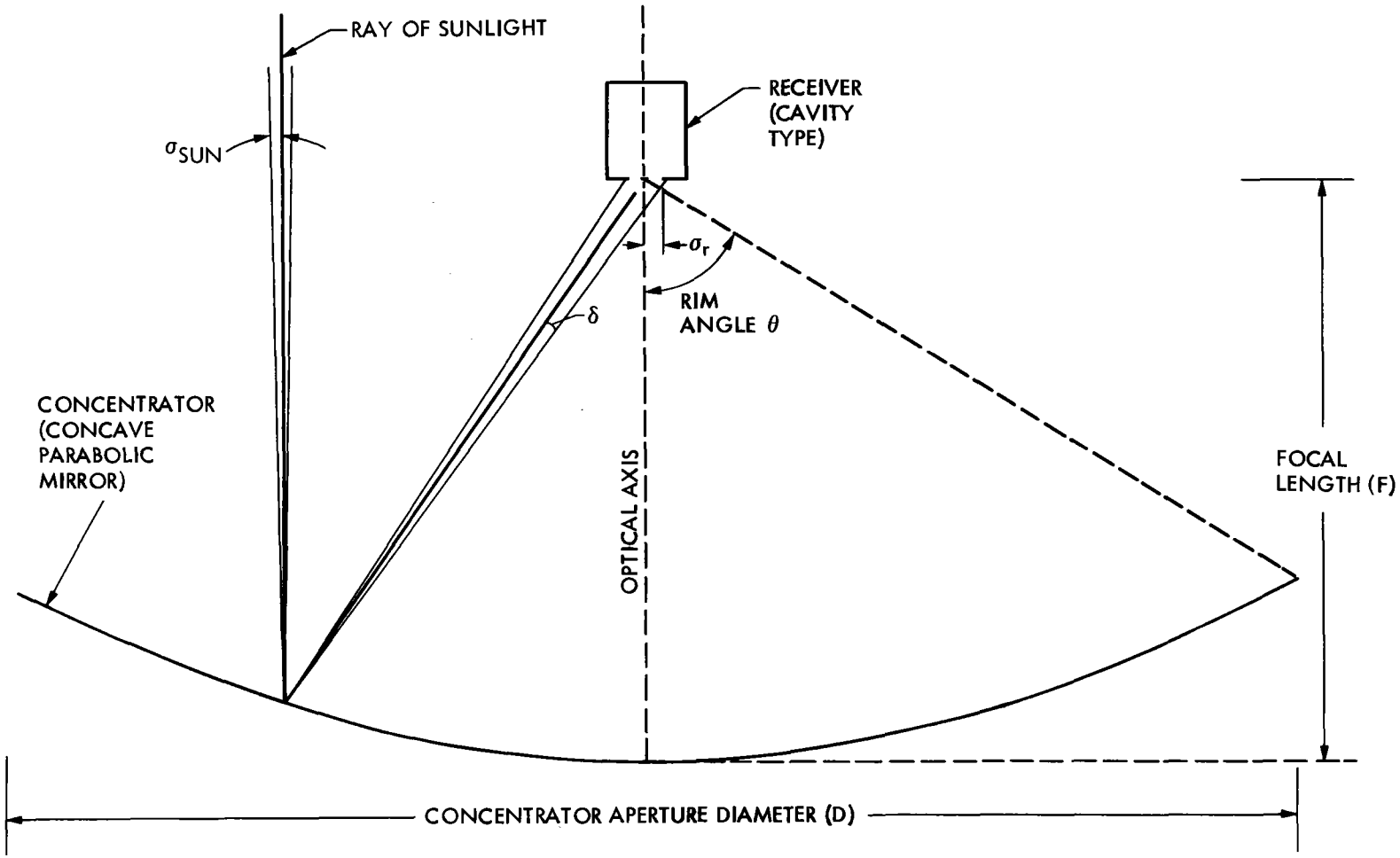

Figure 1. Dish Solar Collector: Geometry.

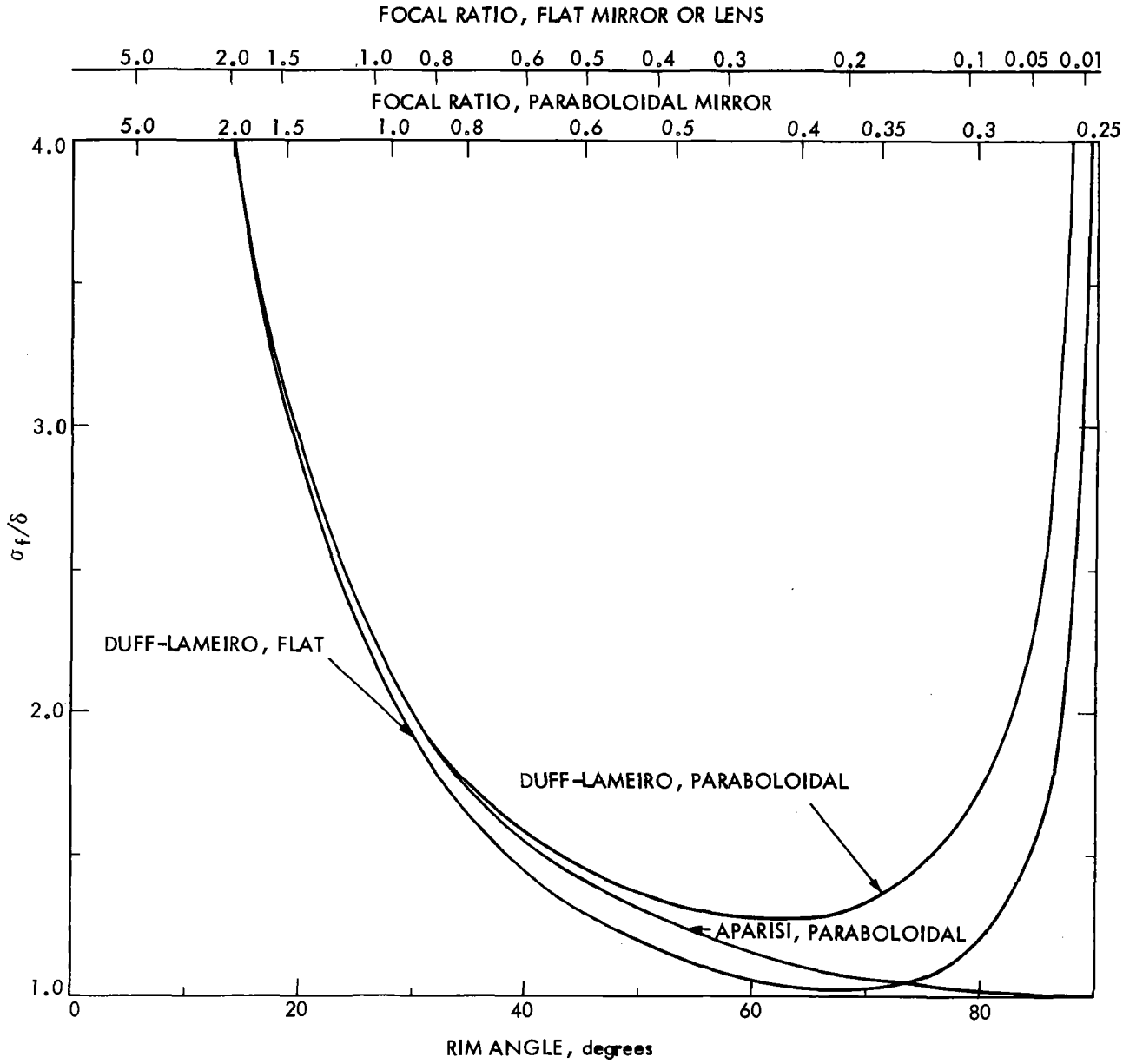

Figure 2. Size of Focal Spot Versus Rim Angle and Focal Ratio.

Compare Duff-Lameiro (Ref. 13) and Aparisi (Refs. 14, 15) approximations for paraboloidal mirrors. Also shown is Duff-Lameiro approximation for planar concentrators. All are for cavity receivers.

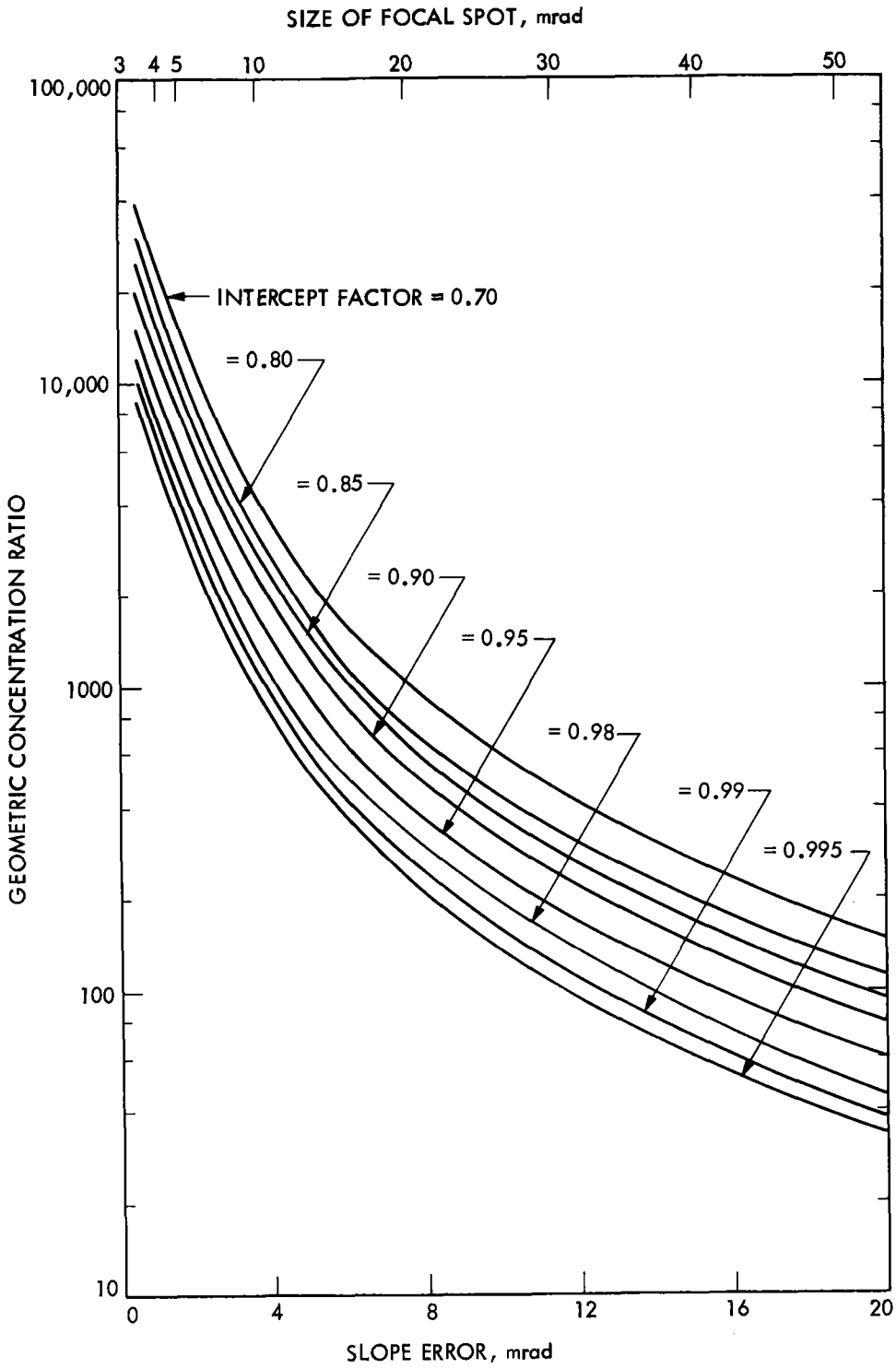

Figure 3. Geometric Concentration Ratio Attainable for Paraboloidal Mirrors As a Function of Slope Error or Size of Focal Spot and Intercept Factor.

Focal ratio $f_r = 0.5$. Angular spread of incoming direct sunlight, σ_{sun}, taken as 2.3 mrad. Specularity spread, σ_ω, and pointing error, σ_p, taken as 0.0. Thus, $\delta^2 = (2\ \sigma_{slope})^2 + 2.3^2$ mrad^2.

Focal spot relative size, σ_f, given by Duff-Lameiro approximation (Eq. 7).

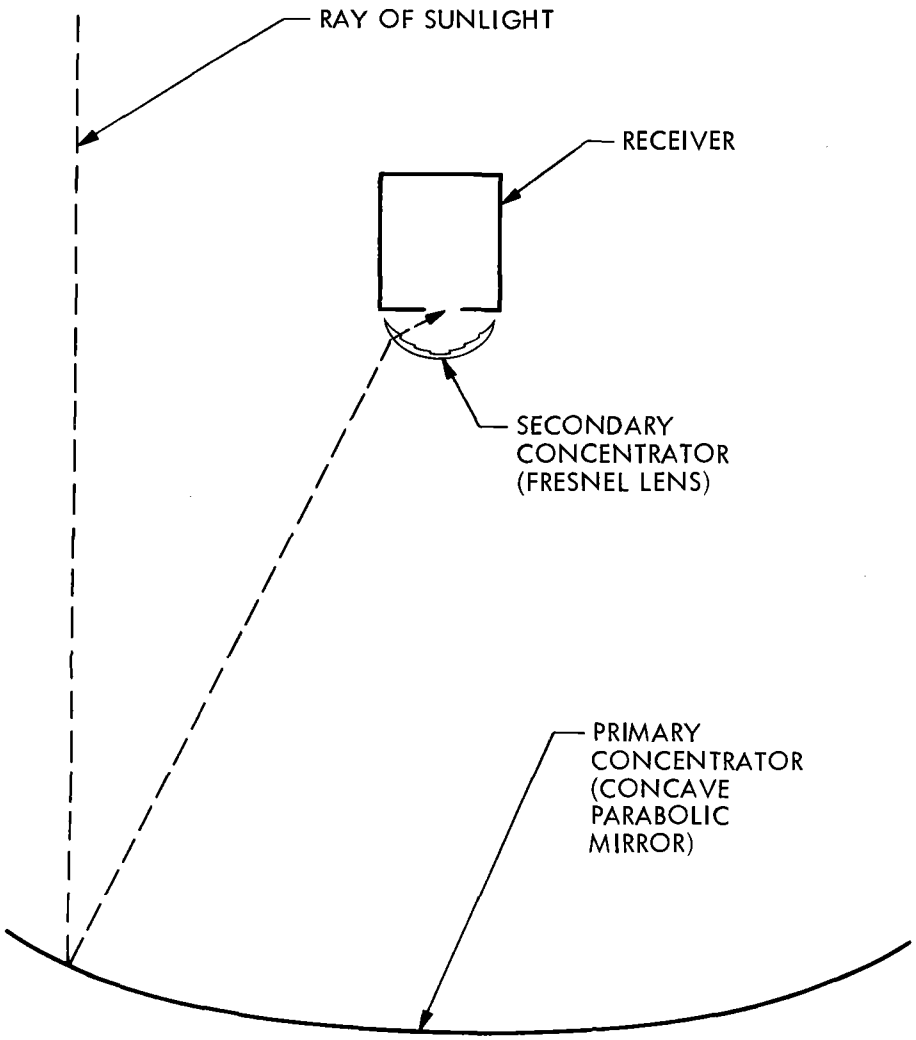

Figure 4a . Example of Secondary Concentrator to Improve Optical Performance: Fresnel Lens.

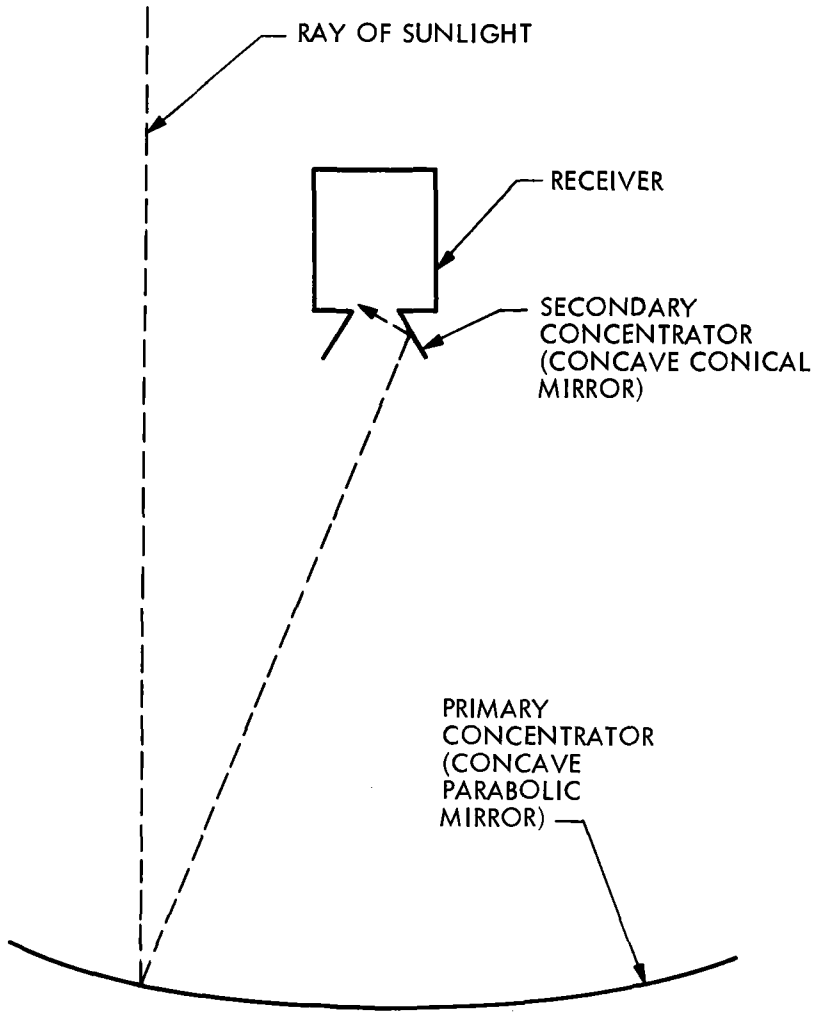

Figure 4b. Example of Secondary Concentrator to Improve Optical Performance: Conical (Truncated, Axicon).

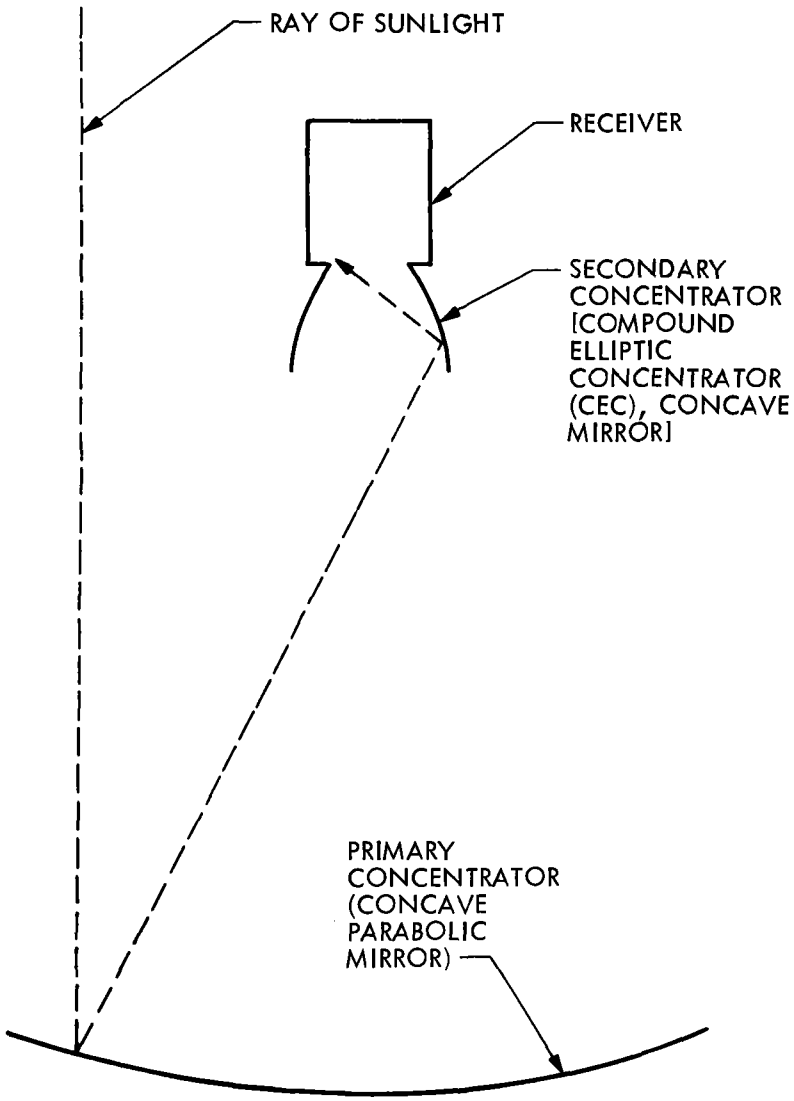

Figure 4c. Example of Secondary Concentrator to Improve Optical Performance: Compound Elliptic Concentrator.

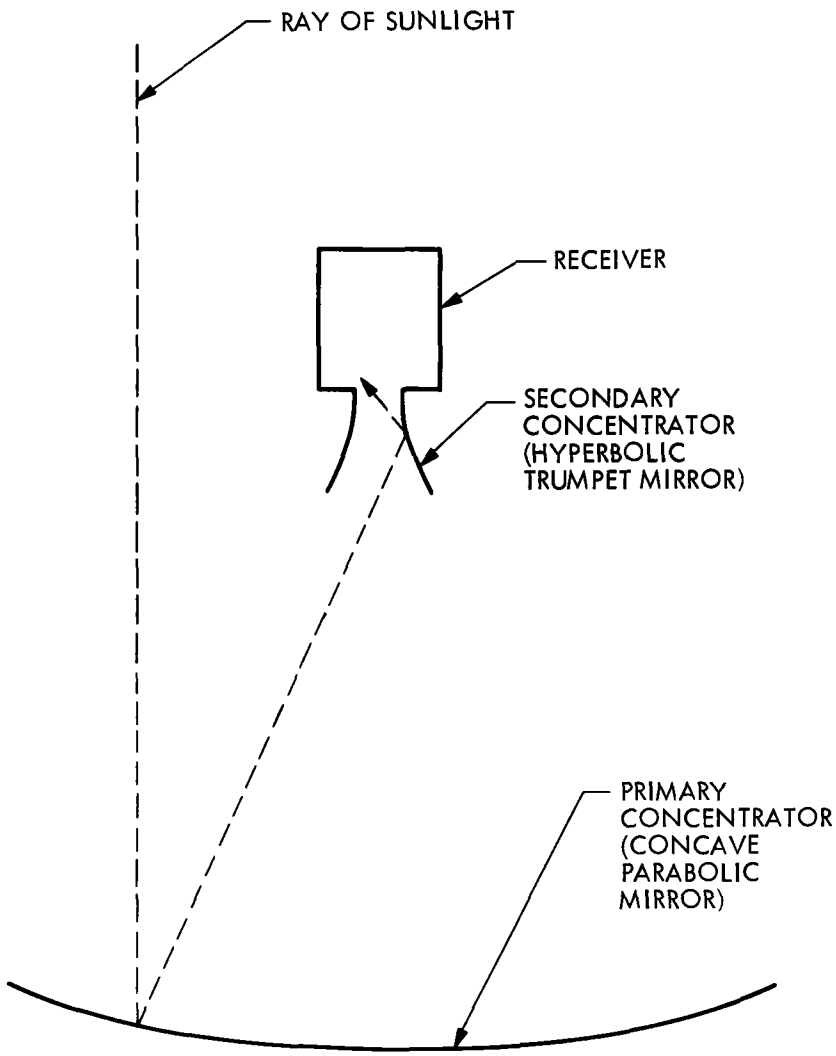

Figure 4d. Example of Secondary Concentrator to Improve Optical Performance: Hyperbolic Trumpet.

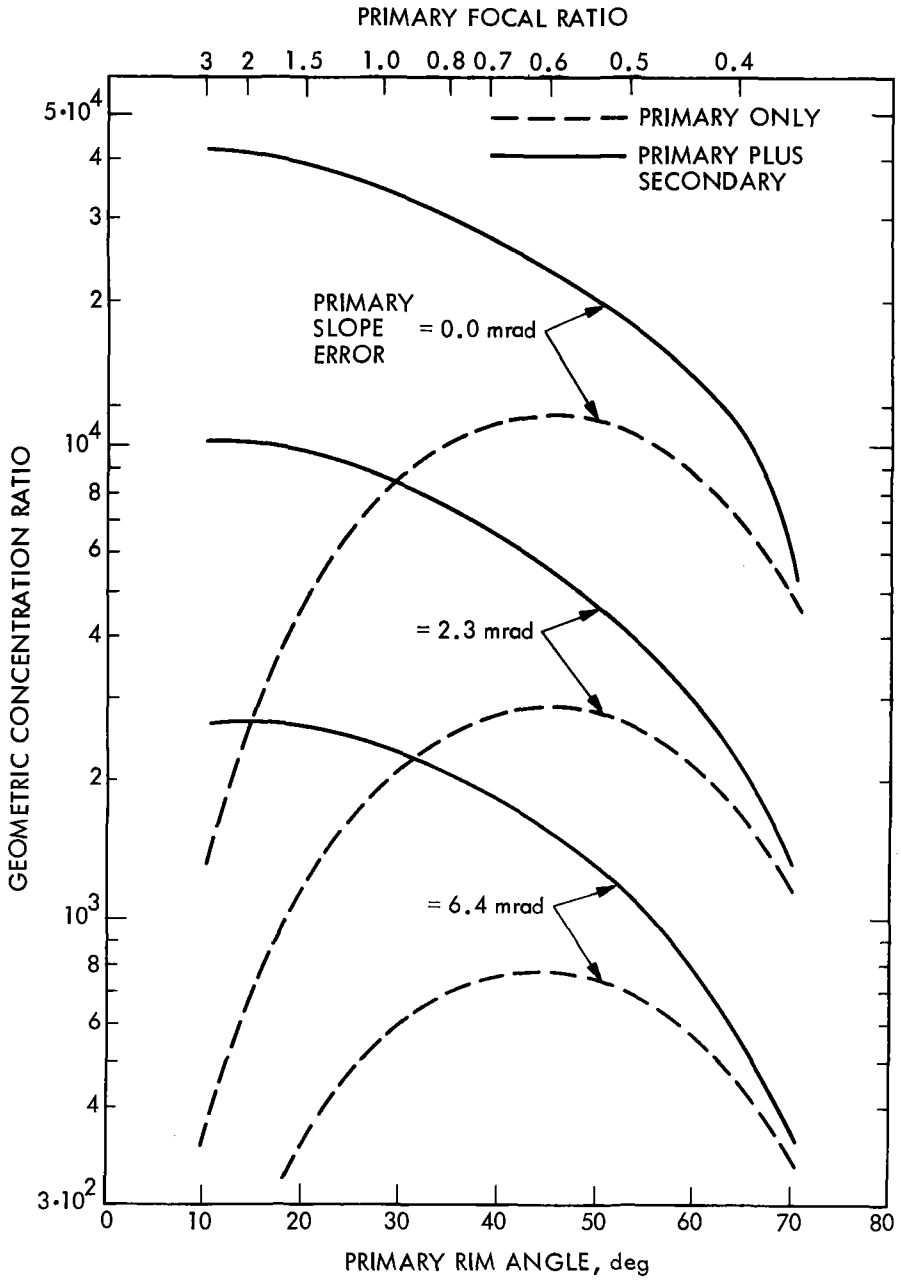

Figure 5. Effect of Focal Ratio upon Attainable Geometric Concentration Ratio of Single and Compound Concentrators.

Rectangular distribution of slope errors. Intercept factor = 1.0.

Adapted from Baranov (Ref. 22).

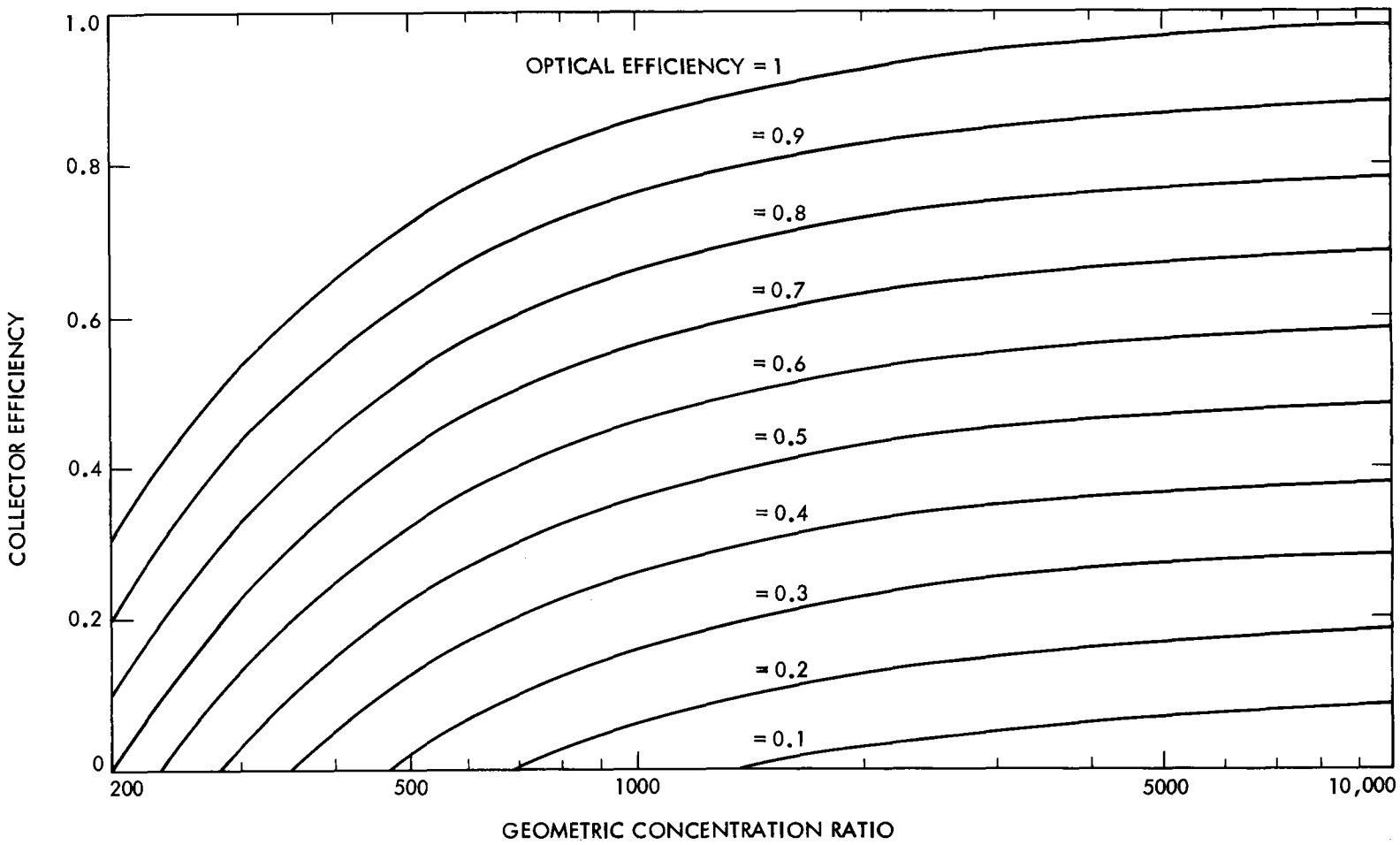

Figure 6a. Effect of Optical Performance upon Collector Efficiency: Idealized System. (Except as noted.)

Intercept factor constant.

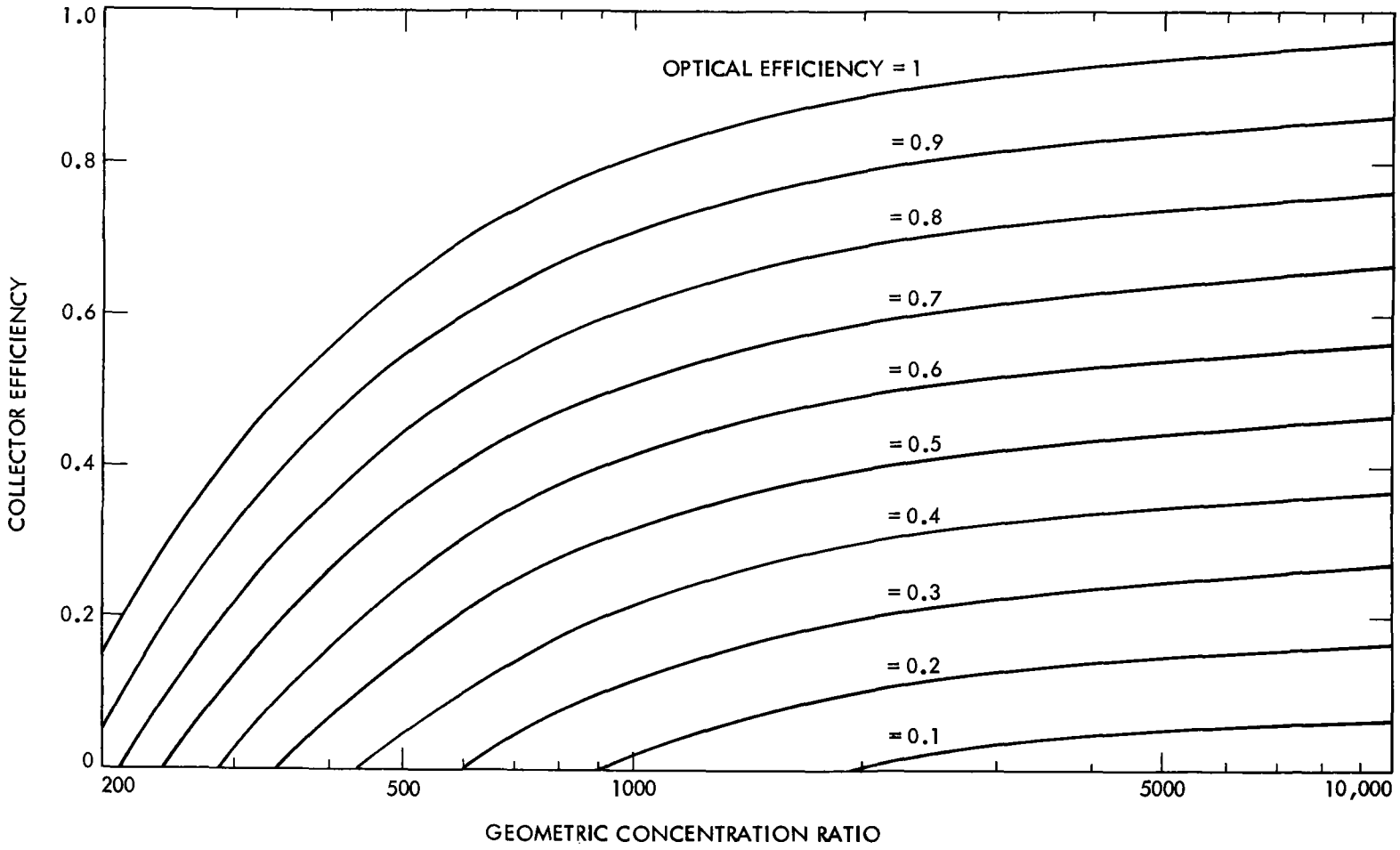

Figure 6b. Effect of Optical Performance upon Collector Efficiency: Baseline System. (Except as noted.)

Intercept factor constant.

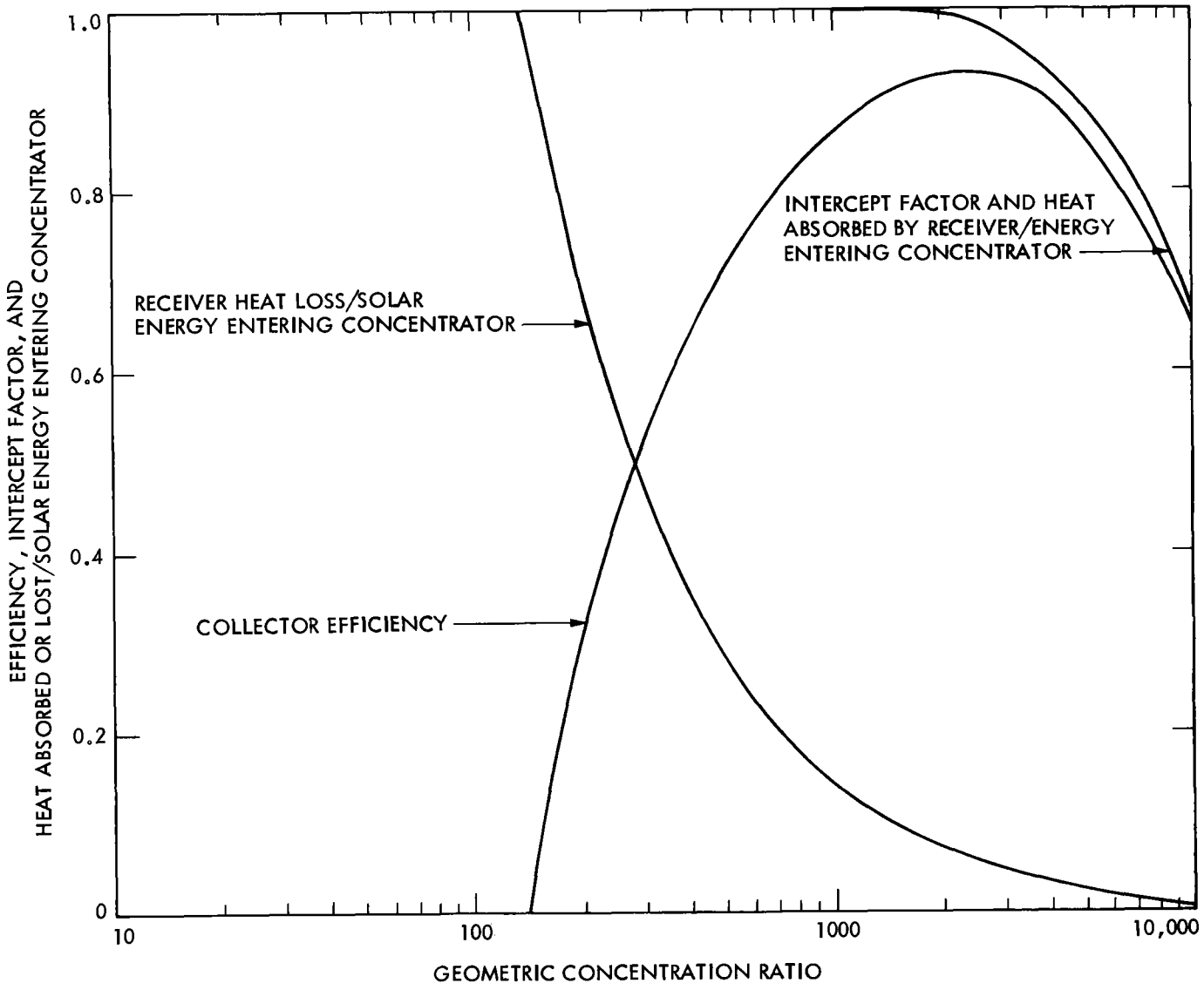

Figure 7a. Receiver Aperture Optimization: Idealized System.

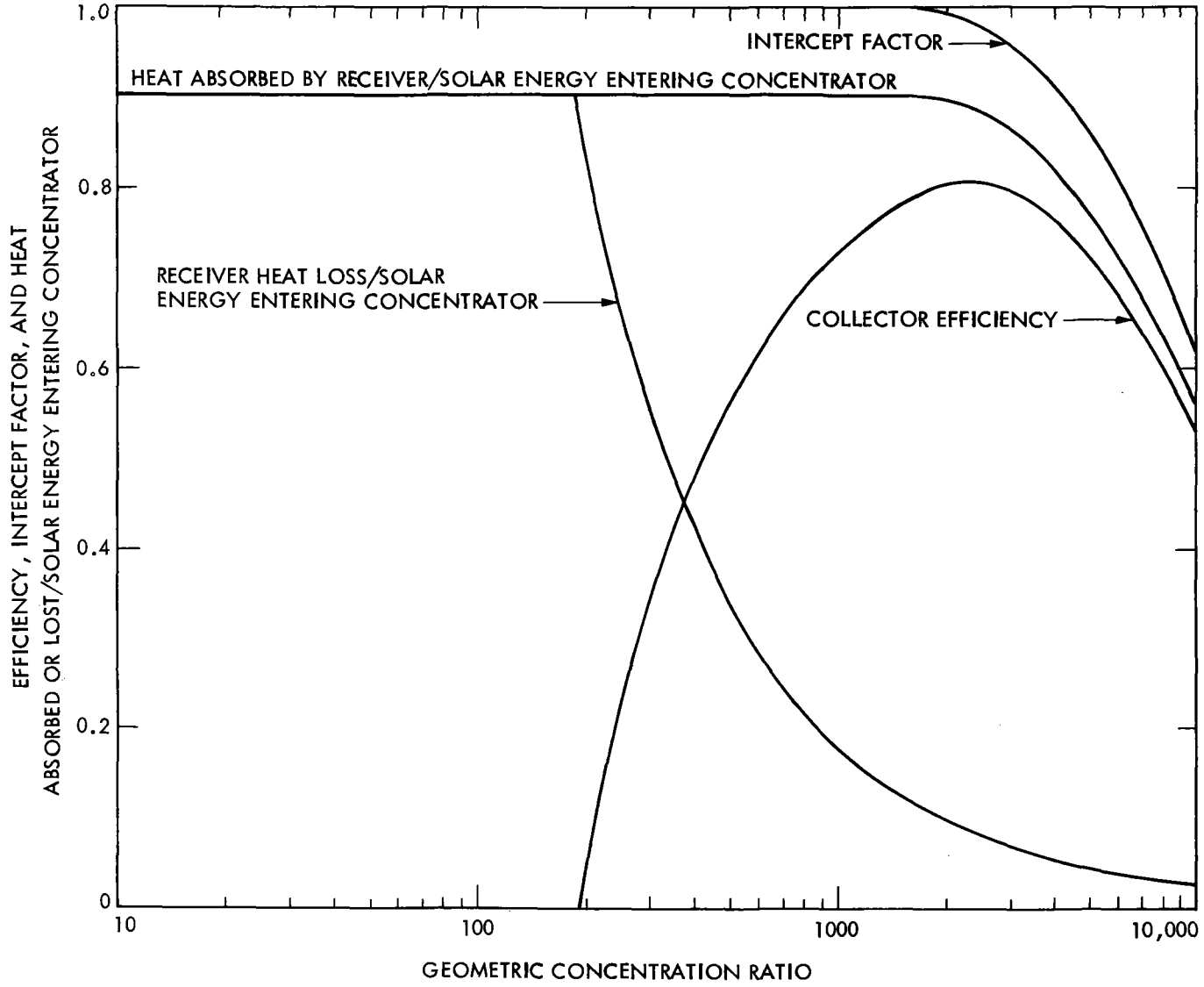

Figure 7b. Receiver Aperture Optimization: Baseline System.

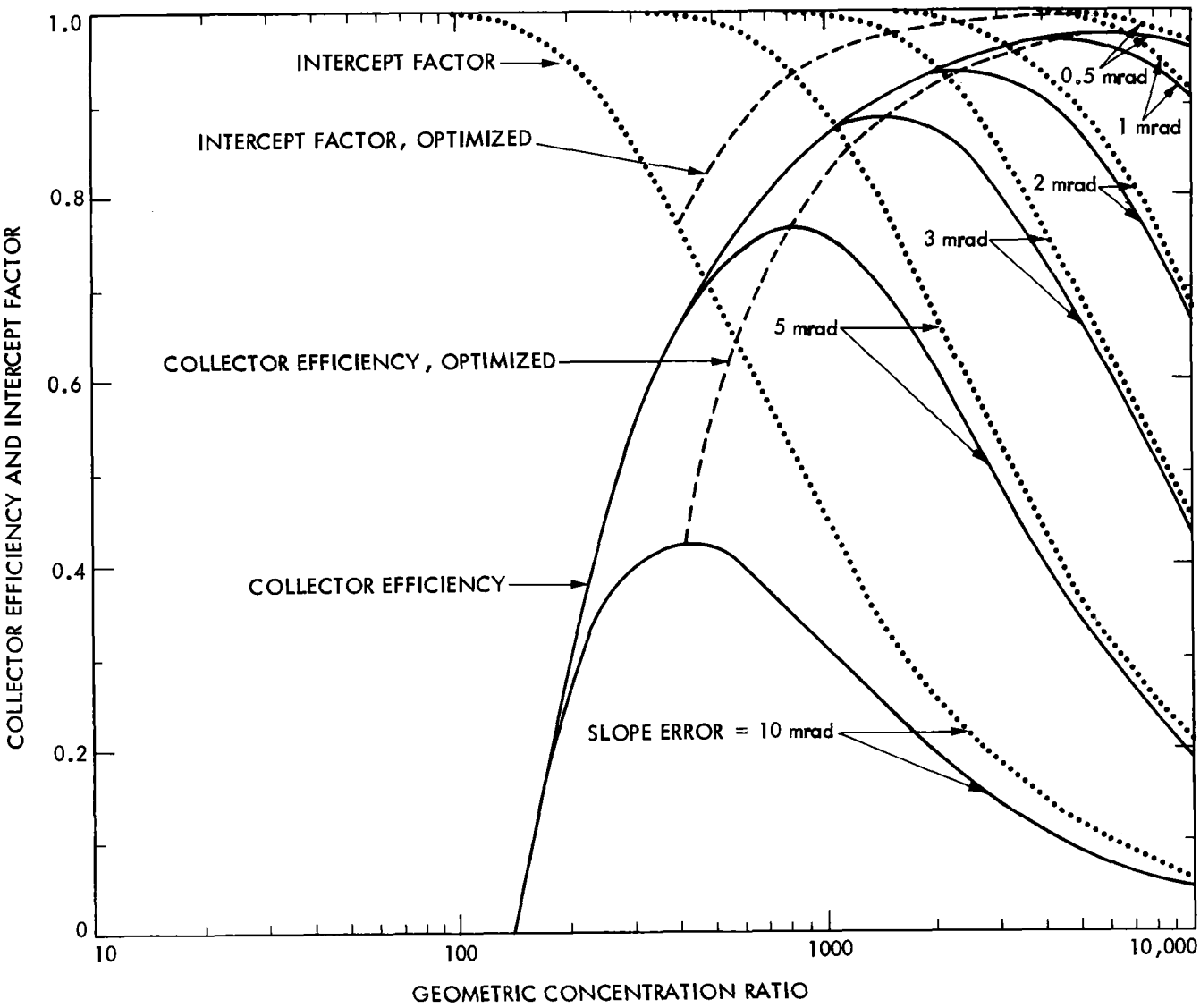

Figure 8a. Effect of Concentrator Slope Errors upon Collector Efficiency and Intercept Factor: Idealized System.

Dotted line: Receiver aperture optimized.

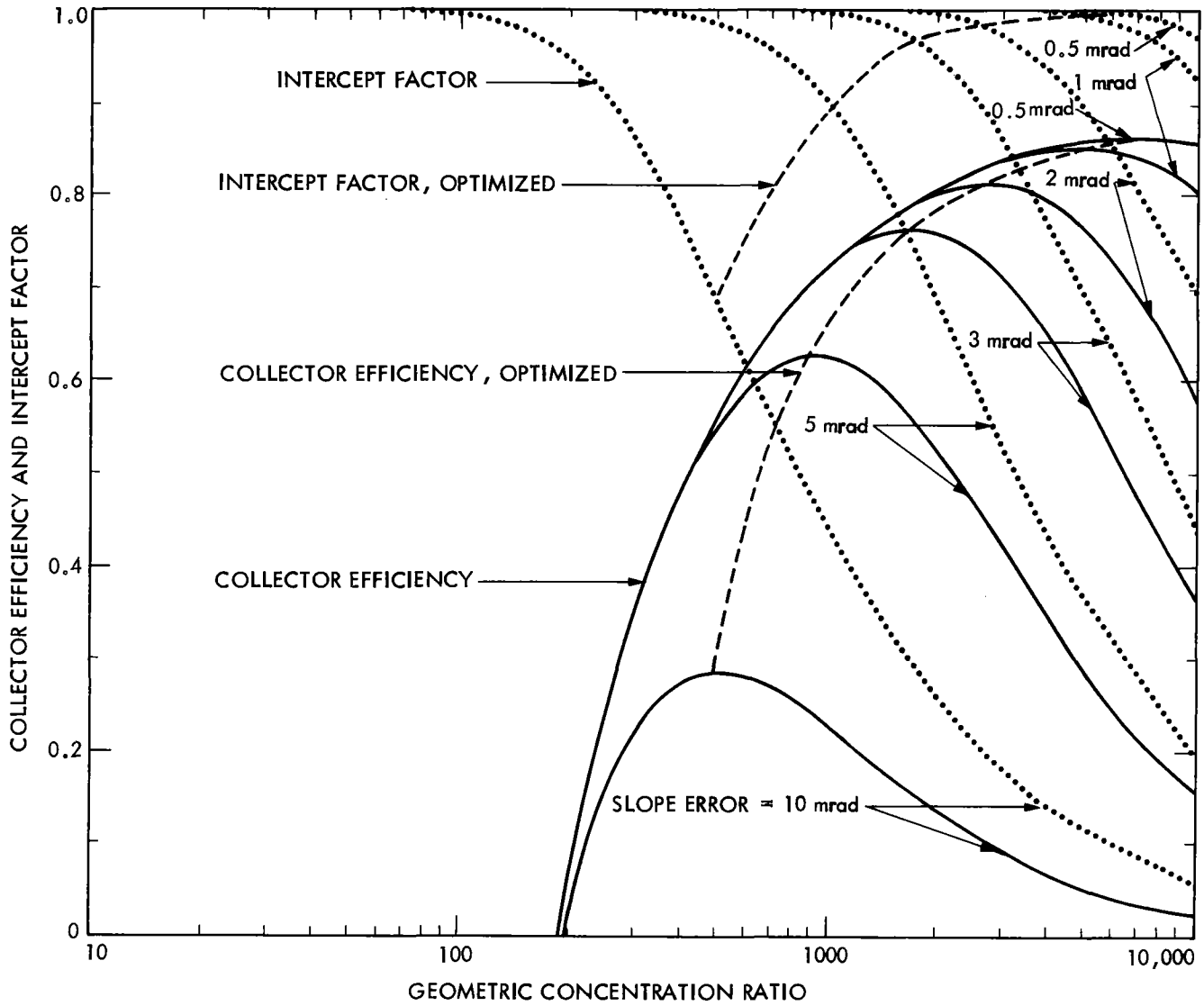

Figure 8b. Effect of Concentrator Slope Errors upon Collector Efficiency and Intercept Factor: Baseline System.

Dotted line: Receiver aperture optimized.

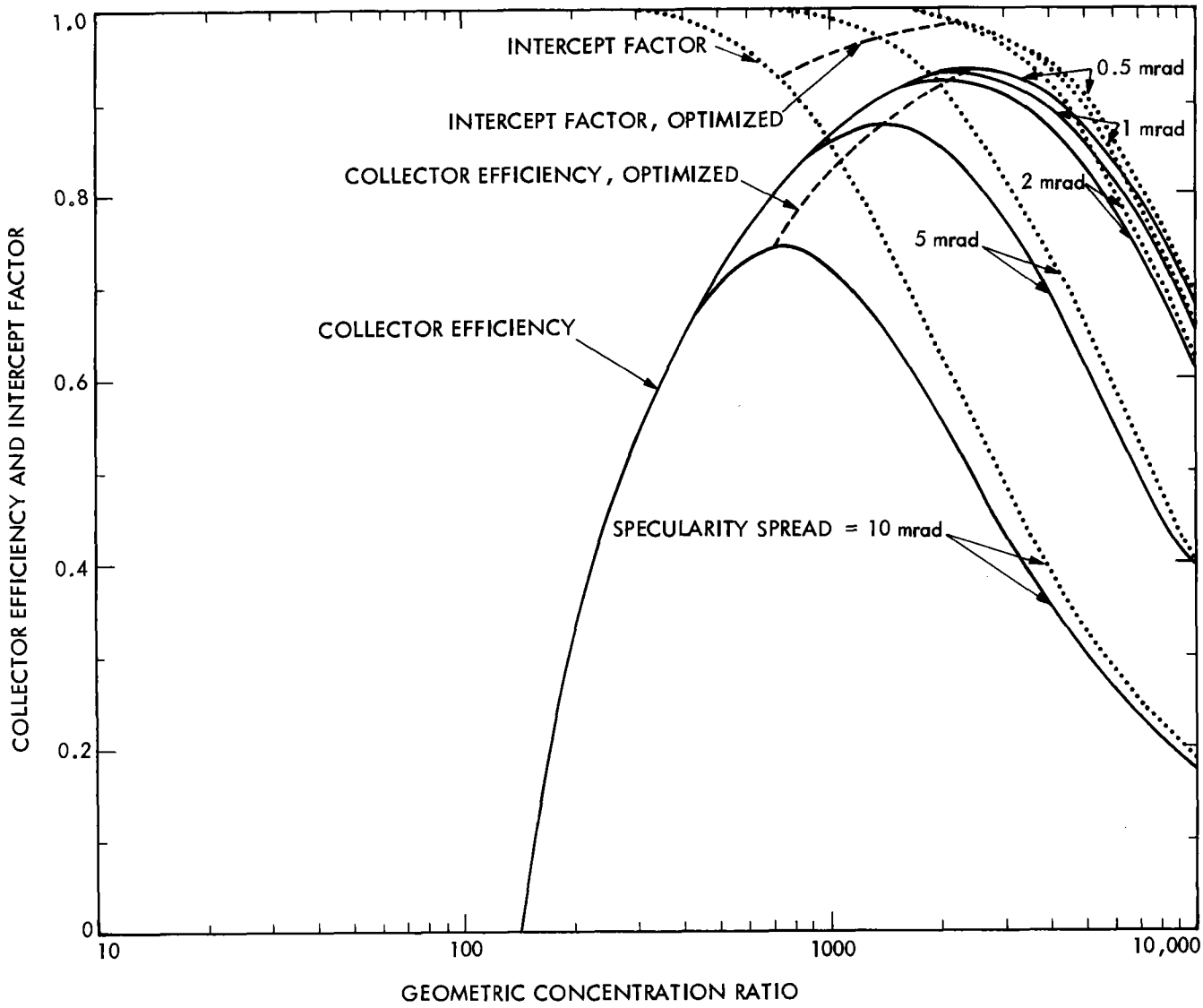

Figure 9a. Effect of Specularity Spread upon Collector Efficiency and Intercept Factor: Idealized System.

Dotted line: Receiver aperture optimized.

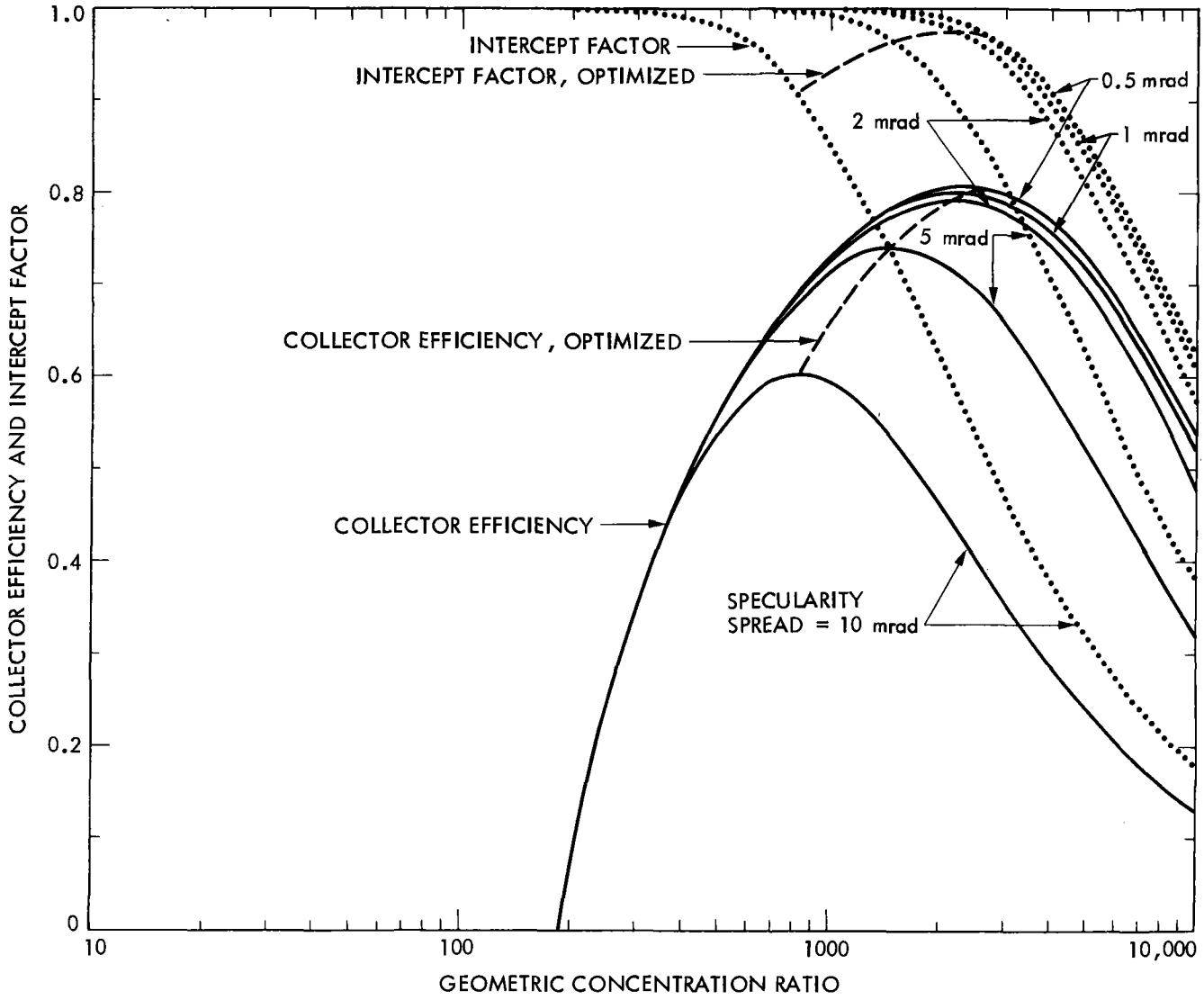

Figure 9b. Effect of Specularity Spread upon Collector Efficiency and Intercept Factor: Baseline System.

Dotted line: Receiver aperture optimized.

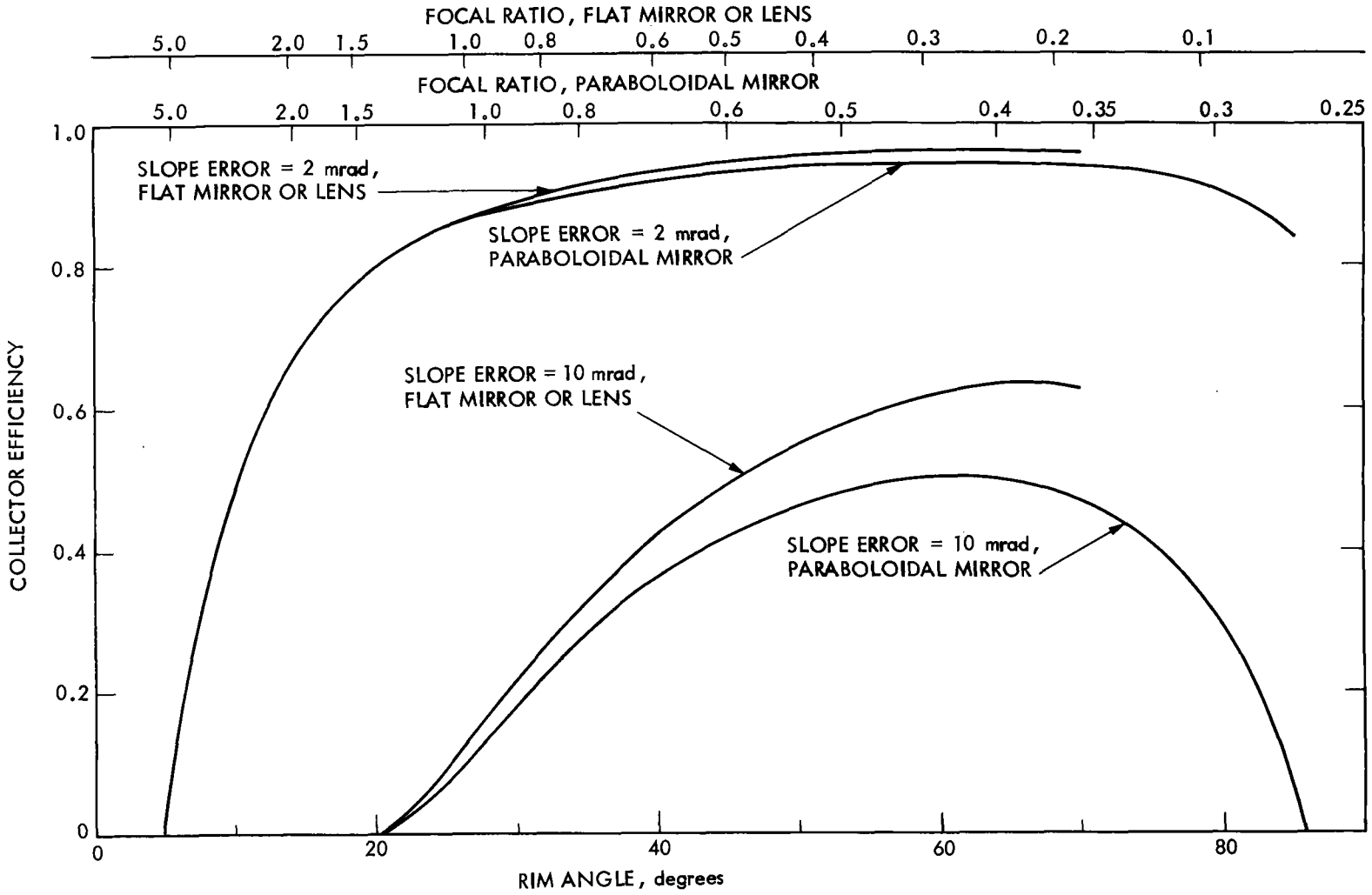

Figure 10. Effect of Focal Ratio or Rim Angle upon Collector Efficiency.

Receiver aperture optimized for each focal ratio (or rim angle). Duff-Lameiro approximation. Idealized System.

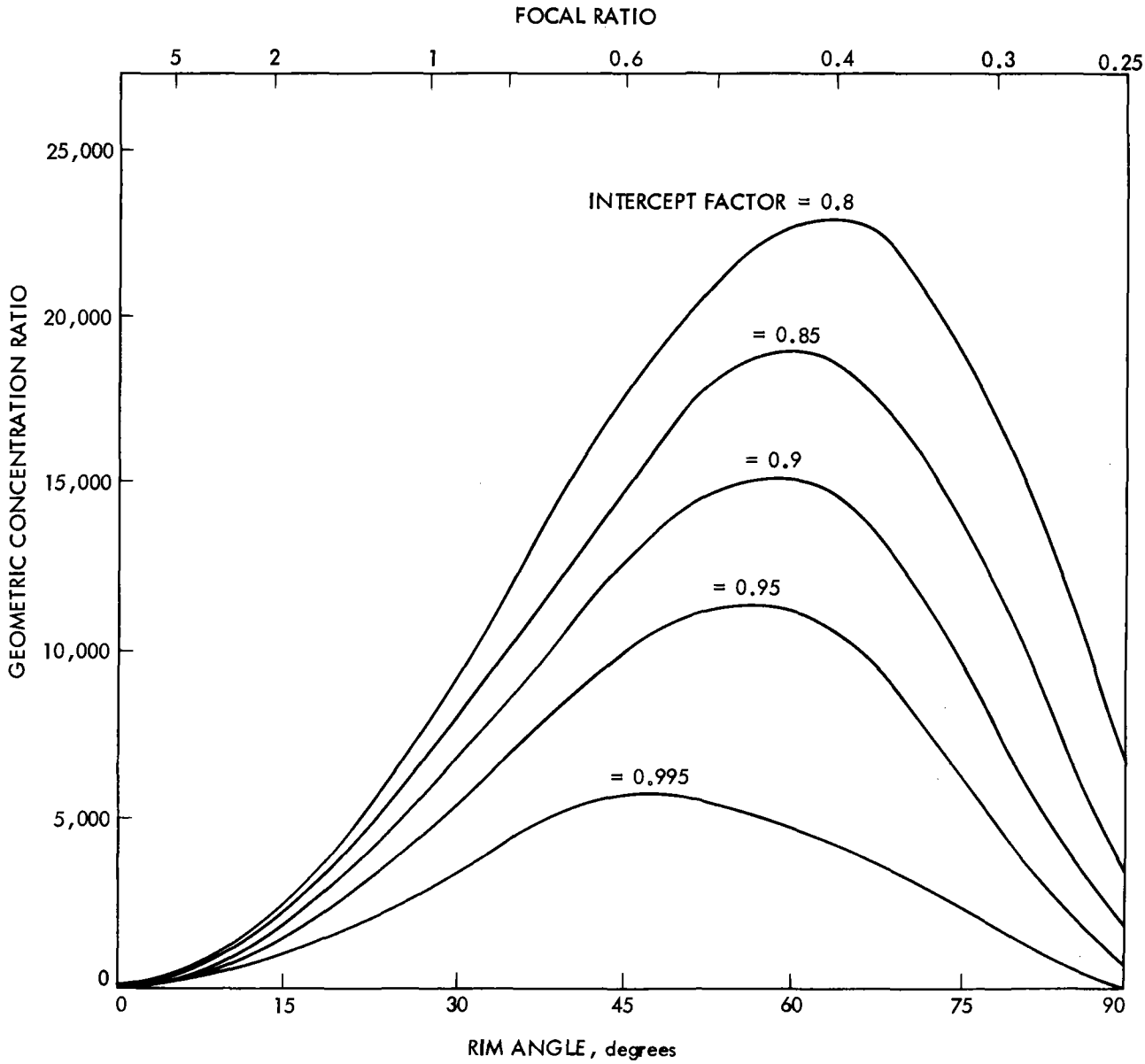

Figure 11. Effect of Rim Angle and Geometric Concentration Ratio upon Intercept Factor.

Flat solar disk profile, diameter 32 arc minutes. Paraboloidal mirror, reflectance 1.0, slope error 3 arc minutes, no other errors.

After O'Neill and Hudson (Ref. 26).

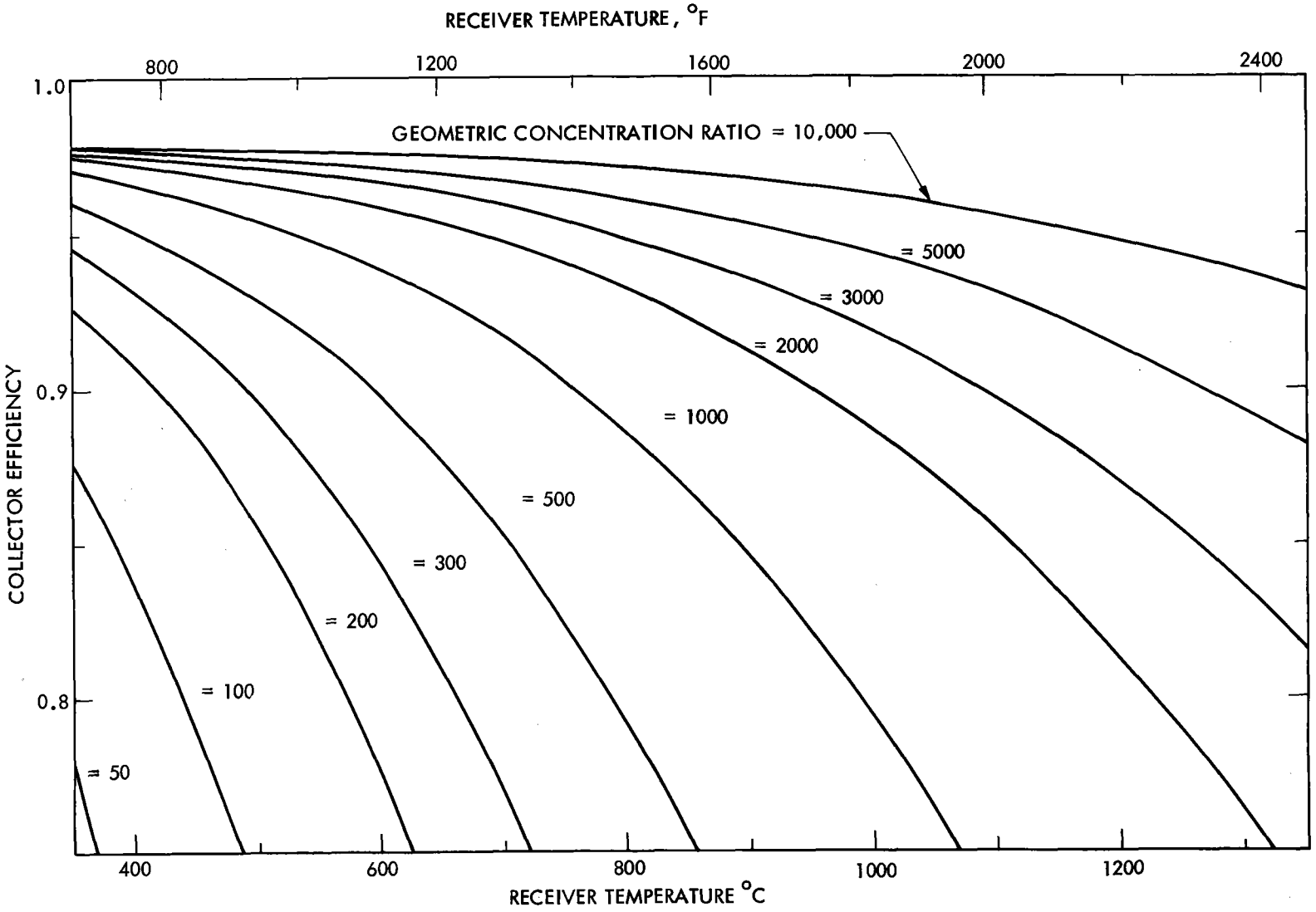

Figure 12a. Effect of Receiver Temperature and Geometric Concentration Ratio upon Collector Efficiency.

Idealized system, except as noted; constant intercept factor (ϕ = 0.98).

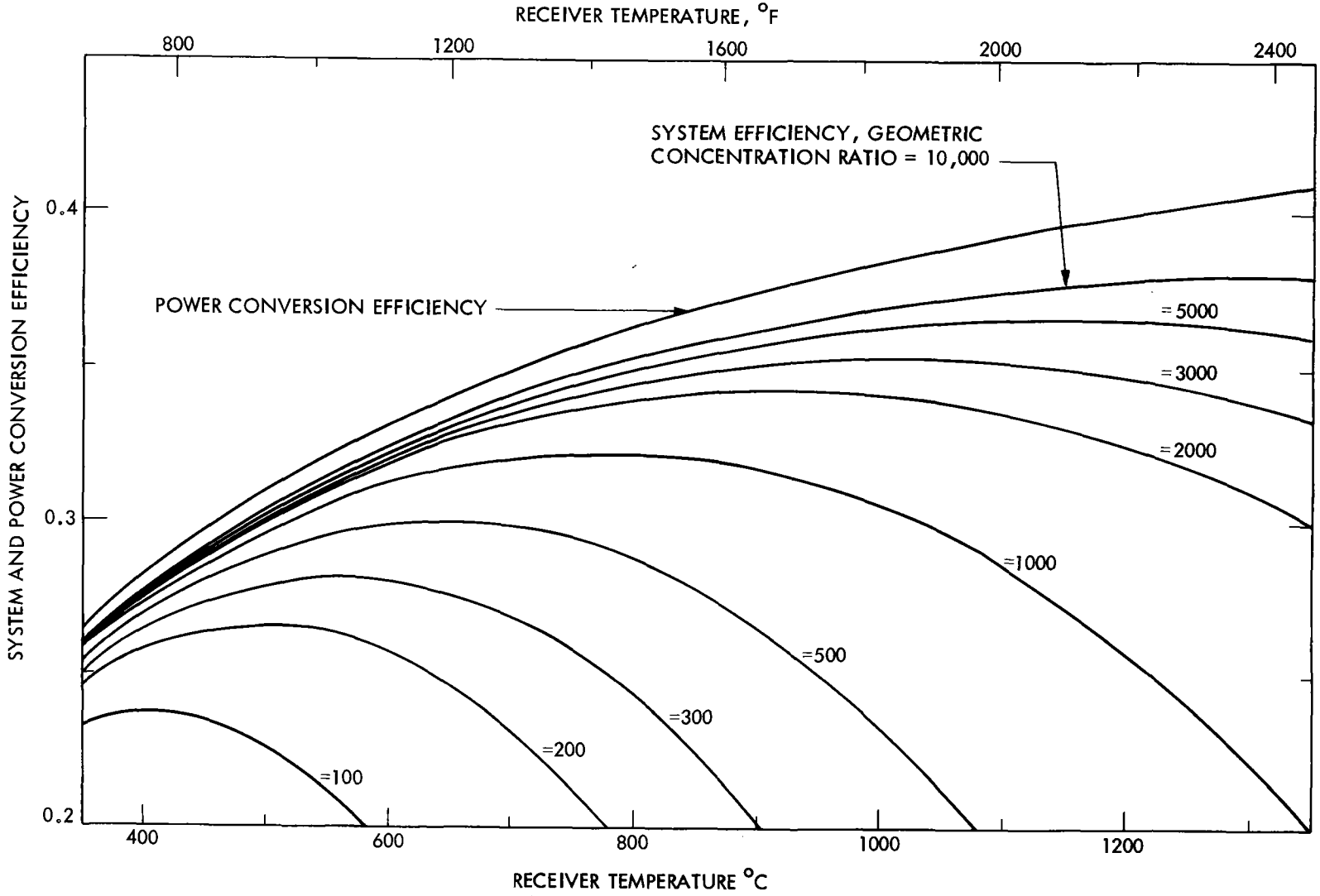

Figure 12b. Effect of Receiver Temperature and Geometric Concentration Ratio upon Power Conversion and System Efficiency.

Idealized system, except as noted; constant intercept factor (ϕ = 0.98), constant power conversion effectiveness.

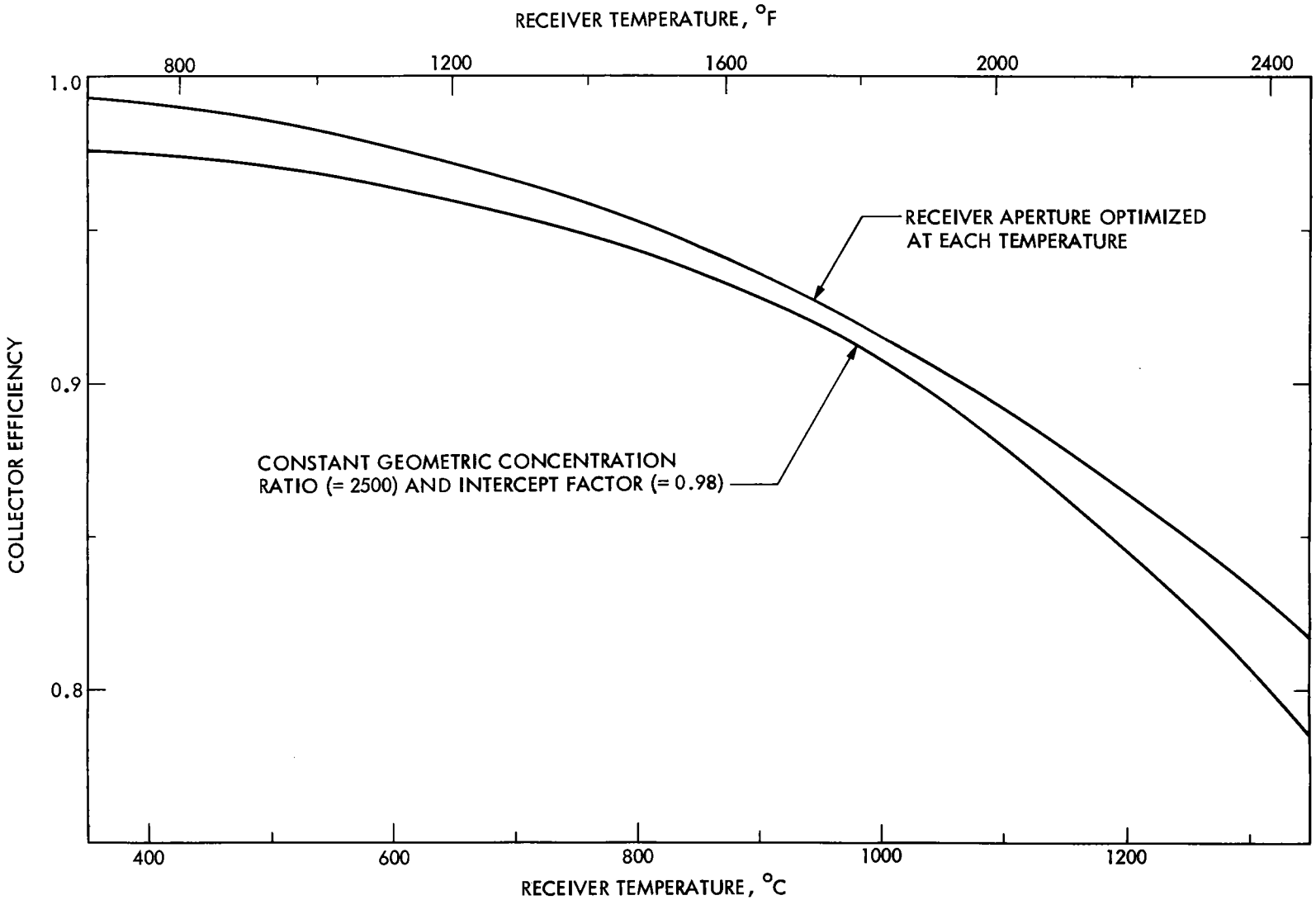

Figure 13. Effect of Receiver Temperature on Collector Efficiency With and Without Optimization of Receiver Aperture at Each Temperature.

Idealized system except as noted.

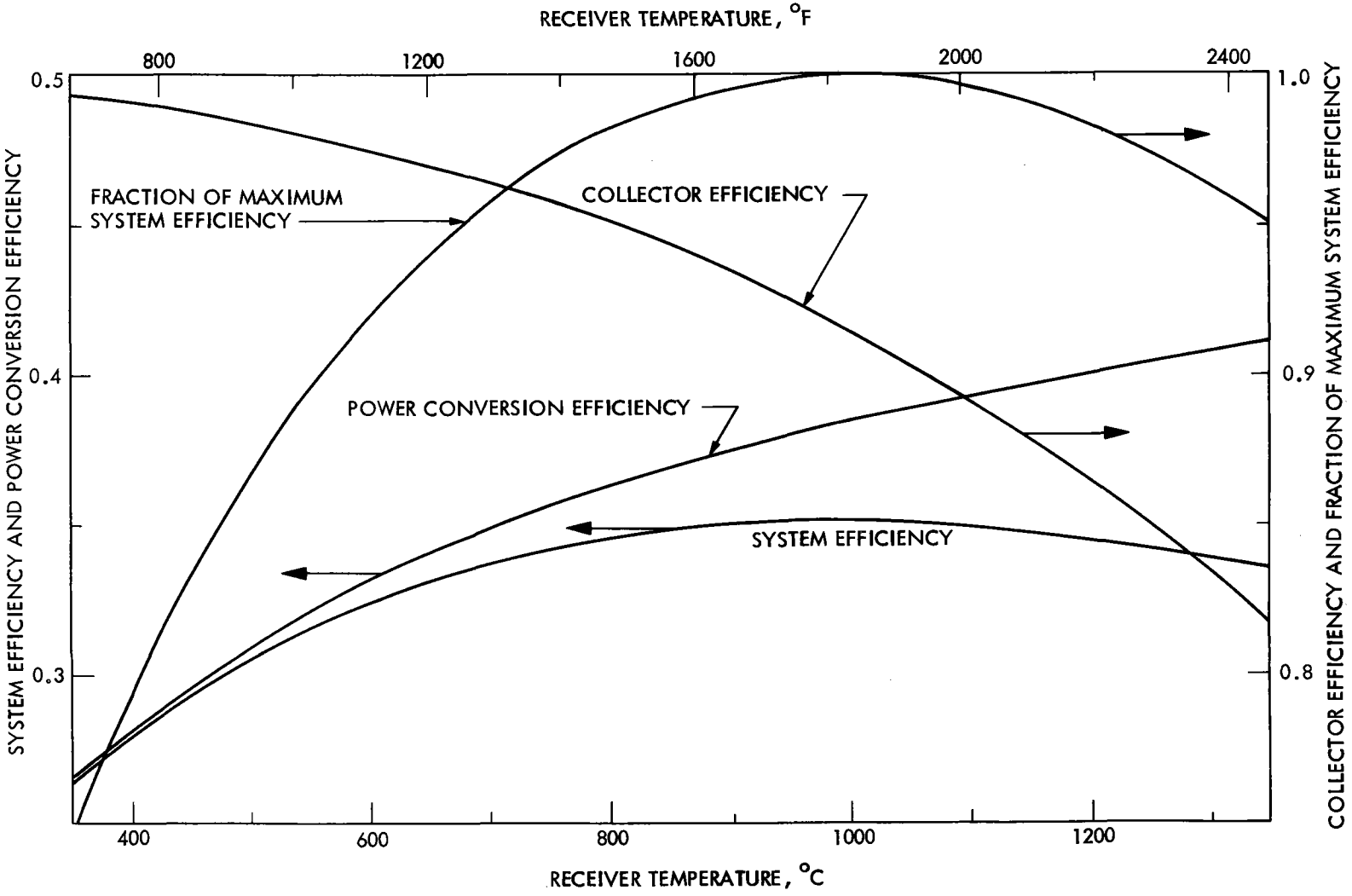

Figure 14. Effect of Receiver Temperature on Collector, Power Conversion, and System Efficiency.

Receiver aperture optimized at each temperature. Idealized system except as noted. Constant power conversion effectiveness.

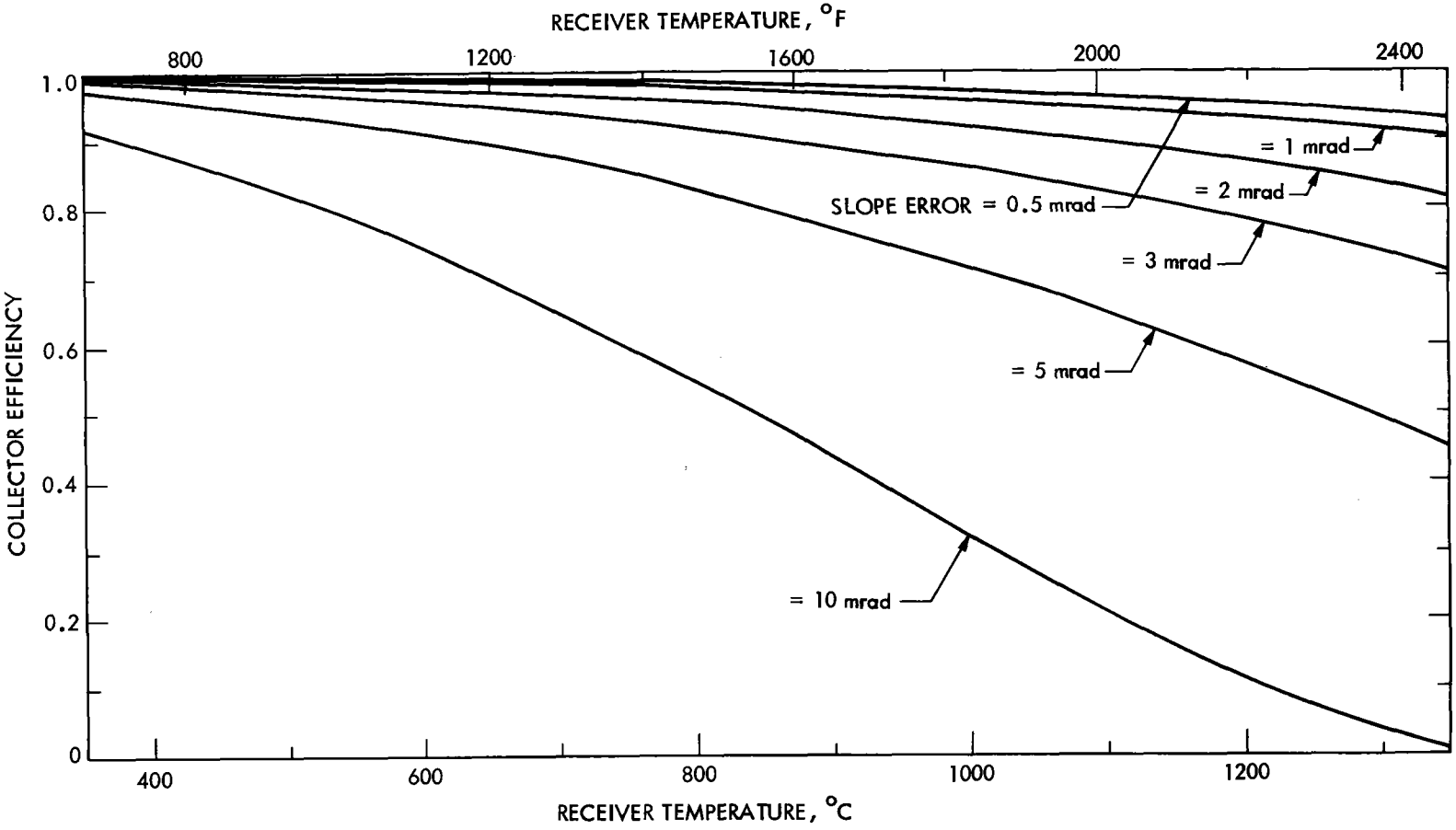

Figure 15a. Effect of Receiver Temperature and Concentrator Slope Error upon Collector Efficiency.

Idealized system except as noted. Receiver aperture optimized at each temperature.

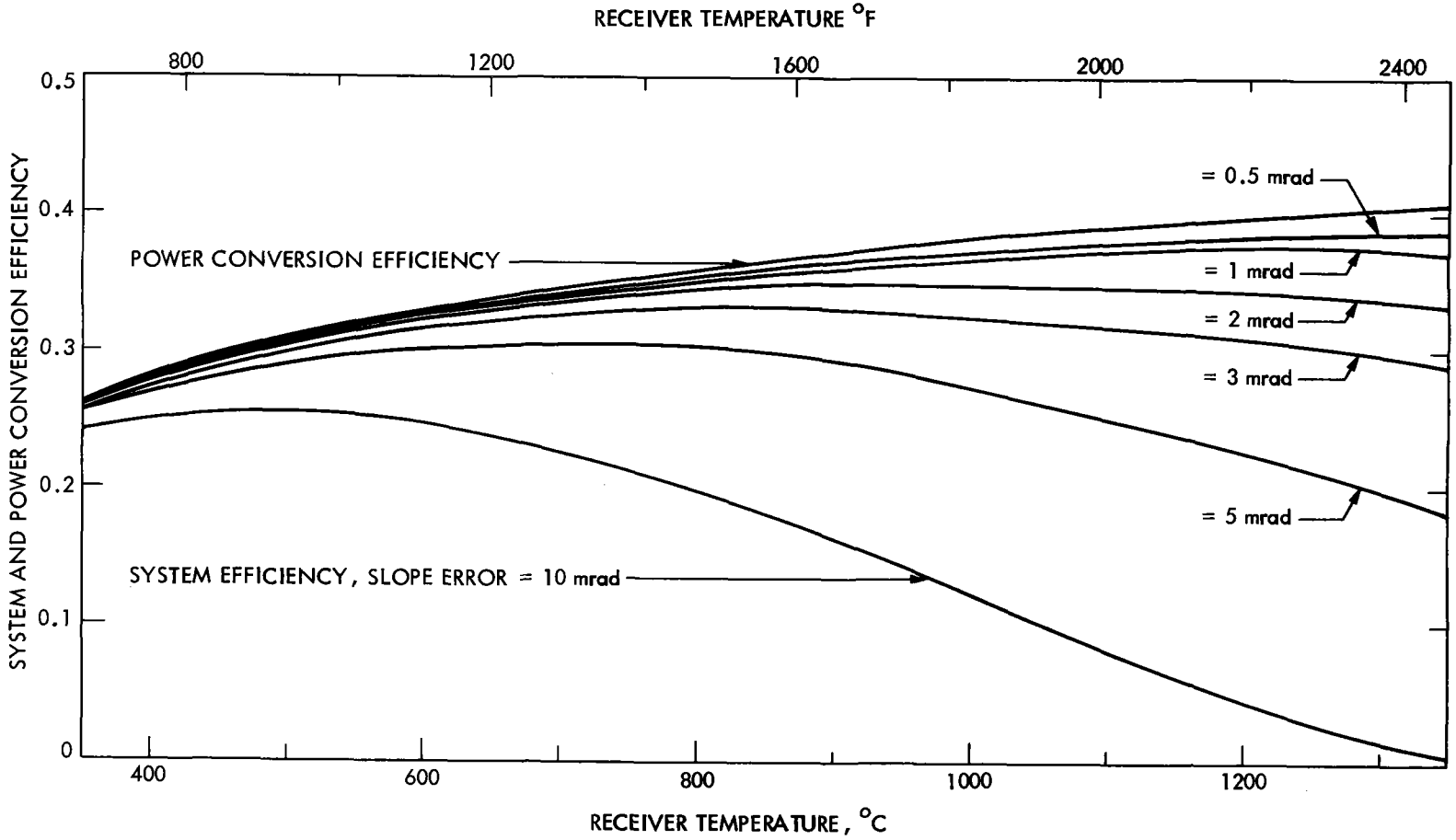

Figure 15b. Effect of Receiver Temperature and Concentrator Slope Error upon Power Conversion and System Efficiency.

Idealized system except as noted. Receiver aperture optimized at each temperature. Constant power conversion effectiveness.

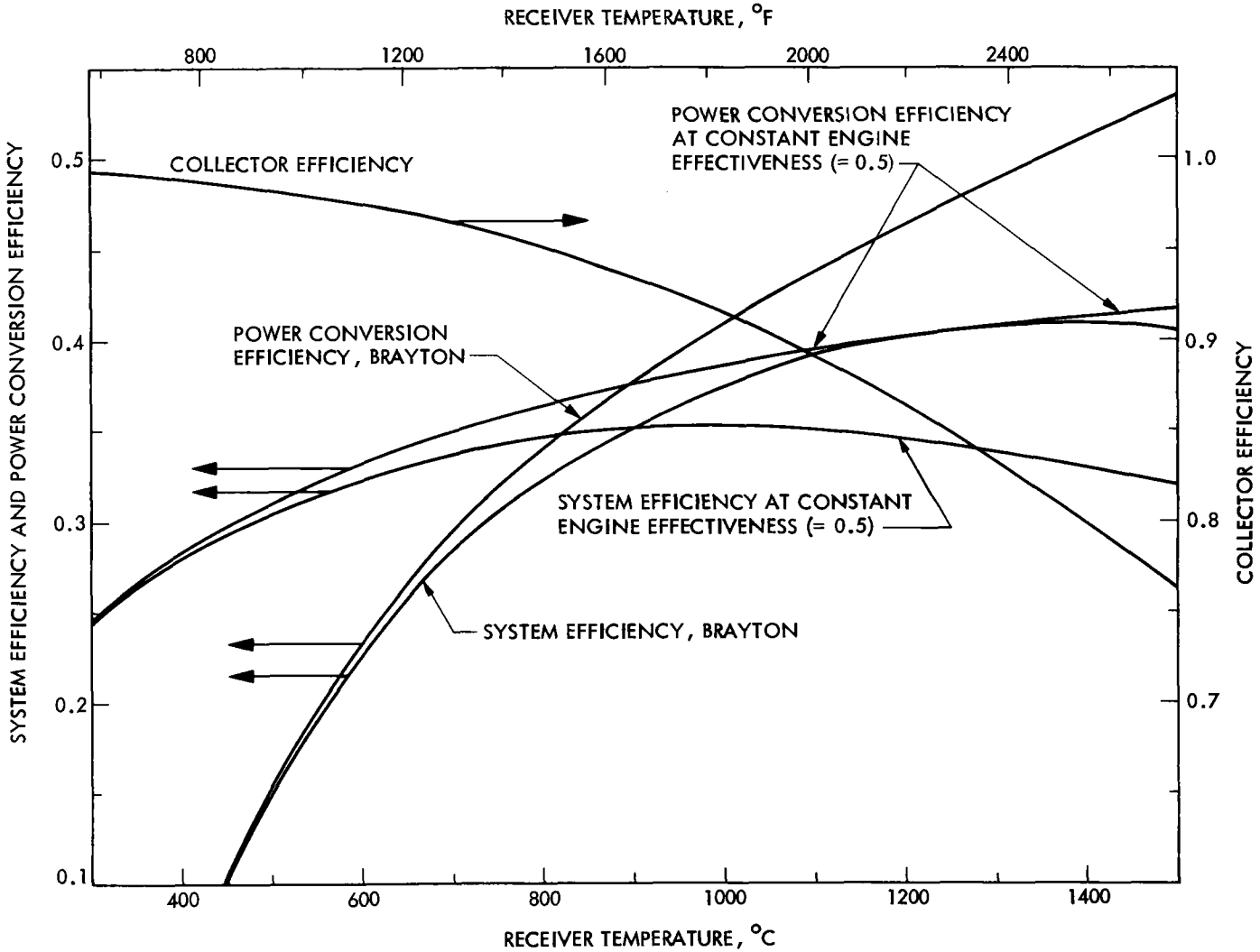

Figure 16a. Effect of Receiver Temperature on Power Conversion and System Efficiency with Engines of Differing Characteristics: Collector, Power Conversion, and System Efficiencies. (Idealized system, except as noted. Receiver aperture optimized at each temperature.)

Constant power conversion effectiveness is characteristic of Rankine and Stirling systems. The numerical value of the effectiveness (here taken as $v = 0.5$) depends on the particular engine.

Brayton systems characteristically have an engine effectiveness that increases with engine inlet temperature. Brayton power conversion efficiencies shown here are based on engine efficiencies from Reference 30 and alternator plus rectifier efficiency of 0.92.

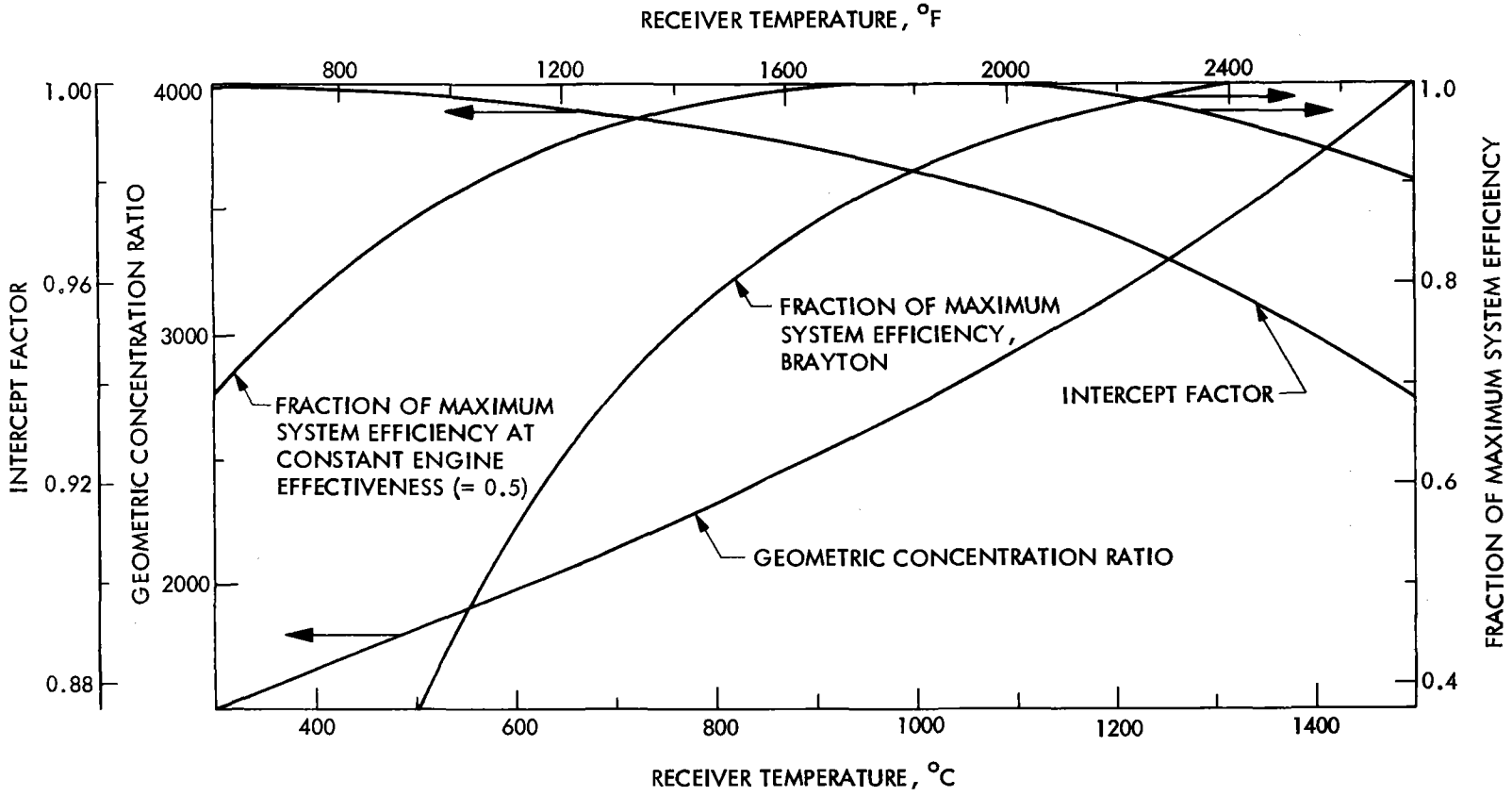

Figure 16b. Effect of Receiver Temperature on Power Conversion and System Efficiency with Engines of Differing Characteristics: System Efficiency As Function of Maximum System Efficiency, Geometric Concentration Ratio, and Intercept Factor. (Idealized system, except as noted. Receiver aperture optimized at each temperature.)

Constant power conversion effectiveness is characteristic of Rankine and Stirling systems. The numerical value of the effectiveness (here taken as $v = 0.5$) depends on the particular engine.

Brayton systems characteristically have an engine effectiveness that increases with engine inlet temperature. Brayton power conversion efficiencies shown here are based on engine efficiencies from Reference 30 and alternator plus rectifier efficiency of 0.92.

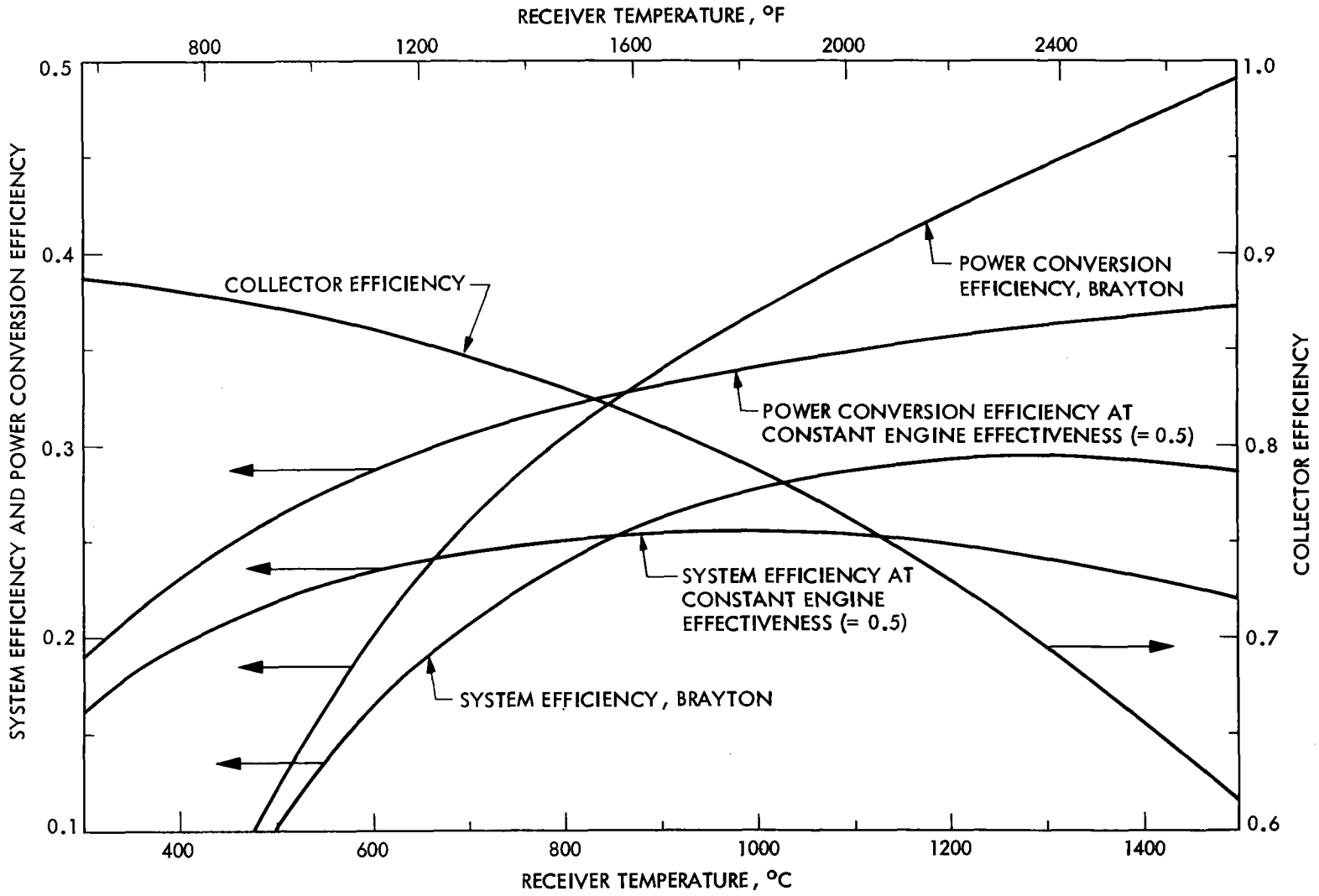

Figure 17a. Effect of Receiver Temperature on Power Conversion and System Efficiency with Engines of Differing Characteristics: Collector, Power Conversion, and System Efficiencies.

Baseline system, except as noted. Other characteristics as in Figure 16.

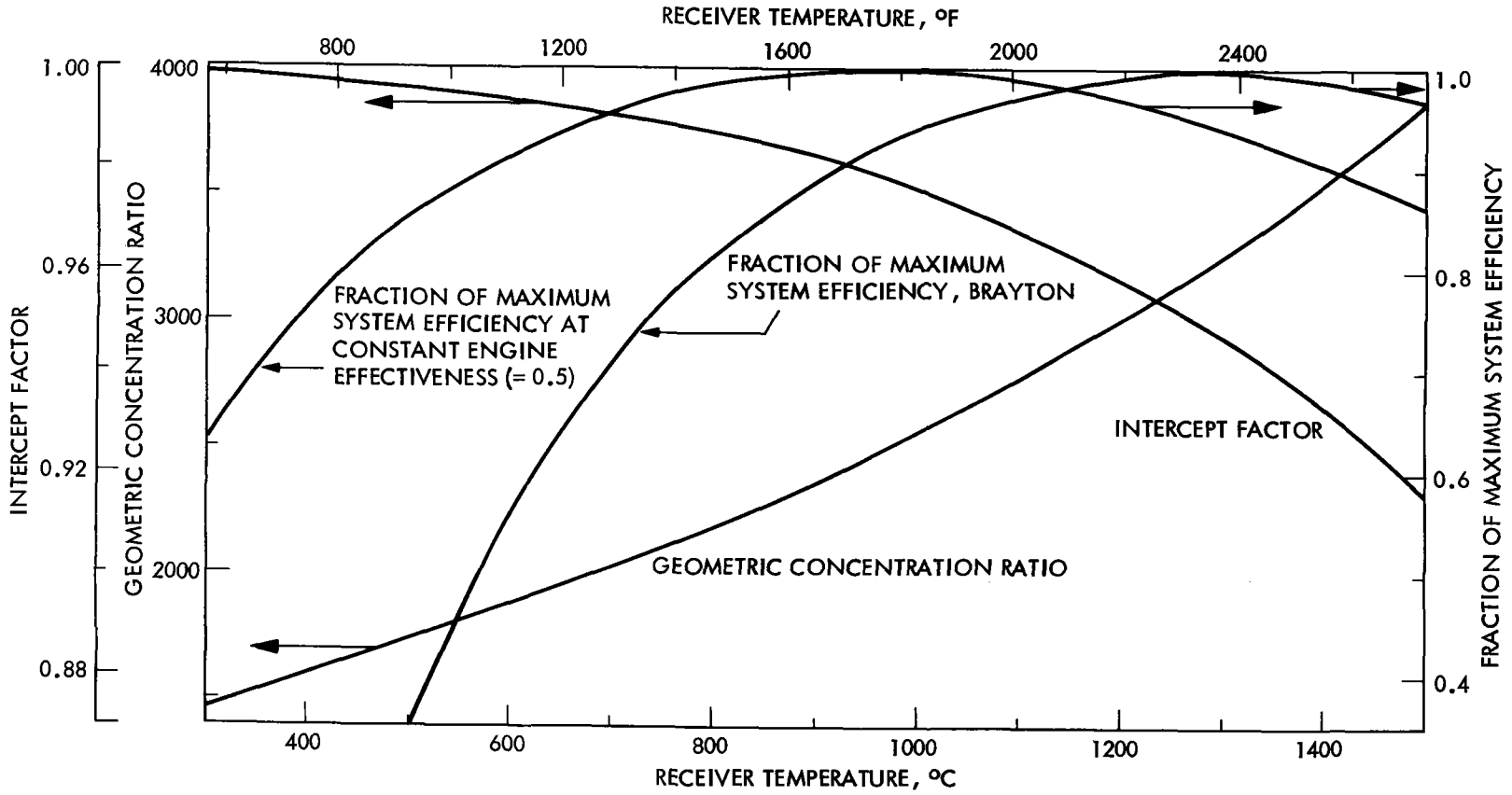

Figure 17b. Effect of Receiver Temperature on Power Conversion and System Efficiency with Engines of Differing Characteristics: System Efficiency As Function of Maximum System Efficiency, Geometric Concentration Ratio, and Intercept Factor.

Baseline system, except as noted. Other characteristics as in Figure 16.

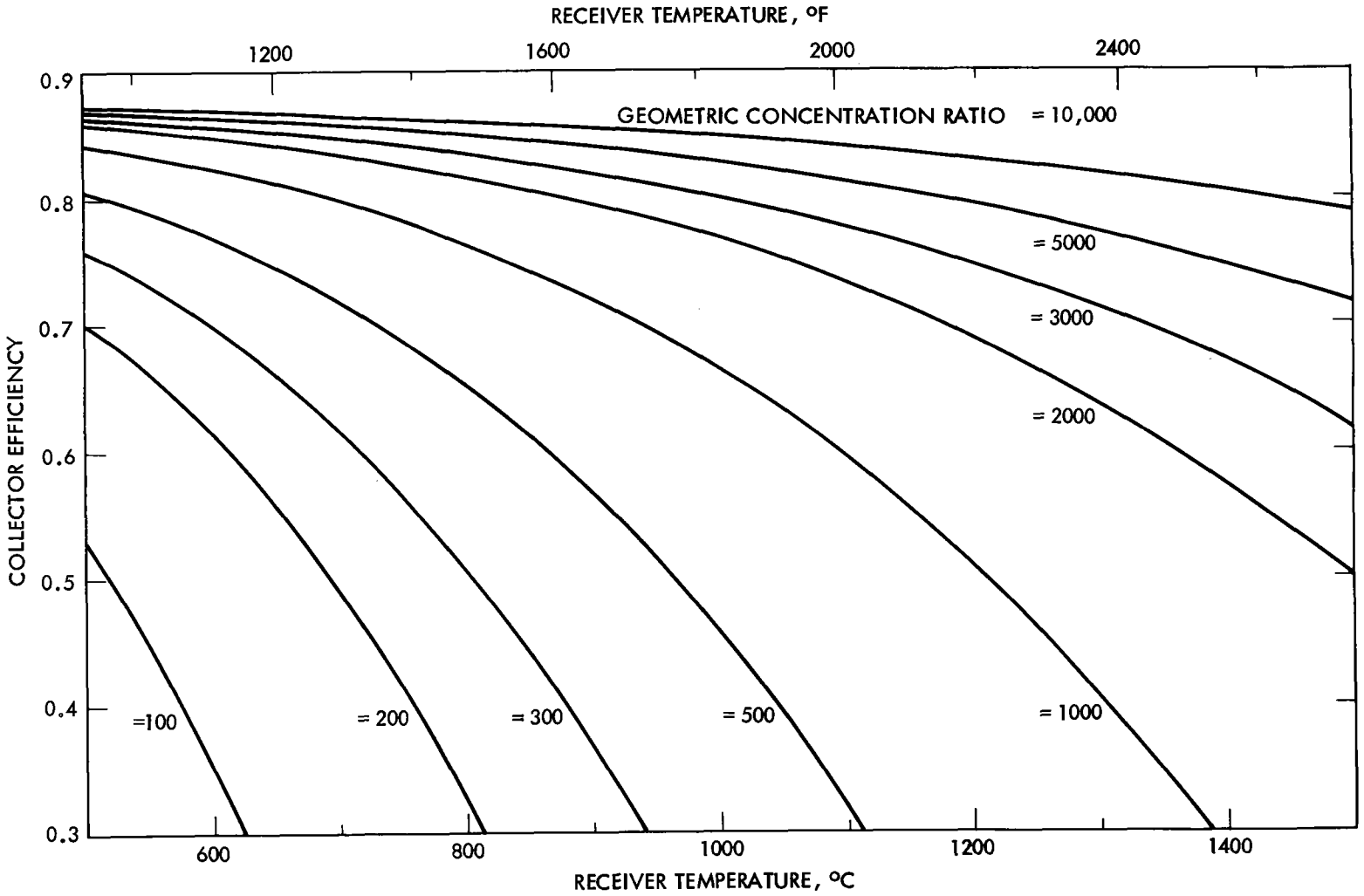

Figure 18a. Effect of Receiver Temperature and Geometric Concentration Ratio upon Collector Efficiency.

Fixed intercept factor. Baseline system except as noted. Brayton power conversion effectiveness as in Figure 16.

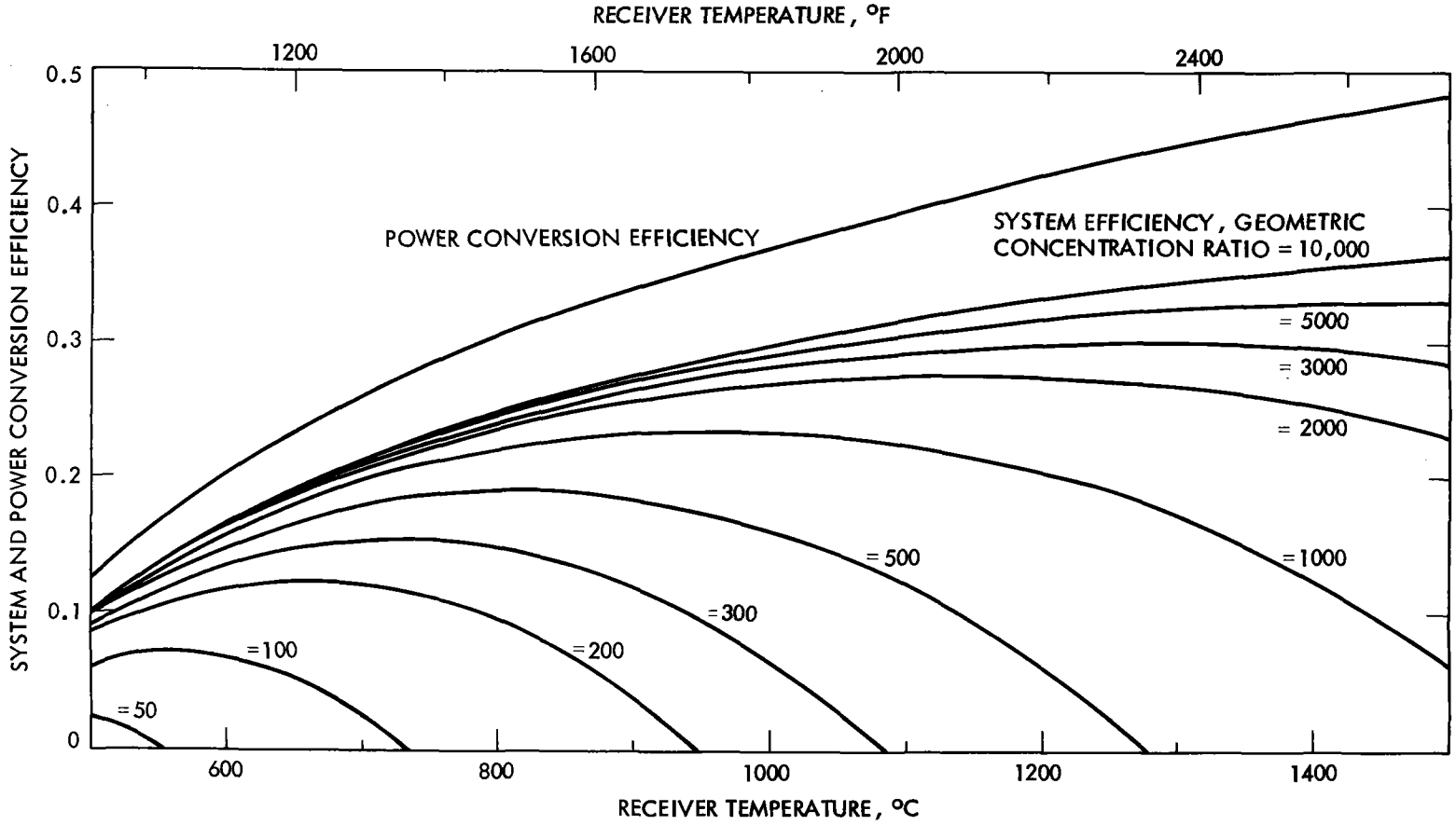

Figure 18b. Effect of Receiver Temperature and Geometric Concentration Ratio upon Power Conversion and System Efficiency.

Fixed intercept factor. Baseline system except as noted. Brayton power conversion effectiveness as in Figure 16.

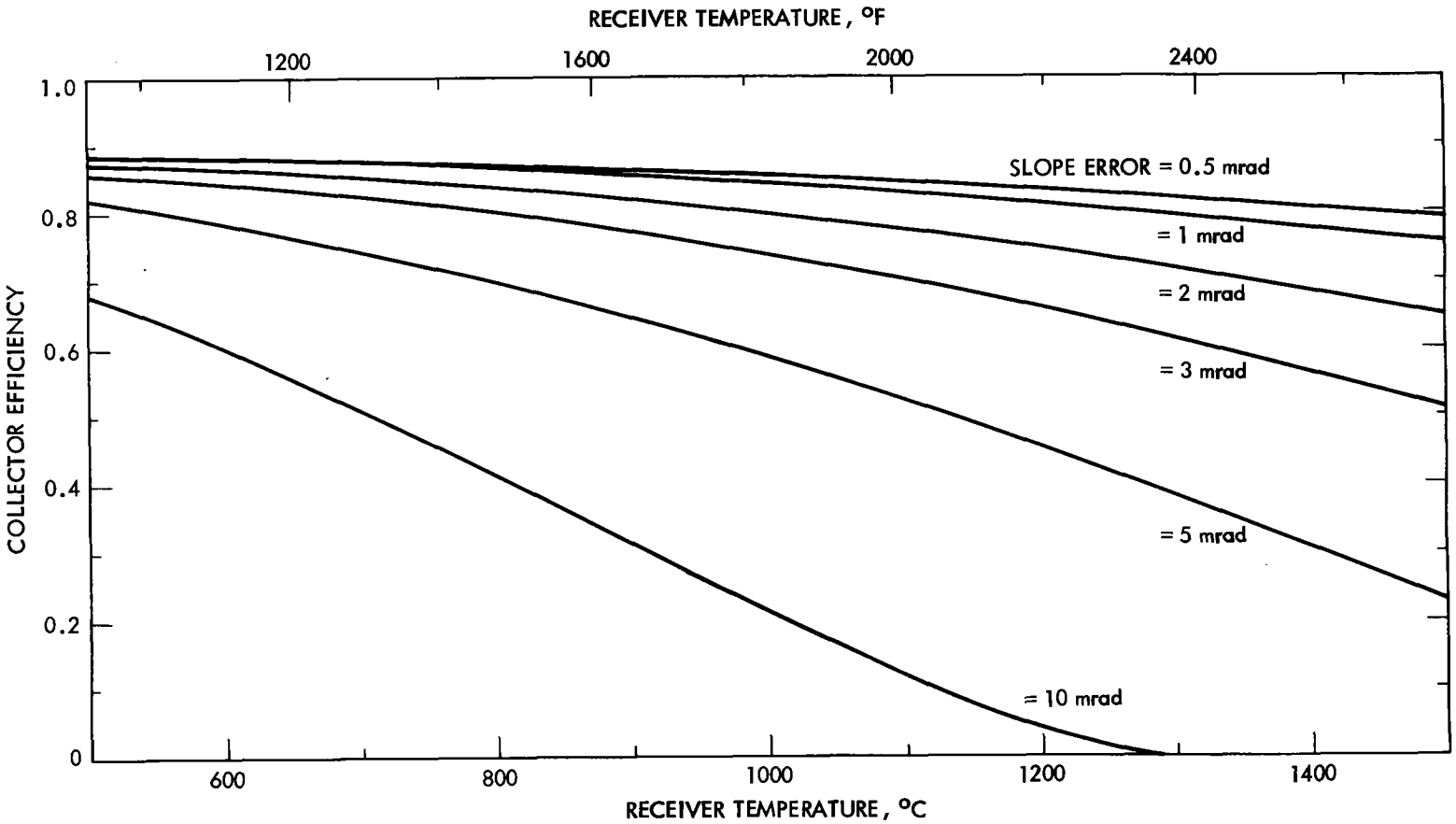

Figure 19a. Effect of Receiver Temperature and Concentrator Slope Error upon Collector Efficiency.

Receiver aperture optimized at each temperature. Baseline system except as noted. Brayton power conversion efficiencies as in Figure 16.

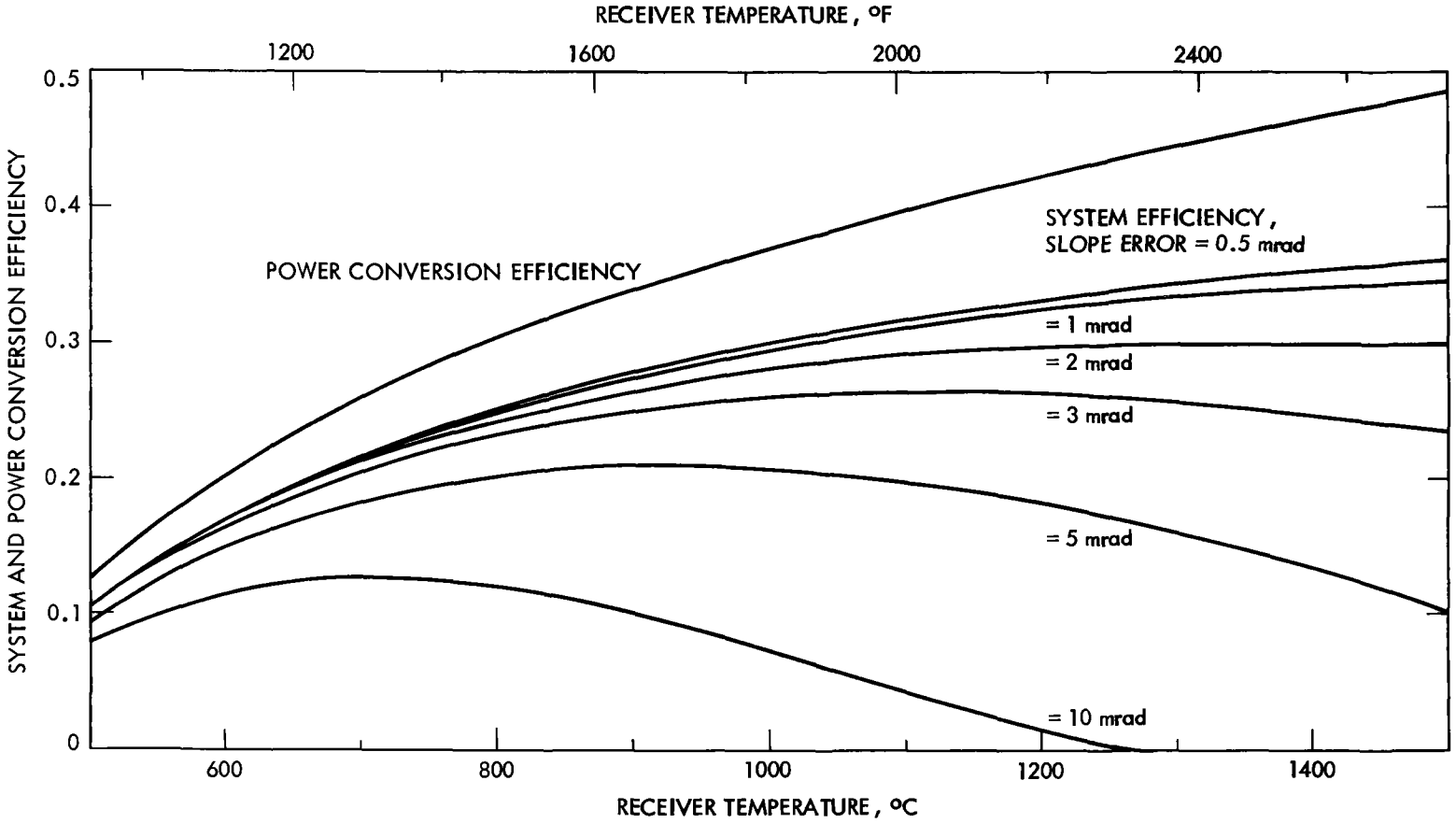

Figure 19b. Effect of Receiver Temperature and Concentrator Slope Error upon Power Conversion and System Efficiency.

Receiver aperture optimized at each temperature. Baseline system except as noted. Brayton power conversion efficiencies as in Figure 16.

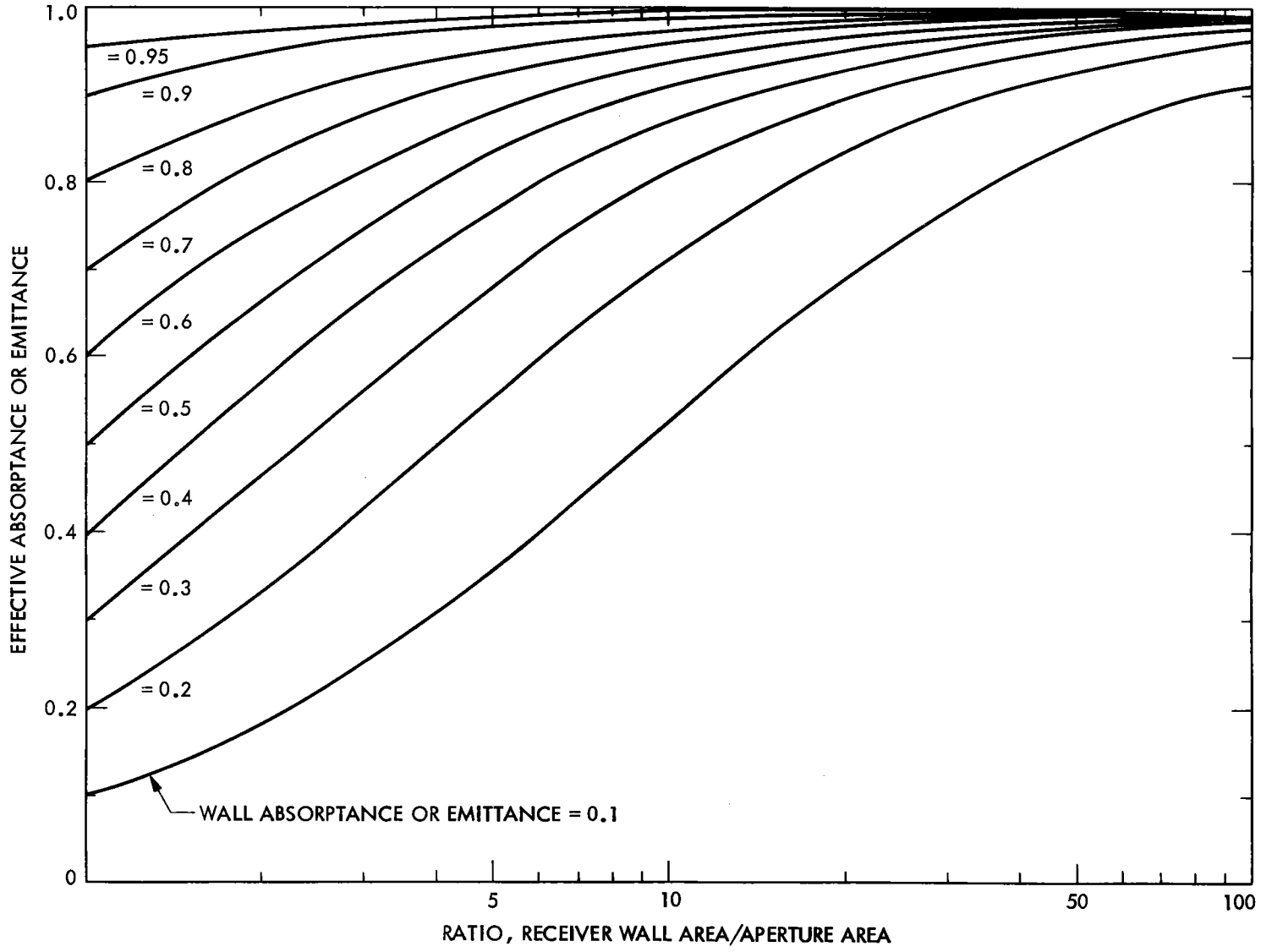

Figure 20. Effective Absorptance or Emittance of Receiver Aperture Versus Absorptance or Emittance of Interior Wall for a Cavity Receiver. (Holraum approximation: Aperture area small compared to total surface of cavity.)

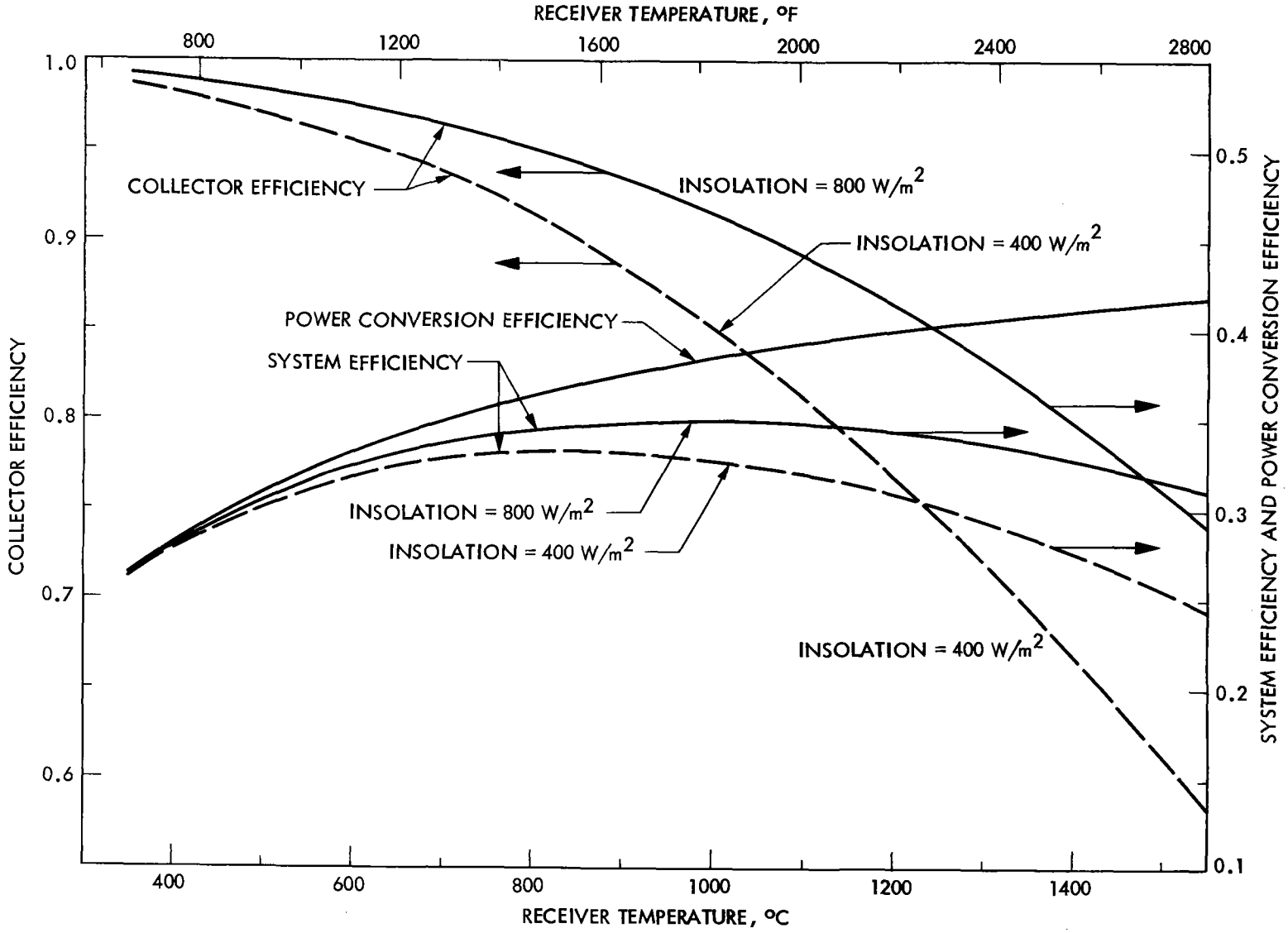

Figure 21. Effect of Insolation Level upon Optimization of Receiver Temperature. Receiver aperture optimized at each temperature. Idealized System.

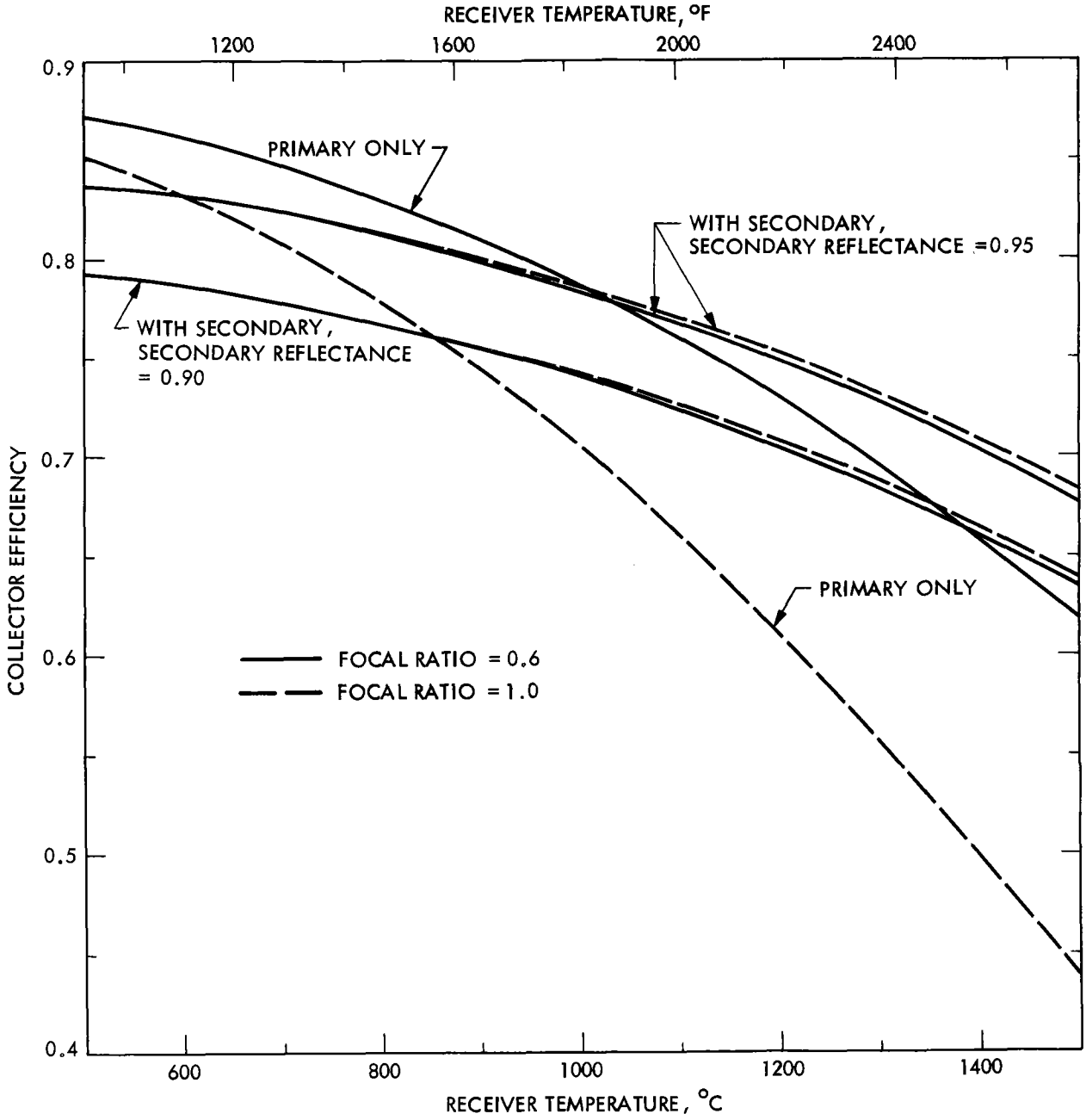

Figure 22a. Effect of Secondary Concentrator on Collector Efficiency. (Baseline system except as noted. Focal ratios 0.6 and 1.0.)

Secondary concentrator reflectances 0.90 and 0.95. Exit aperture of secondary concentrator coincident with receiver aperture. Secondary geometric concentration ratio maximized at each focal ratio of the primary concentrator (1.96 at $f_r = 0.6$; 4.43 at $f_r = 1.0$).

Receiver aperture (= secondary concentrator exit aperture) optimized at each temperature for each design.

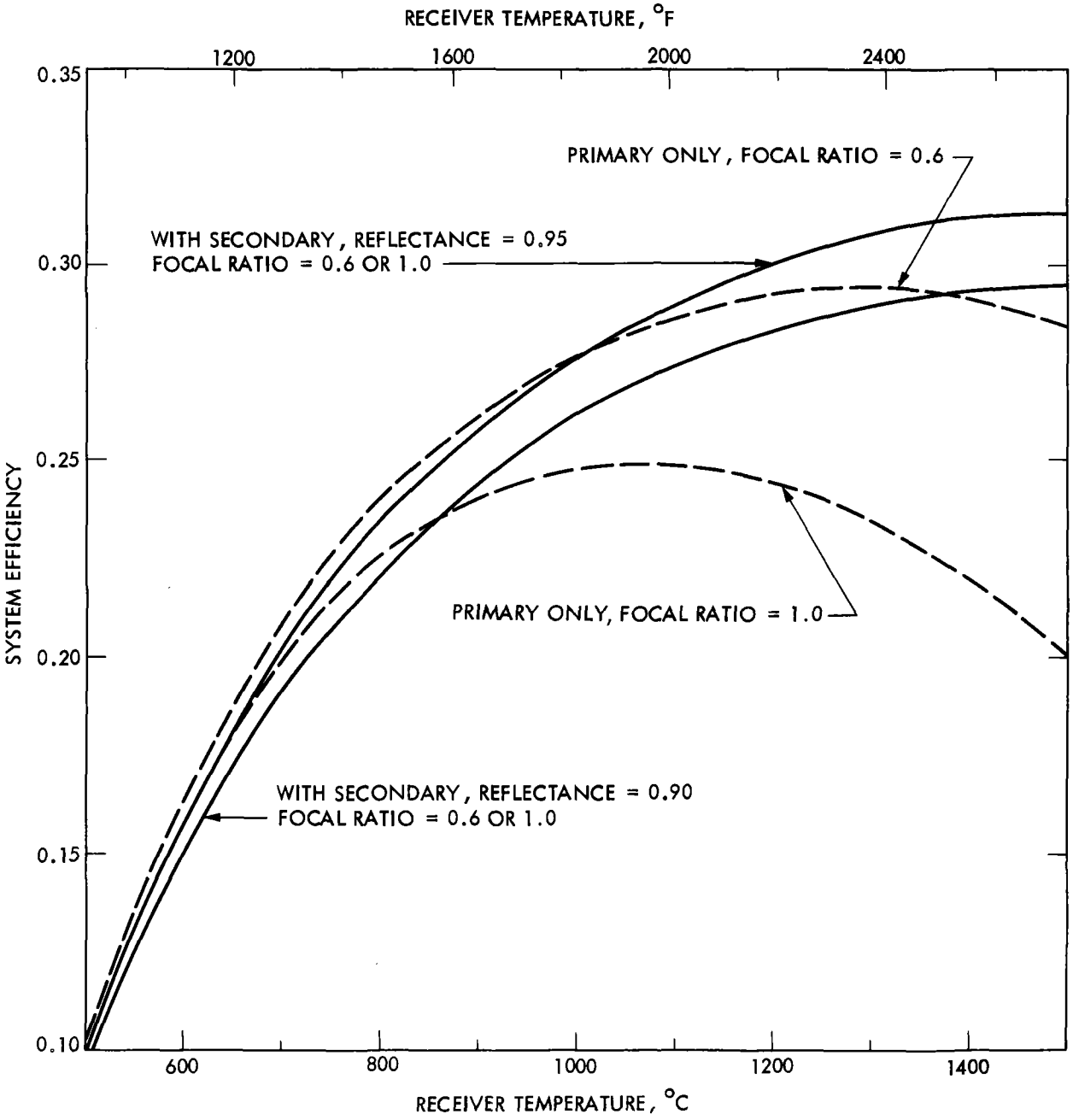

Figure 22b. Effect of Secondary Concentrator on System Efficiency. (Baseline system except as noted. Focal ratios 0.6 and 1.0.)

Secondary concentrator reflectances 0.90 and 0.95. Exit aperture of secondary concentrator coincident with receiver aperture. Secondary geometric concentration ratio maximized at each focal ratio of the primary concentrator (1.96 at $f_r = 0.6$; 4.43 at $f_r = 1.0$).

Receiver aperture (= secondary concentrator exit aperture) optimized at each temperature for each design.

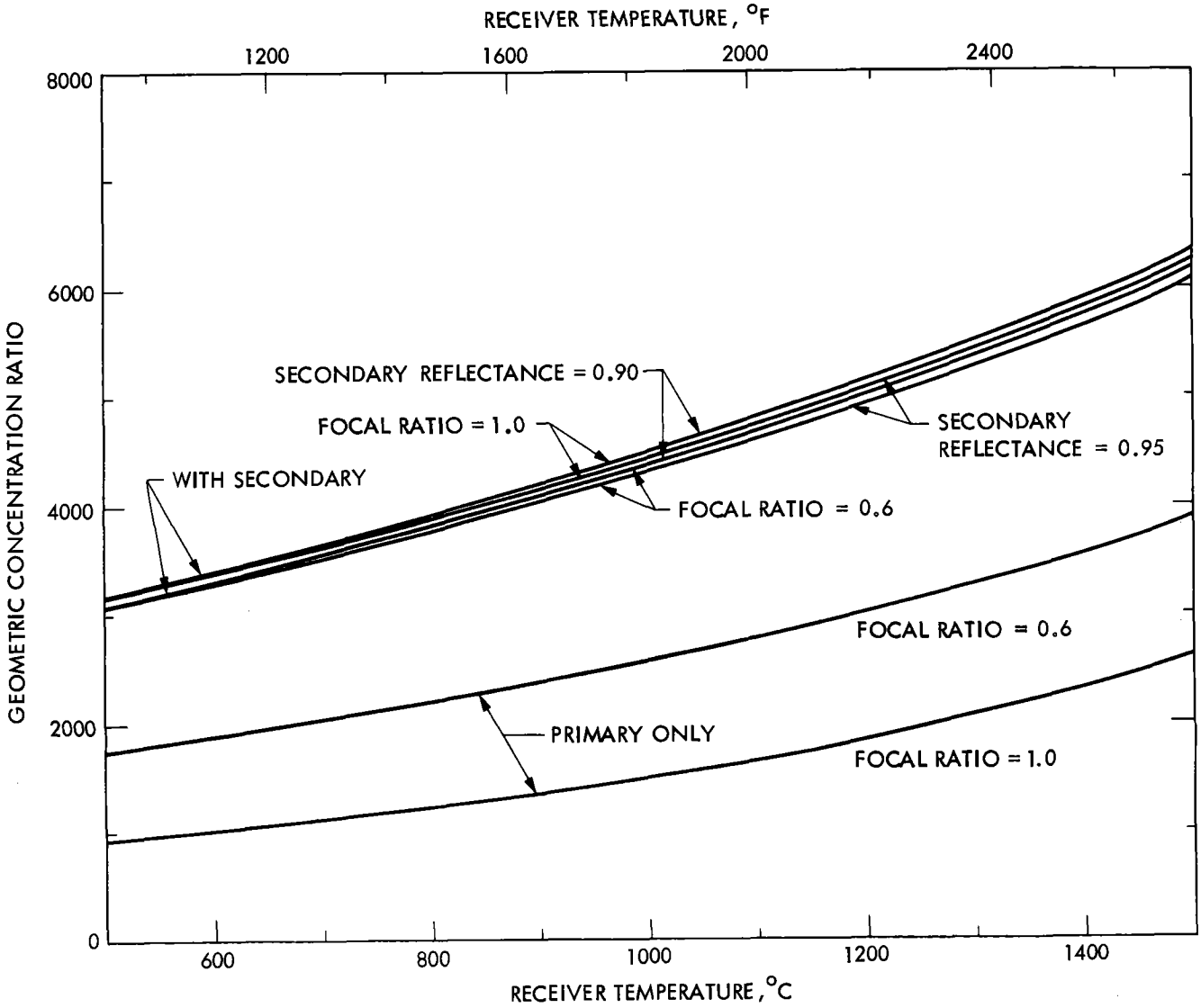

Figure 22c. Effect of Secondary Concentrator on Overall Geometric Concentration Ratio. (Baseline system except as noted. Focal ratios 0.6 and 1.0.)

Secondary concentrator reflectances 0.90 and 0.95. Exit aperture of secondary concentrator coincident with receiver aperture. Secondary geometric concentration ratio maximized at each focal ratio of the primary concentrator (1.96 at $f_r = 0.6$; 4.43 at $f_r = 1.0$).

Receiver aperture (= secondary concentrator exit aperture) optimized at each temperature for each design.

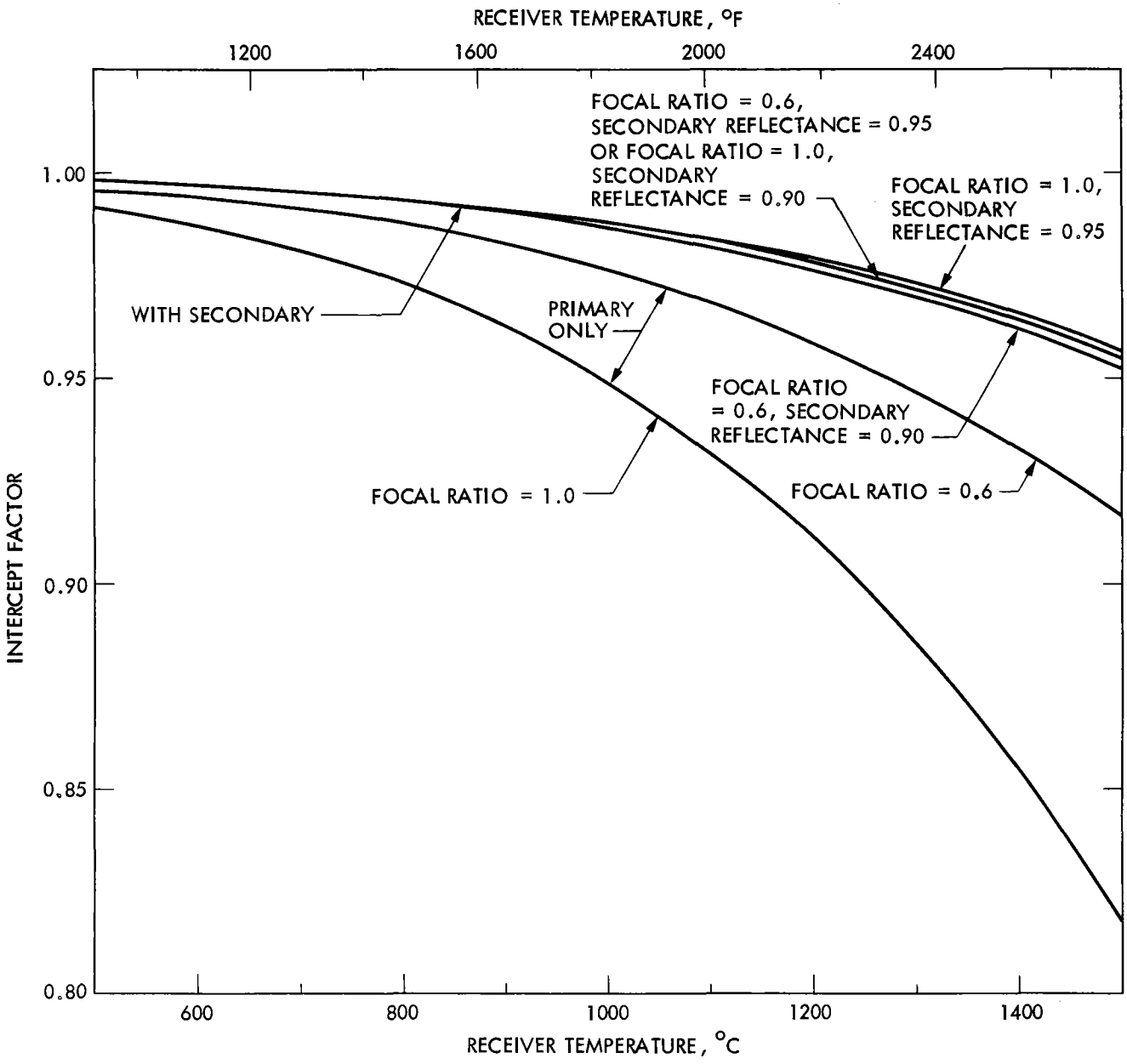

Figure 22d. Effect of Secondary Concentrator on Intercept Factor. (Baseline system except as noted. Focal ratios 0.6 and 1.0.)

Secondary concentrator reflectances 0.90 and 0.95. Exit aperture of secondary concentrator coincident with receiver aperture. Secondary geometric concentration ratio maximized at each focal ratio of the primary concentrator (1.96 at f_r = 0.6; 4.43 at f_r = 1.0).

Receiver aperture (= secondary concentrator exit aperture) optimized at each temperature for each design.

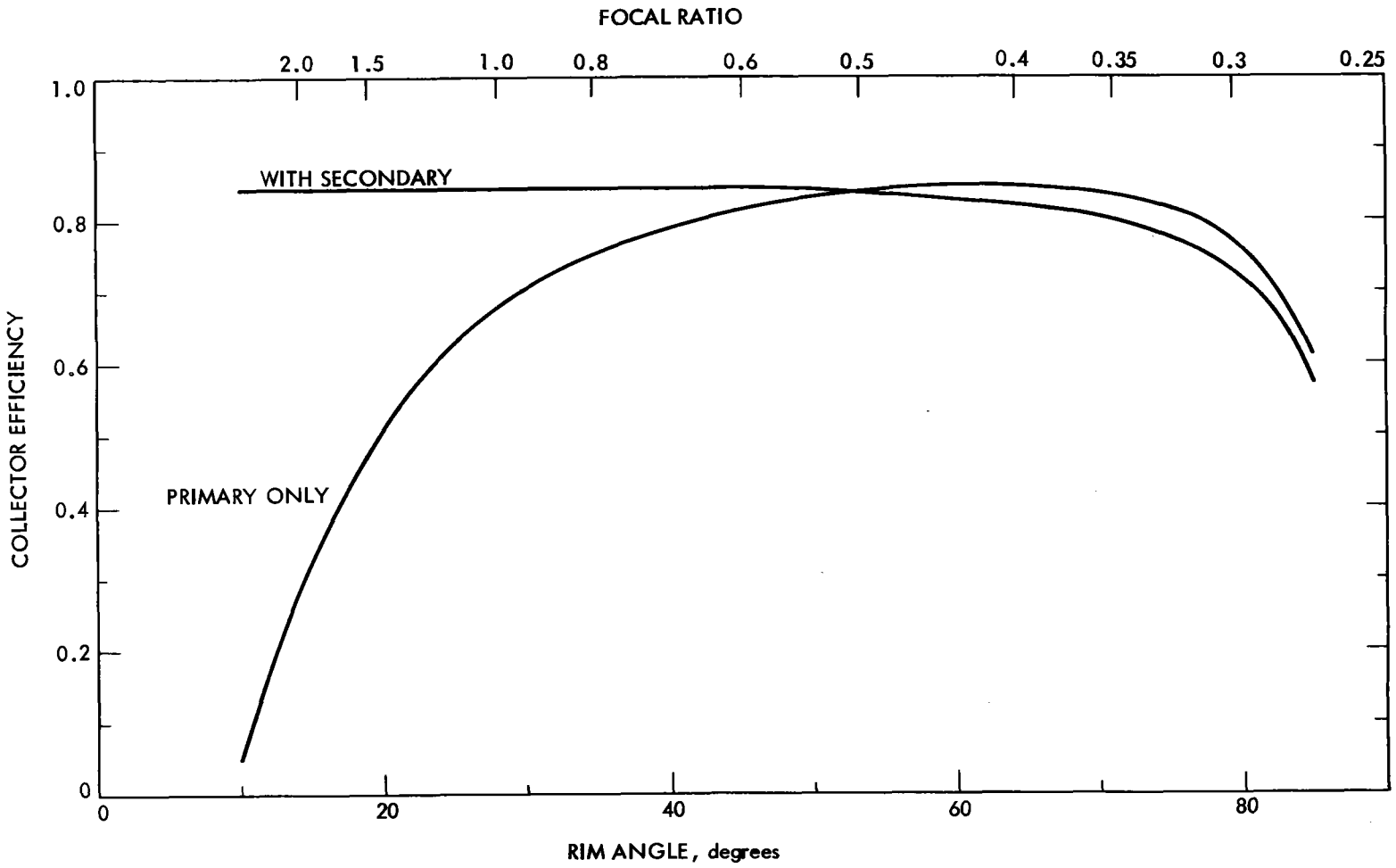

Figure 23a. Effect of Focal Ratio upon Collector Efficiency of Simple and Compound Concentrators. (Based on Duff-Lameiro approximation for primary (Ref.13). Idealized system except as noted.)

Secondary concentrator reflectance 0.95. Exit aperture of secondary concentrator coincident with receiver aperture. Secondary geometric concentration ratio maximized at each focal ratio of the primary concentrator.

Receiver aperture optimized for each design. Receiver temperature 1350°C (2460°F).

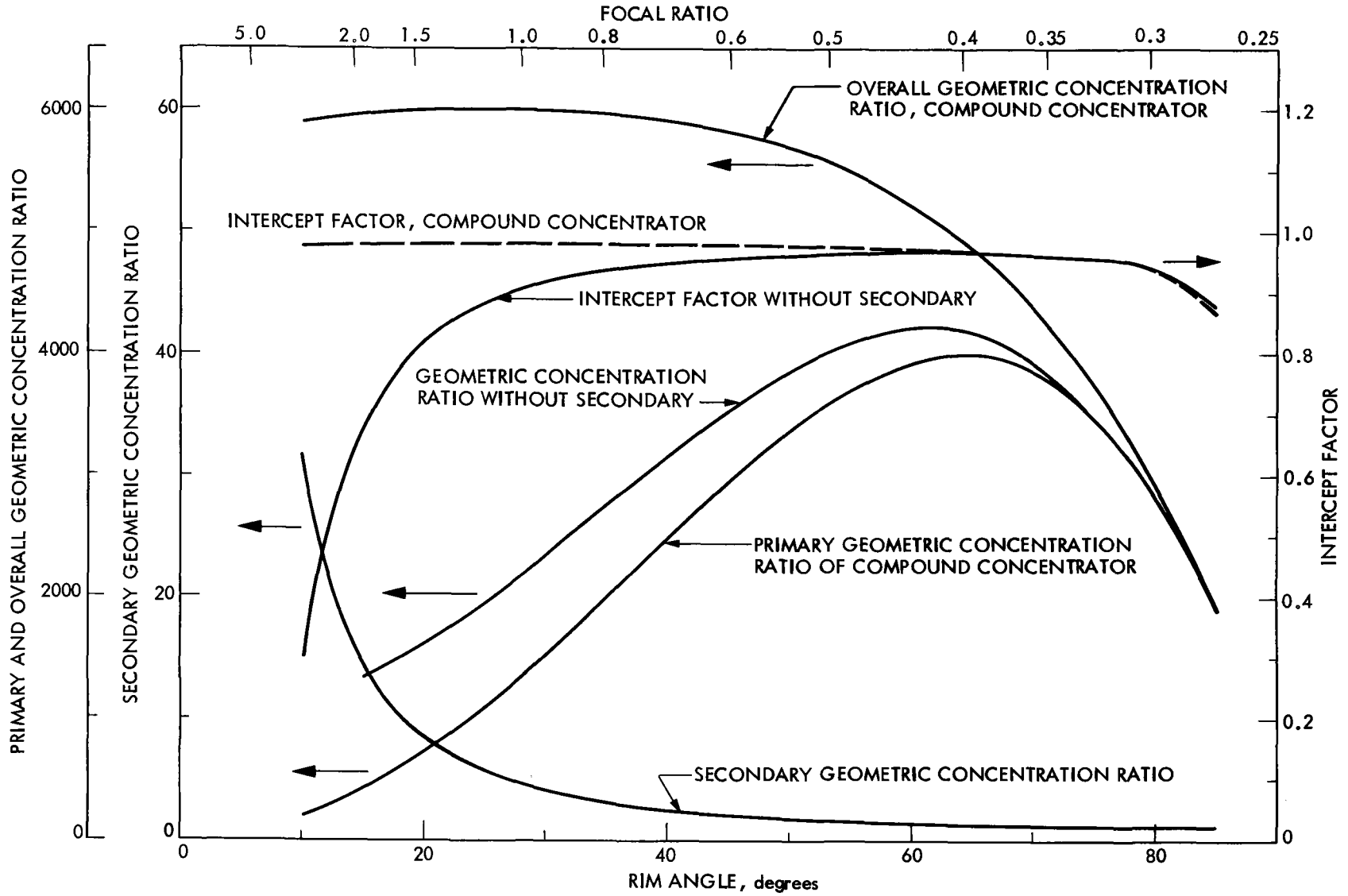

Figure 23b. Effect of Focal Ratio upon Geometric Concentration Ratio and Intercept Factor of Simple and Compound Concentrators. (Based on Duff-Lameiro approximation for primary (Ref. 13). Idealized system except as noted.)

Secondary concentrator reflectance 0.95. Exit aperture of secondary concentrator coincident with receiver aperture. Secondary geometric concentration ratio maximized at each focal ratio of the primary concentrator.

Receiver aperture optimized for each design. Receiver temperature 1350°C (2460°F).

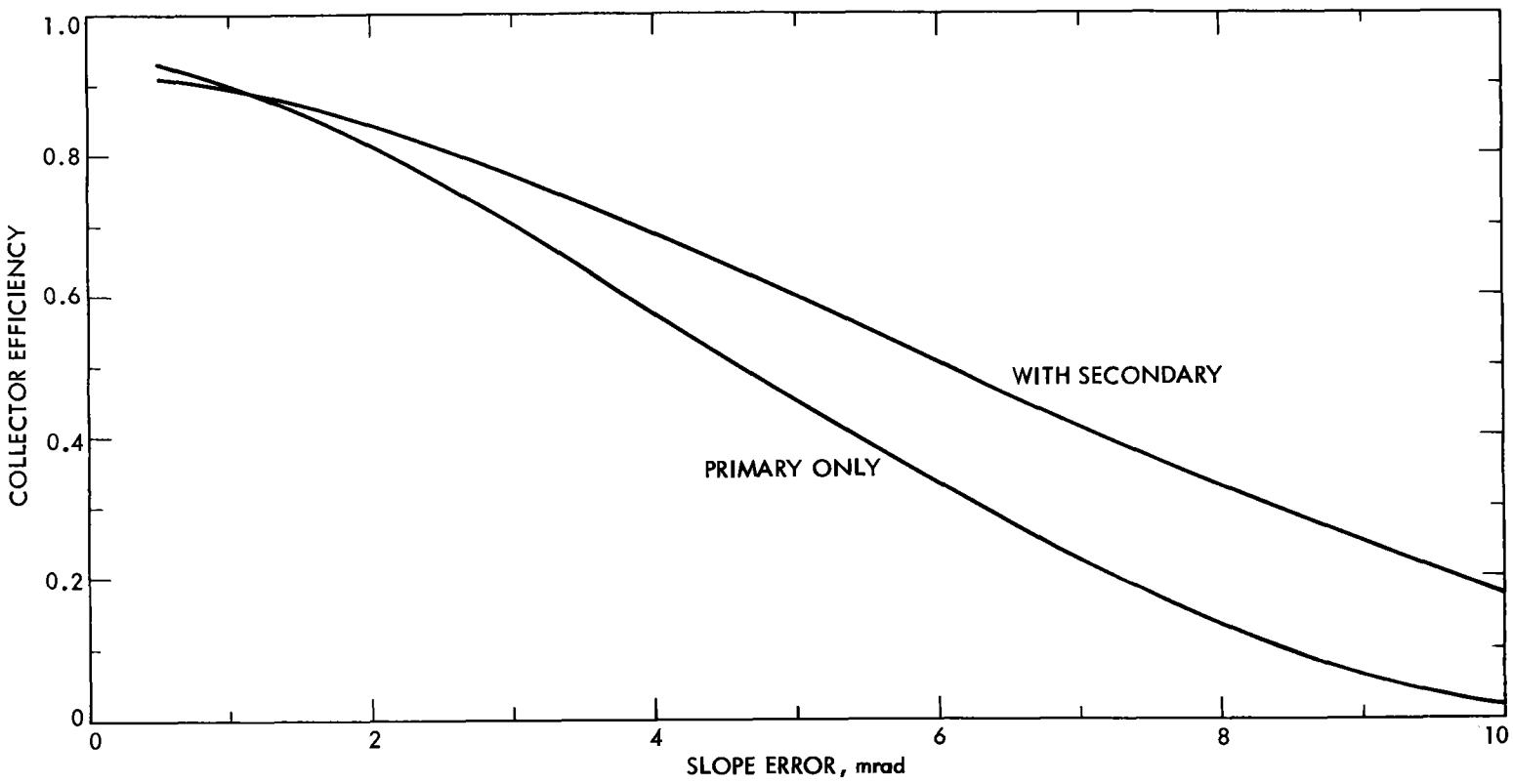

Figure 24a. Effect of Secondary Concentrator on Collector Efficiency with Primary Concentrators of Various Accuracies.

Collector characteristics as for Figure 23. Focal ratio 0.6.

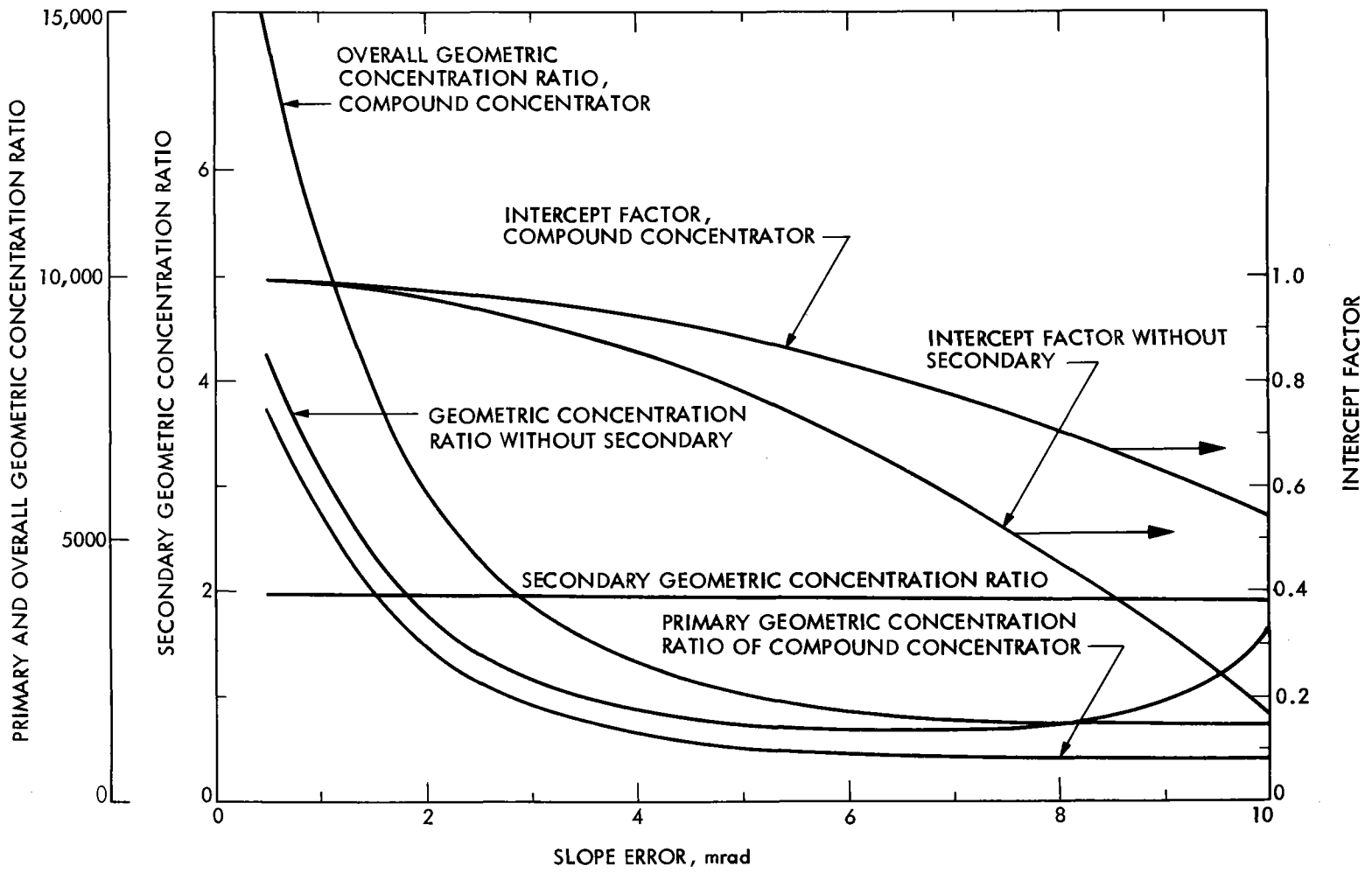

Figure 24b. Effect of Secondary Concentrator on Geometric Concentration Ratio and Intercept Factor with Primary Concentrators of Various Accuracies.

Collector characteristics as for Figure 23. Focal ratio 0.6.

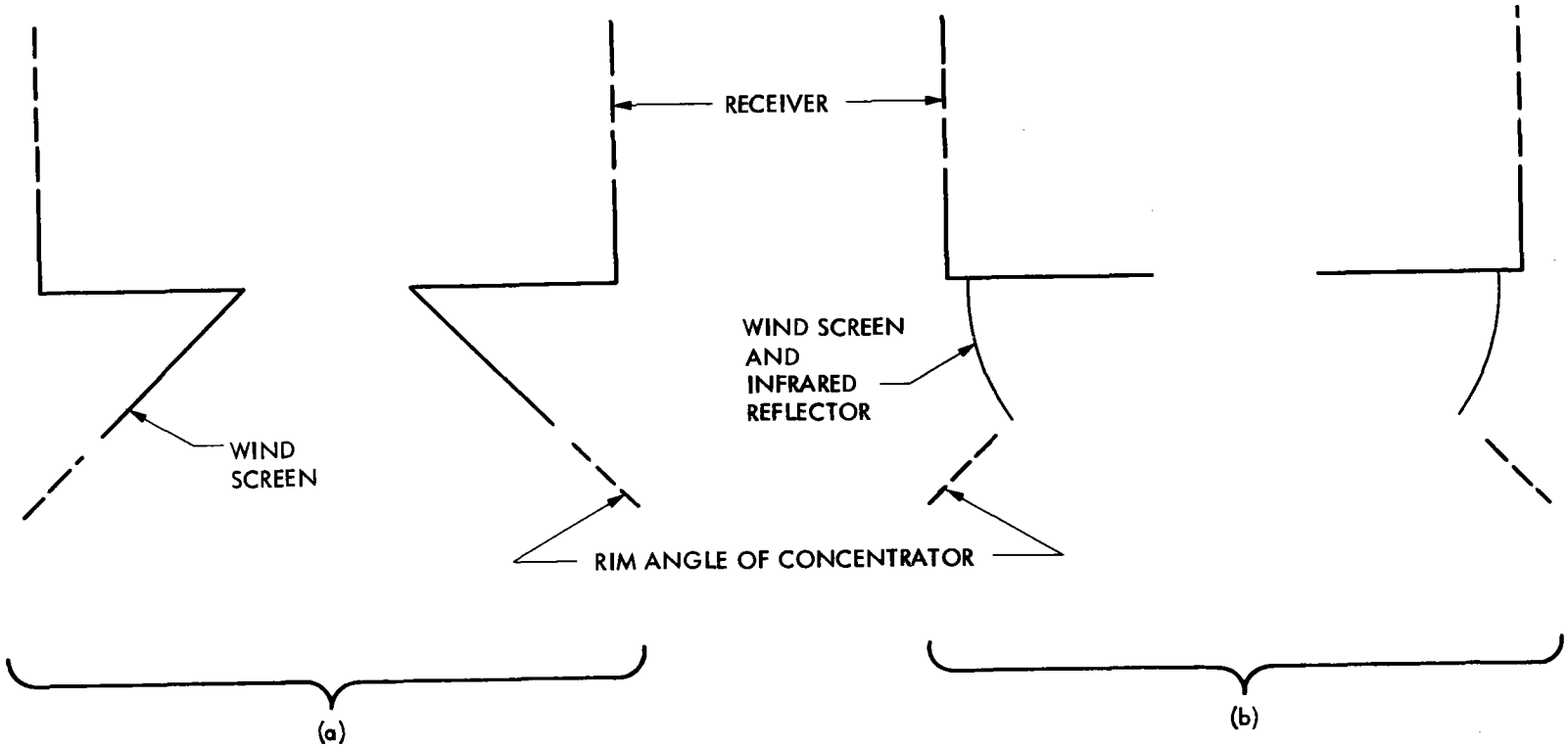

Figure 25. Wind Screens and Infrared Reflector.

a) Conical wind screen. Can also serve as secondary concentrator; compare Figure 4b.

b) Spherical section wind screen. Can also serve as infrared reflector to return emitted radiation to receiver.

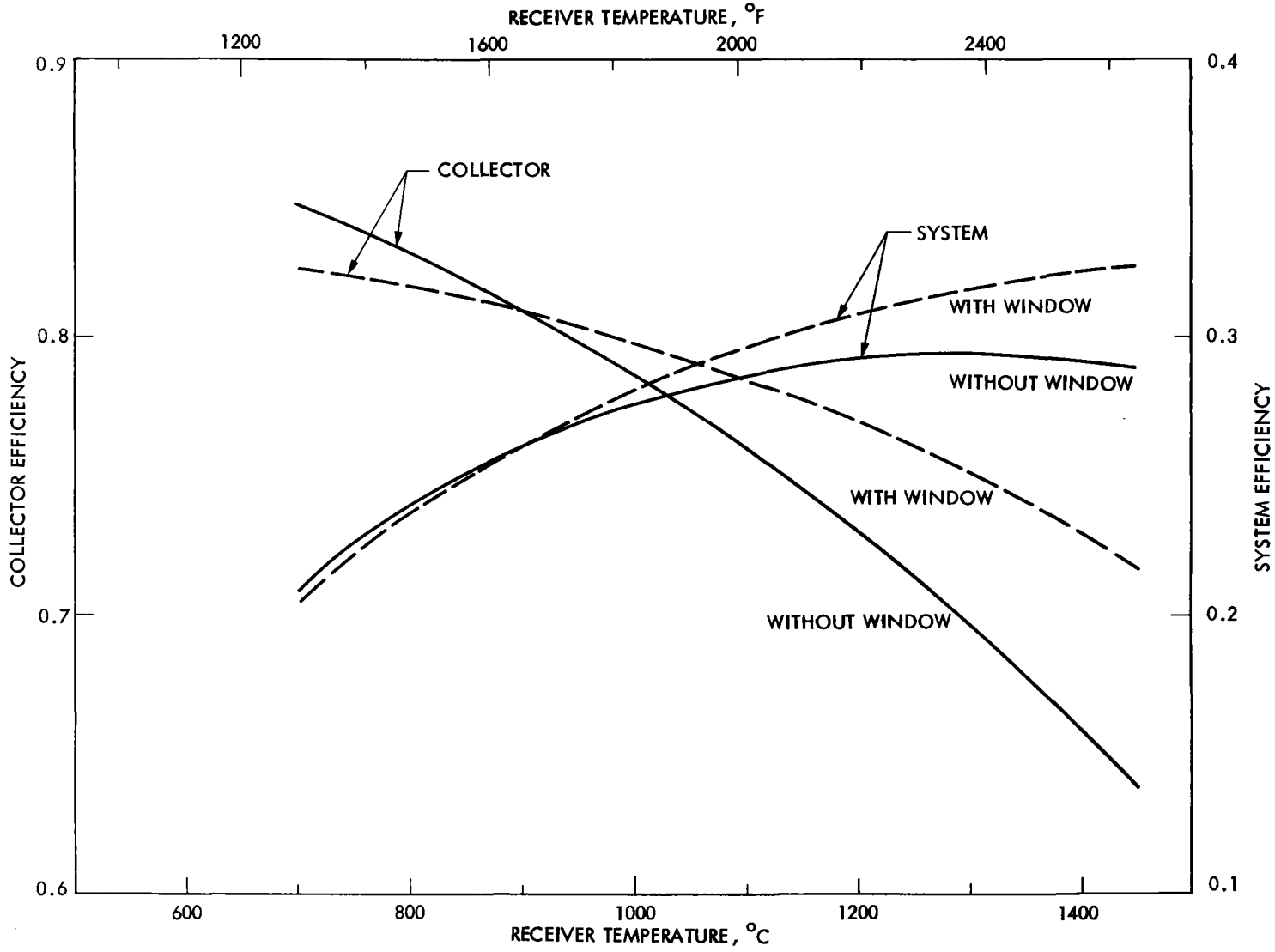

Figure 26. Effect of Receiver Temperature on Collector and System Efficiency With and Without a Window.

Receiver aperture optimized. Baseline system, except as noted. With window, effective receiver absorptance 0.92 (due to reflection), convection coefficient 0.0, effective emittance 0.236, 0.245, 0.261, 0.288, 0.305, 0.322, 0.339, 0.356 at 704, 760, 871, 982, 1093, 1204, 1316, 1427°C, respectively (based on data of Ref. 32). Brayton power conversion effectivess as in Figure 16.

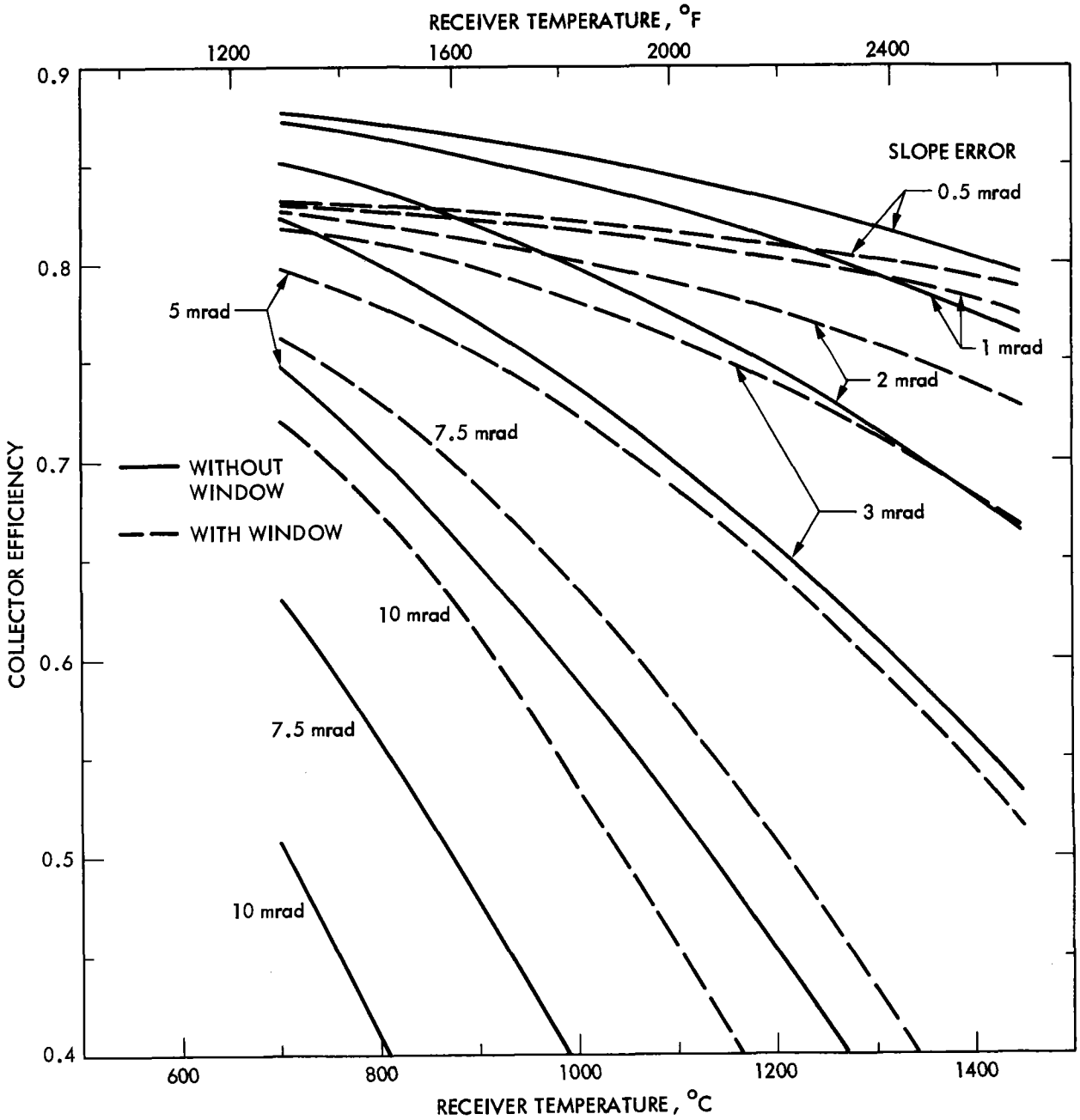

Figure 27. Effect of Window on Collector Performance at Various Concentrator Slope Errors and Receiver Temperatures.

Receiver aperture optimized. Baseline system except as noted. Receiver loss coefficients with window: same as for Figure 2b.

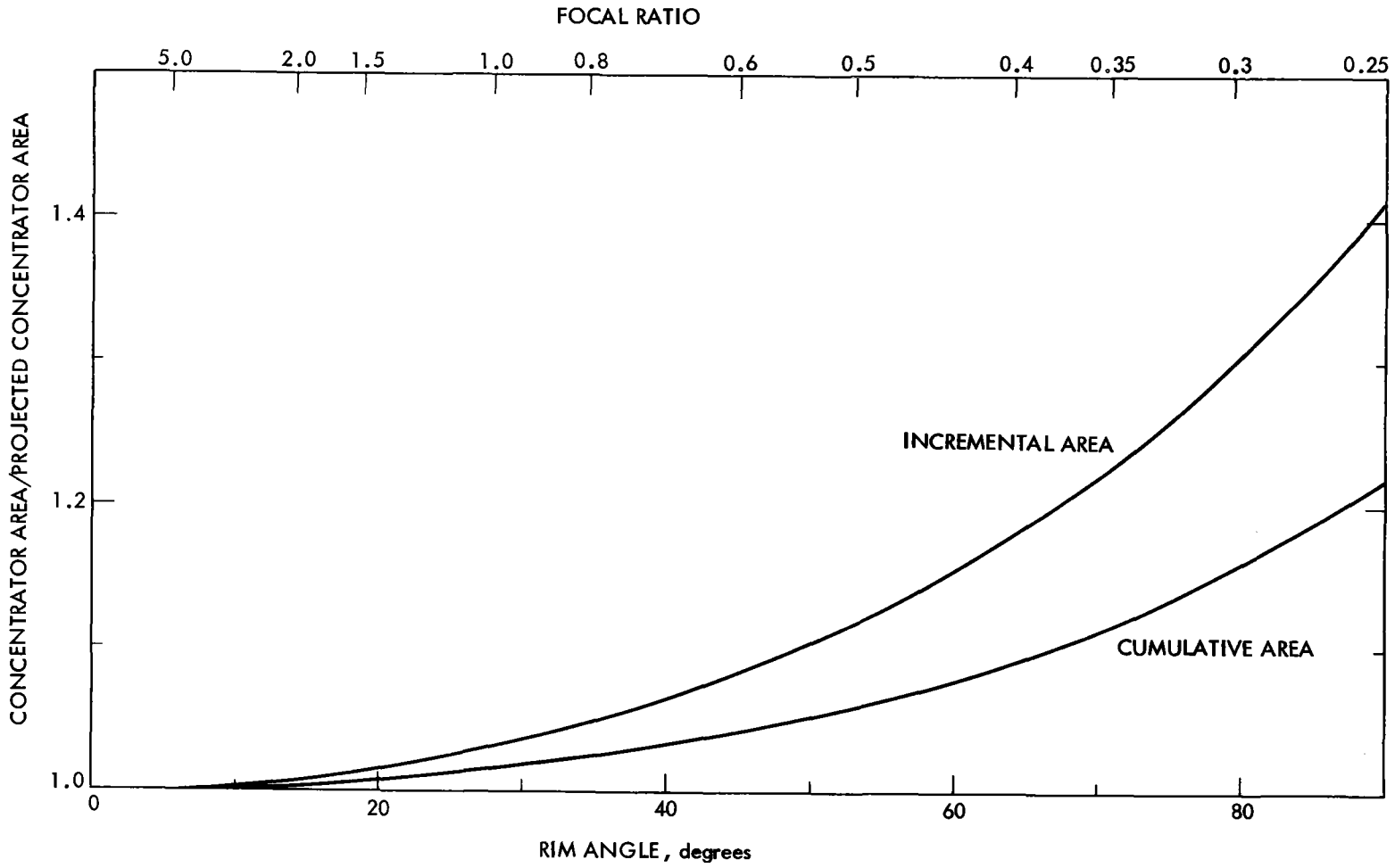

Figure 28. Effect of Focal Ratio upon Ratio of Concentrator Area to Projected Concentrator Area.

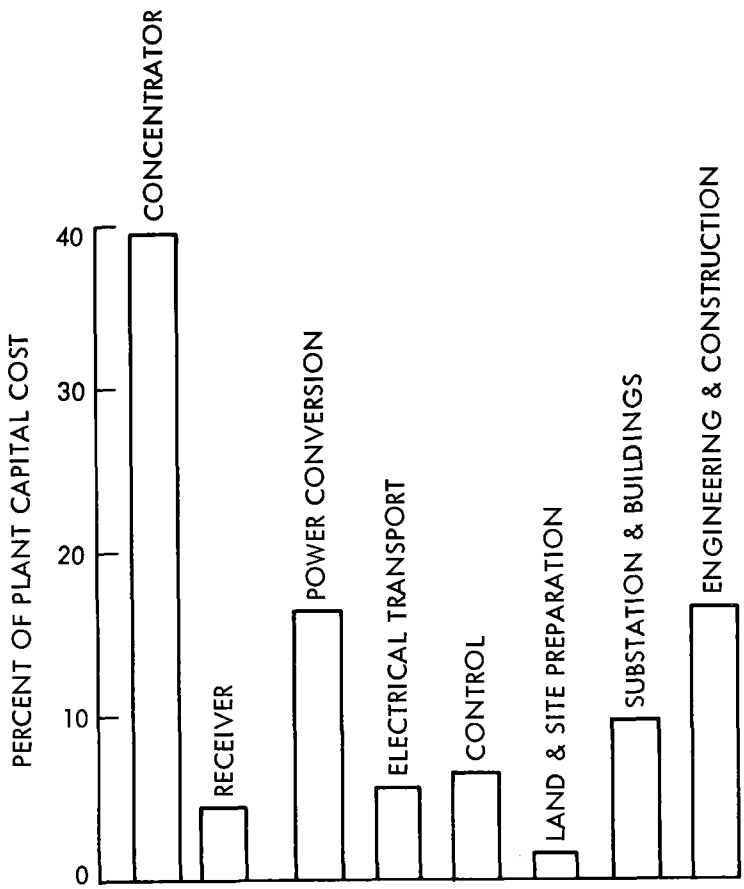

Figure 29. Distribution of Capital Costs for Solar Thermal Power Plant. (Projected.)

System type: dish-Brayton electric. Production rate: 25,000 modules per year. Plant size: 5 MWe.

Based on data from Reference 25.

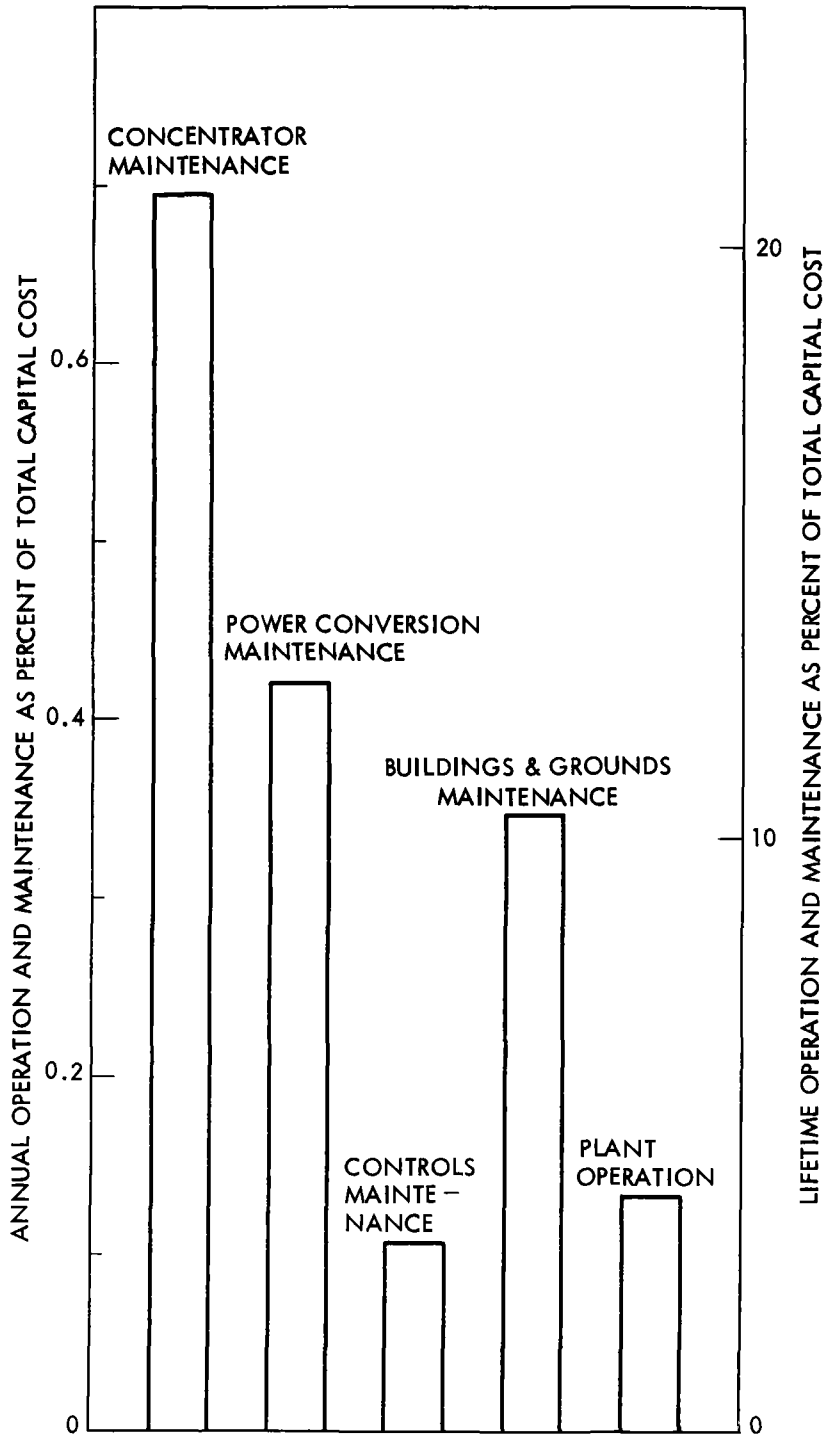

Figure 30. Distribution of Operations and Maintenance Costs for Solar Thermal Power Plant as Percent of Total Cost in Constant Dollars. (Projected.)

Same plant as Figure 29. Plant lifetime 30 years. Based on data of Reference 25.

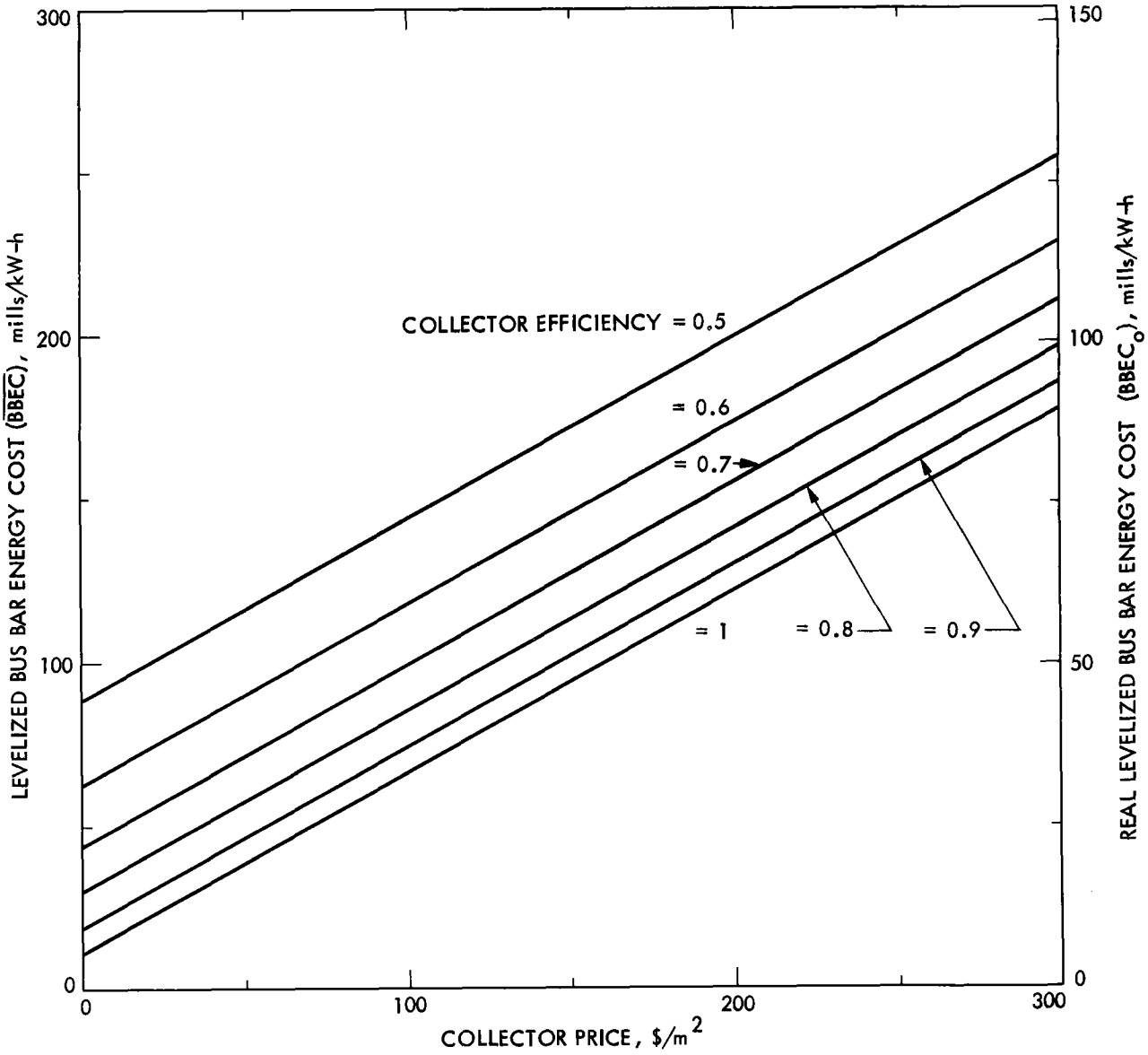

Figure 31. Effect of Collector Price and Efficiency upon Cost of Electricity Produced. (Projected.)

Baseline system except as noted.

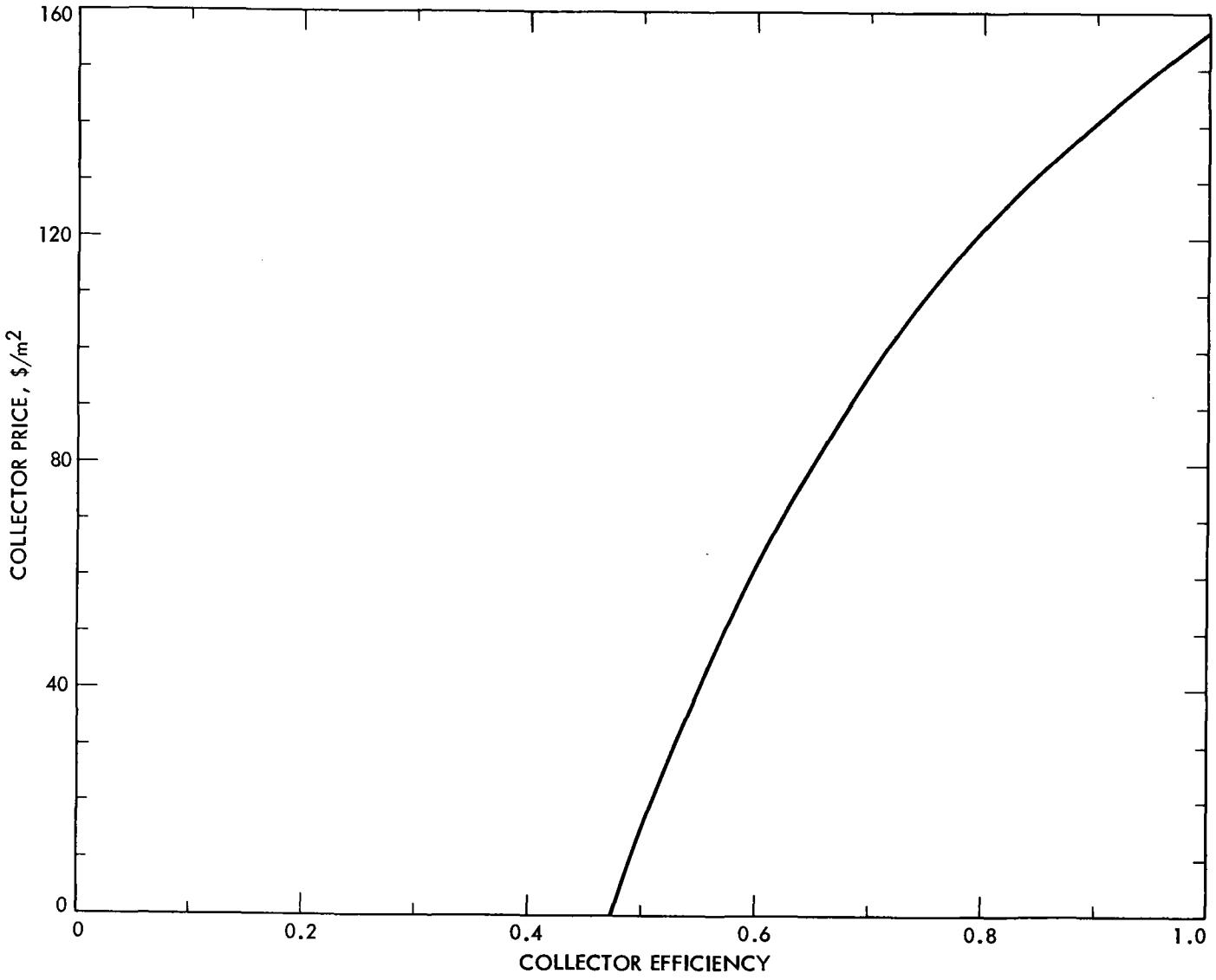

Figure 32. Trade-Off of Collector Price Versus Collector Efficiency at Constant Cost of Electricity Produced. (Projected.)

$\overline{\text{BBEC}}$ = 97 mills/kW-h. Baseline system, except as noted.

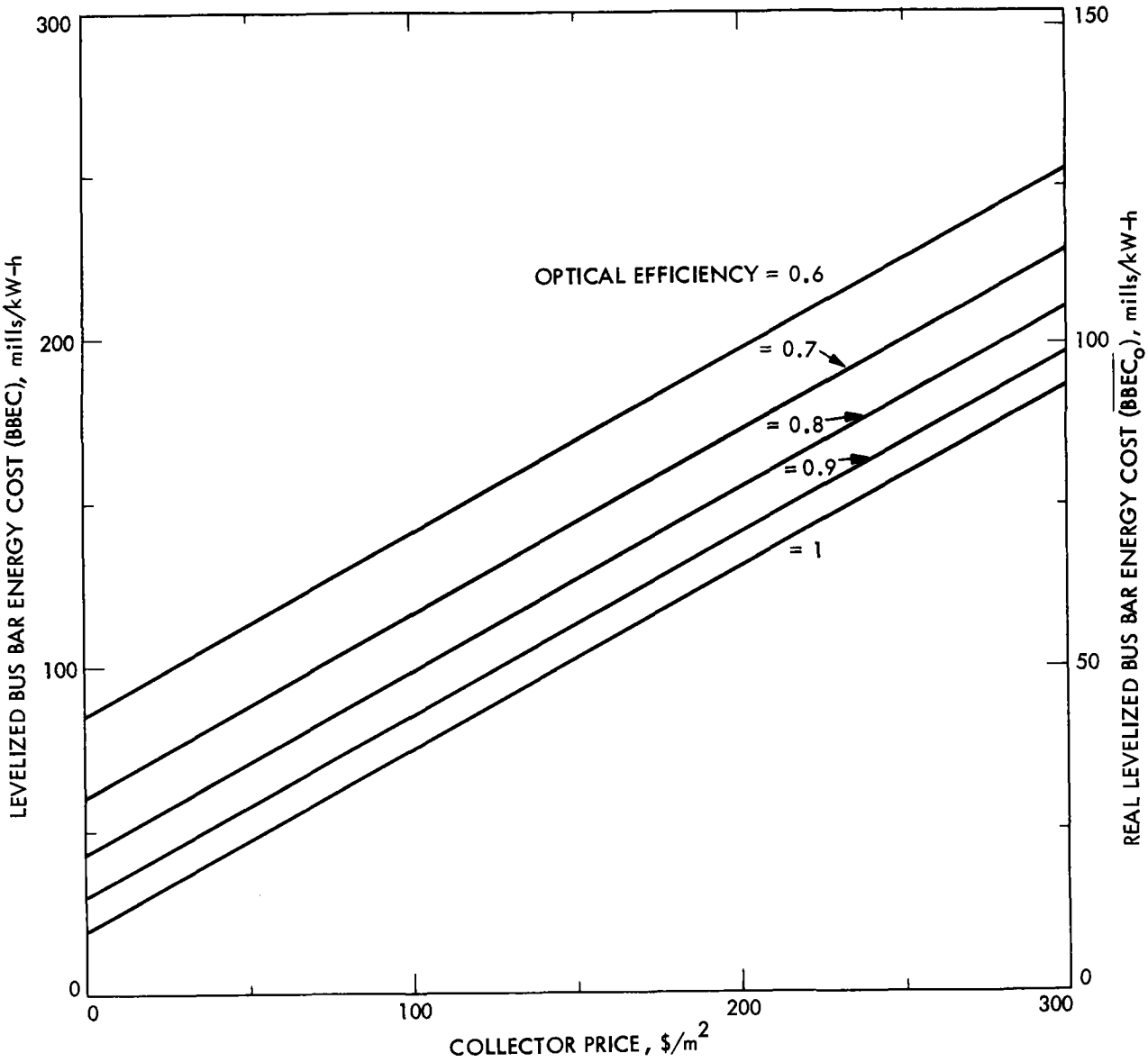

Figure 33. Effect of Optical Efficiency and Collector Price upon Cost of Electricity Produced. (Projected.)

Baseline system except as noted.

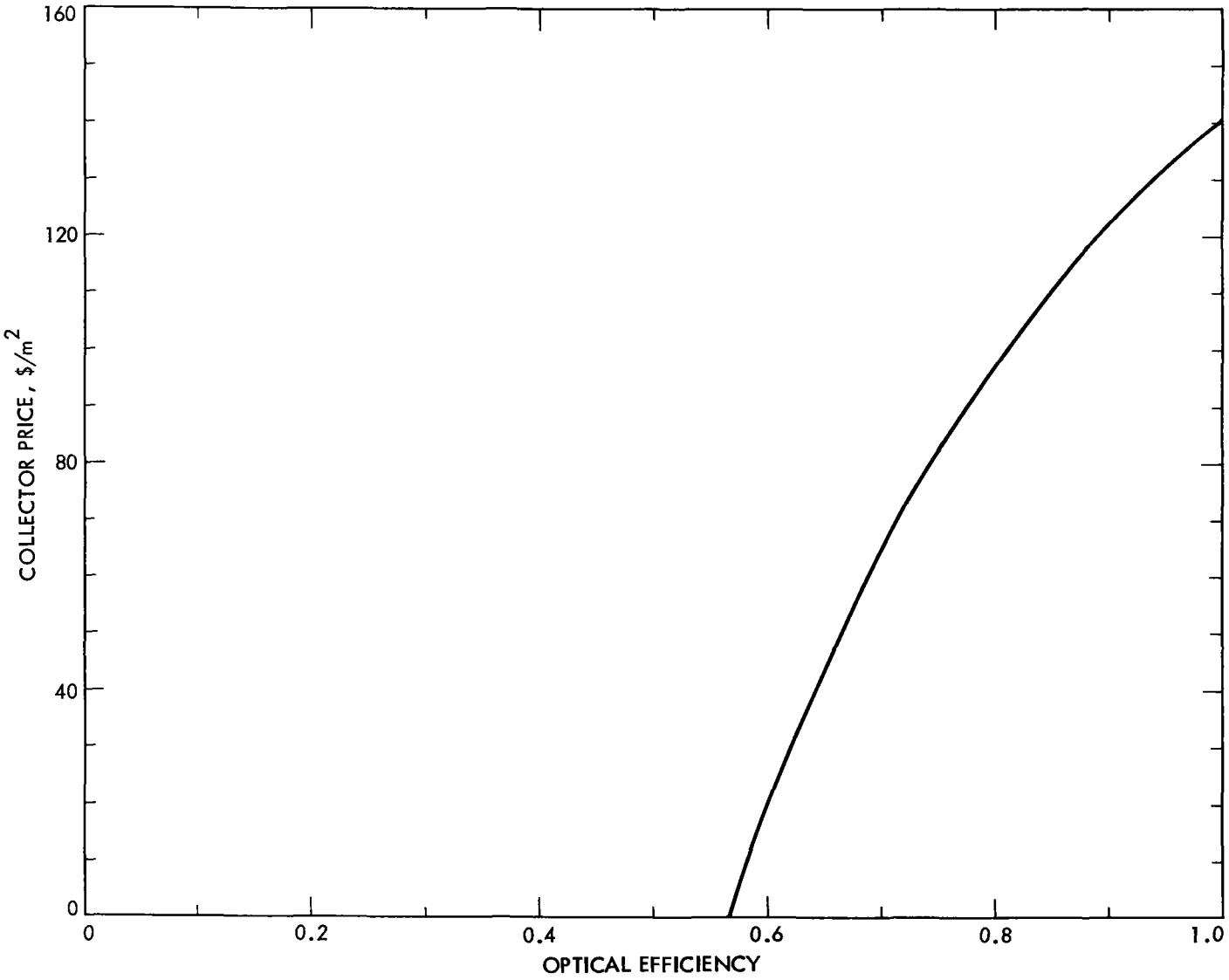

Figure 34. Trade-Off of Collector Price Versus Optical Efficiency at Constant Cost of Electricity Produced. (Projected.)

Baseline system except as noted.

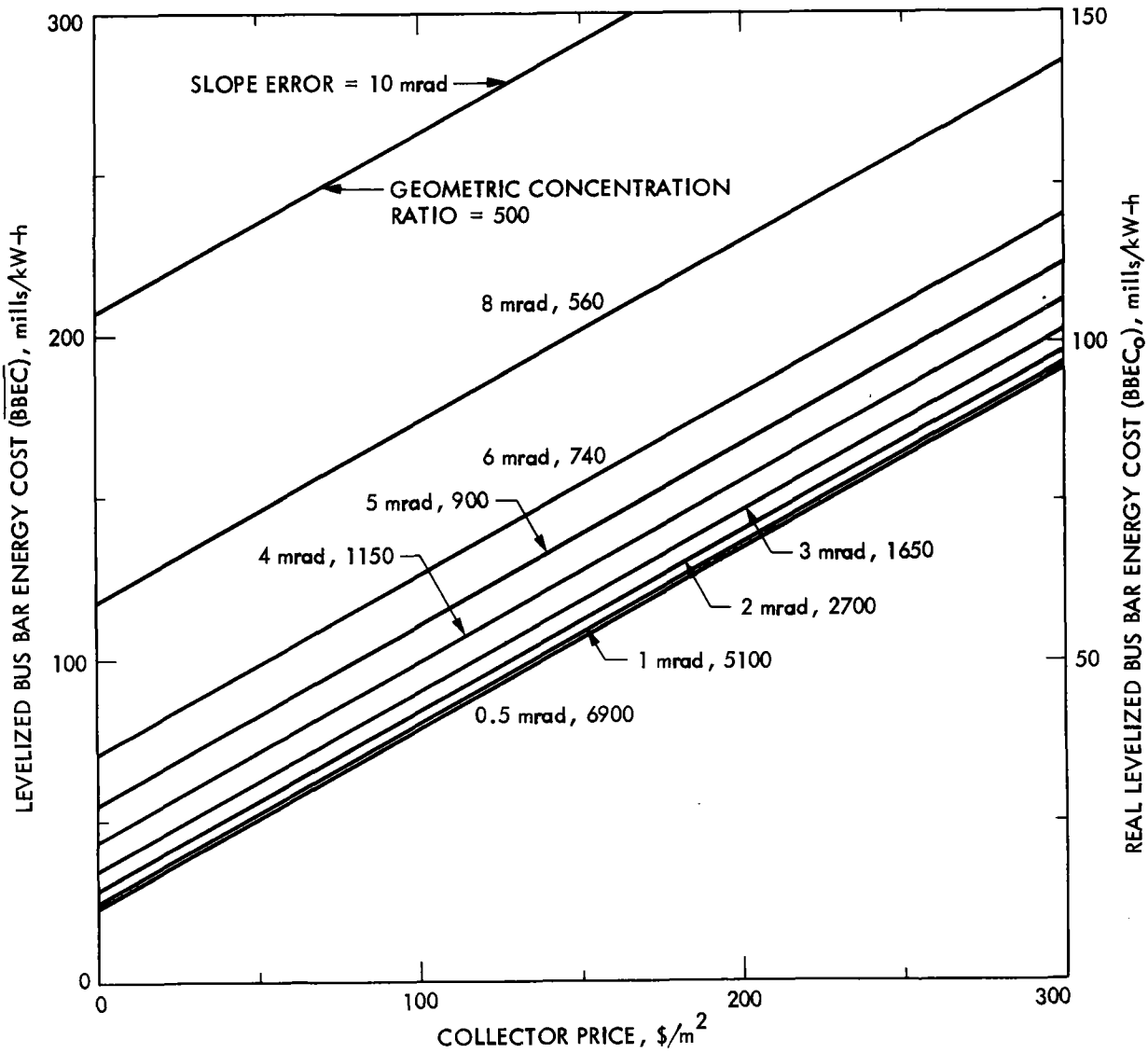

Figure 35. Effect of Slope Error, Geometric Concentration Ratio, and Collector Price upon Cost of Electricity Produced. (Projected.)

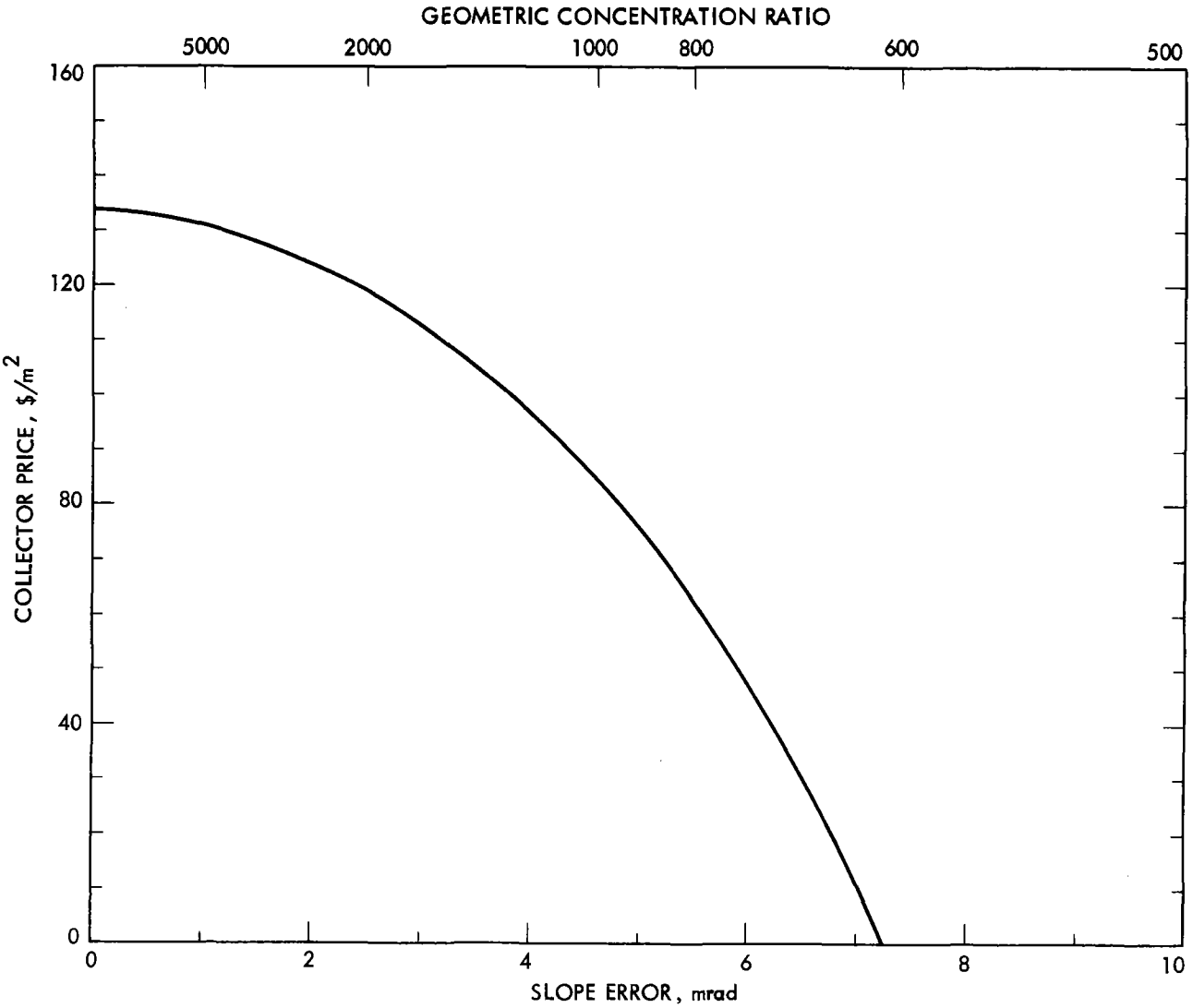

Figure 36. Trade-Off of Collector Price Versus Slope Error and Geometric Concentration Ratio at Constant Cost of Electricity Produced. (Projected.) $\overline{\text{BBEC}}$ = 97 mills/kW-h. Baseline system except as noted. Receiver aperture optimized for each slope error.

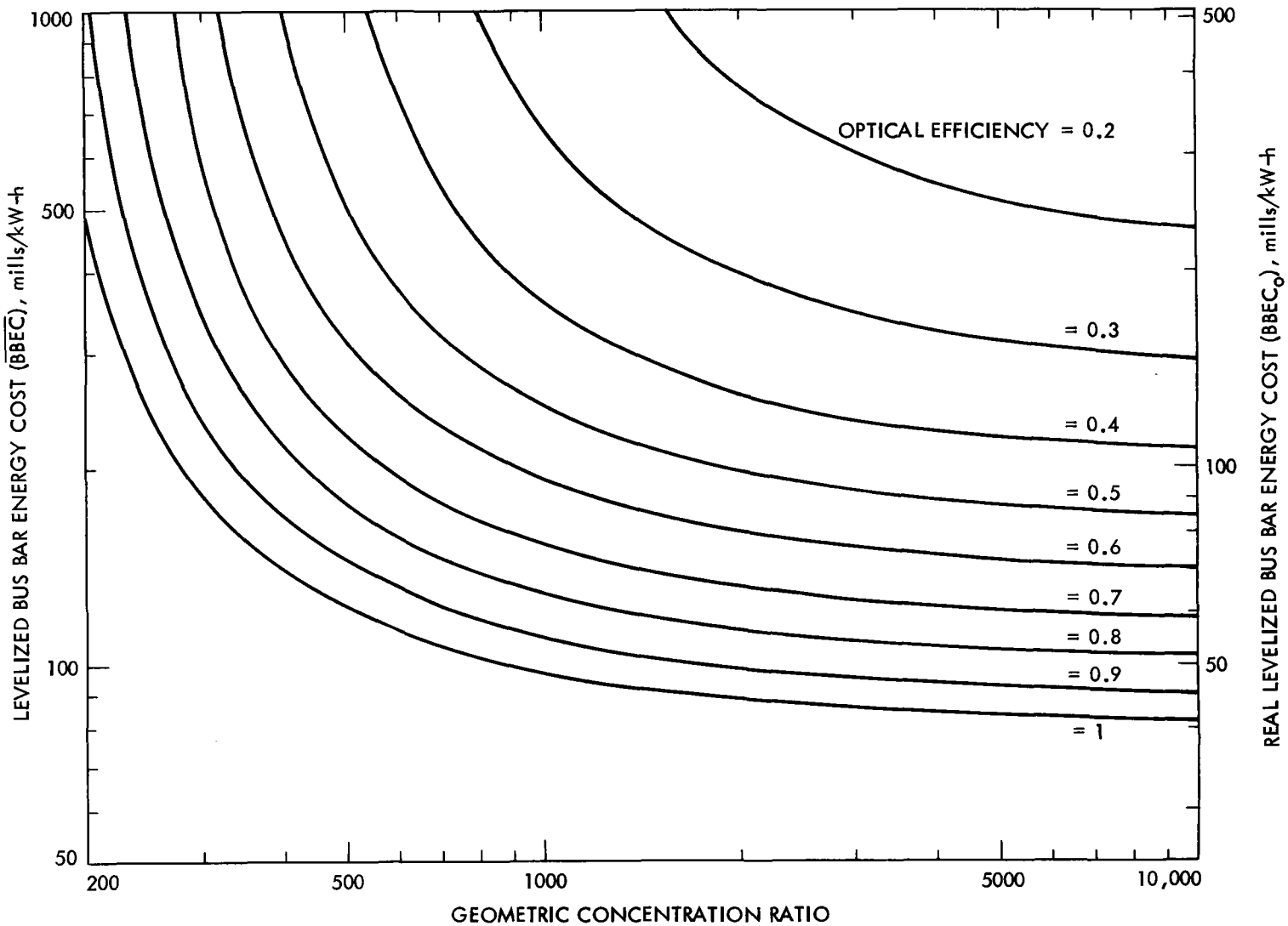

Figure 37. Effect of Optical Performance upon Cost of Electricity Produced. (Projected.) Baseline system except as noted. (For collector efficiencies, see Figure 5.)

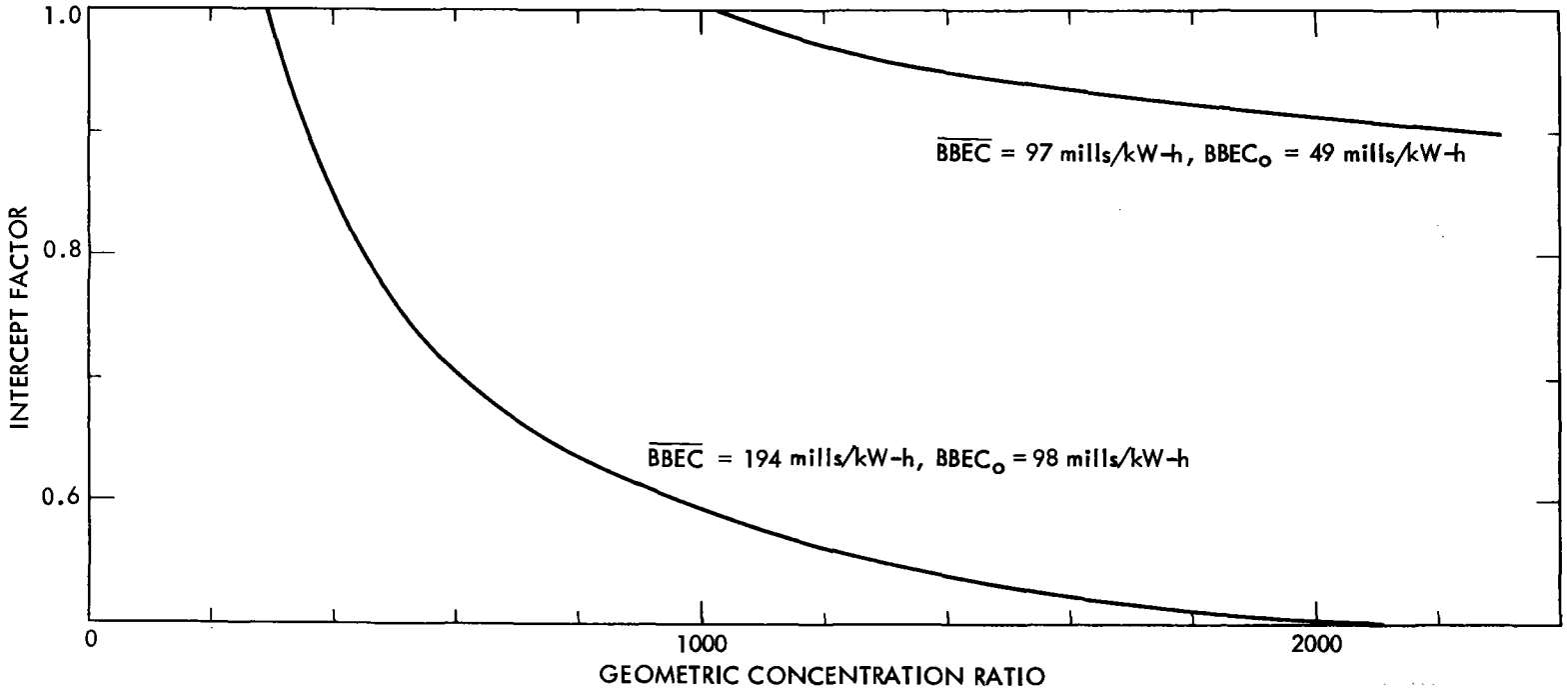

Figure 38. Trade-Off of Optical Efficiency Versus Geometric Concentration Ratio at Constant Cost of Electricity Produced. (Projected.)

Baseline system except as noted.

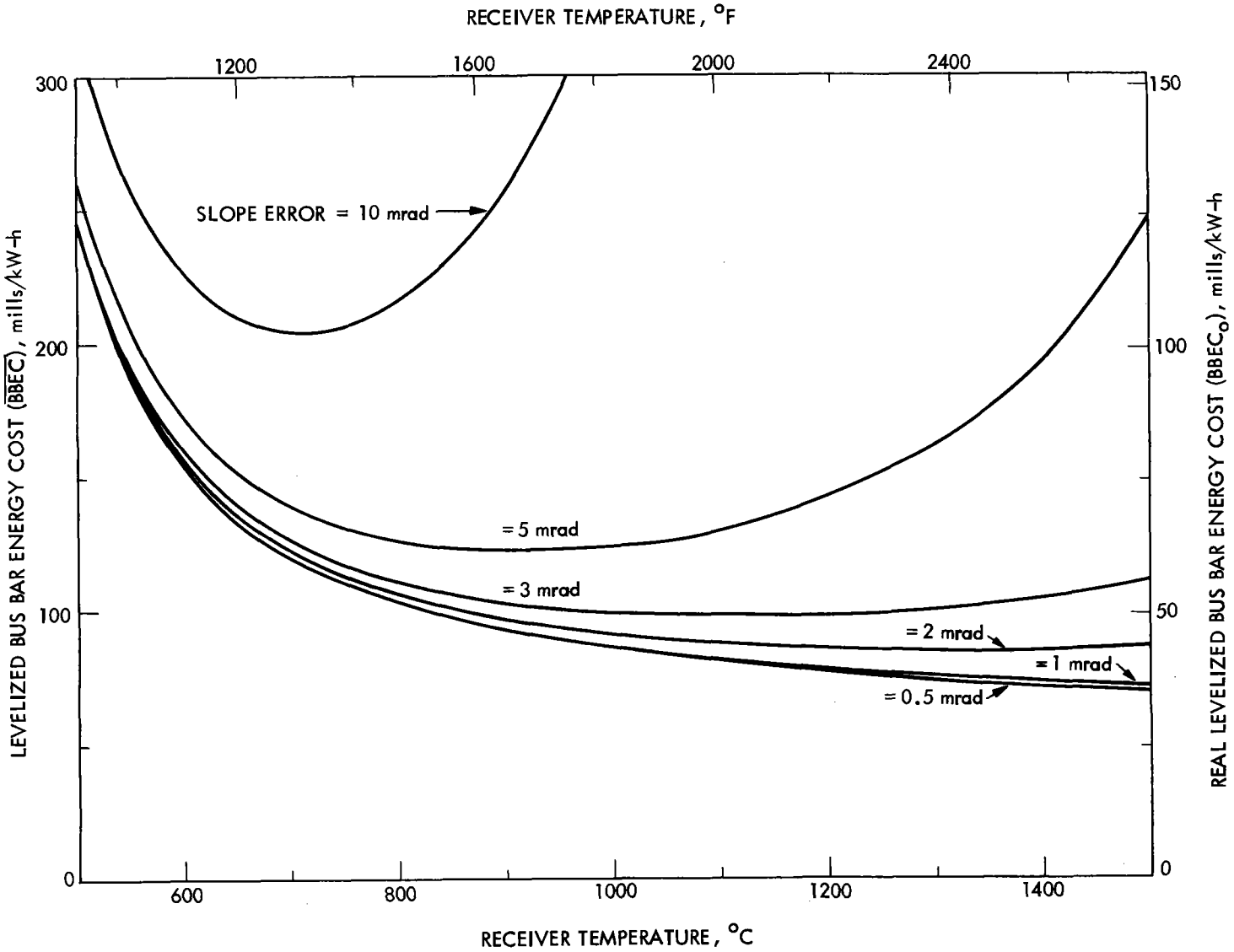

Figure 39. Effect of Slope Error upon Cost of Electricity Produced at Various Receiver Temperatures (Projected)

Baseline system except as noted. Receiver aperture optimized. Plant costs assumed to depend on efficiencies, but to be otherwise independent of temperature. (For collector efficiencies, see Figure 19; for power conversion efficiencies, see Figure 17a.)